Aus dem Med. Institut für Physiologische chemie

Geschäftsführender Direktor: Prof. Dr. Gerhard Schratt

Des Fachbereichs Medizin der Philipps-Universität Marburg

Role of endosomal toll-like receptors in epilepsy

Inaugural Dissertation

Zur

Erlangung des Doktorgrades

Der gesamten Naturwissenschaften

(Dr. rer. nat.)

dem

Fachbereich Medizin

der Philipps-Universität Marburg

Vorgelegt von

Chinmaya Sadangi

Aus New Delhi, Indien

Marburg, 2017

Angenommen vom Fachbereich Medizin der Philipps-Universität Marburg am:

Gedruckt mit Genehmigung des Fachbereichs.

Dekan: Prof. Dr. H. Schafer

Referent: Prof. Dr. G. Schratt

Korreferent: Prof. S. Bauer

To my family.

"My hope is that understanding the brain and the mind will ultimately allow humanity to enter a more enlightened state."
Ed Boyden

Table of Contents

List of abbreviations

AChR: Acetylcholine receptor
ACTH: Adrenocorticotropic hormone
AED: Anti-epileptic drugs
AMPARs: α-amino-3-hydroxy-5-methyl-4-isoxazolepropionic acid receptors
BBB: Blood brain barrier
CA: *Cornu ammonis*
CNS: Central nervous system
COX-2: Cyclooxygenase-2
CSF: Cerebrospinal fluid
DAMP: Damaged associated molecular pattern
DC: Dendritic cells
DG: Dentate gyrus
DRG: Dorsal root ganglion
dsRNA: double stranded RNA
EC: Entorhinal cortex
ELISA: Enzyme Linked Immunosorbent Assay
eTLRs: endosomal toll-like receptors
FCD: Focal cortical dysplasia
GABA: Gamma-aminobutyric acid
HI: Hypoxia ischemia
HSV: Herpex simplex virus
HMGB1: High-mobility group box protein 1
HS: Hippocampal sclerosis
i.p: Intraperitoneal
IFN: Interferons
IKK: IκB kinase
IL-1: Interleukin 1
IL-1β: Interleukin-1β
IL: Interleukin
ILAE: International League Against Epilepsy
IRAK: Interleukin-1 receptor-associated kinase
IRAK4: Interleukin-1 receptor-associated kinase 4
IRF: Interferon regulatory transcription factor

KA: Kainic acid

KaL: Kainate-lorazepam

KAR: Kainic acid receptors

LPS: Lipopolysaccharide

MCP-1: Monocyte chemokine protein-1

mTLE: Mesial temporal lobe epilepsy.

MVBs: Multivesicular bodies

MyD88: Myeloid differentiation factor 88

NF-κB: Nuclear factor kappa-light-chain-enhancer of activated B cells

PAMP: Pathogen-associated molecular pattern

PPS: Perforant path stimulation

PRR: Pattern recognition receptor

PTZ: Pentylenetetrazole

qPCR: Quantitative real-time PCR

RNA: Ribonucleotide acid

SARM: Sterile-alpha and Armadillo motif containing protein

SE: Status epilepticus

siRNA: Small interfering RNA

ssRNA: Single stranded RNA

TAK1: Transforming growth factor beta-activated kinase 1

TBI: Traumatic brain injury

TICAM1: Toll-like receptor adaptor molecule 1

TLE: Temporal lobe epilepsy

TLRs: Toll-like receptors

TNFα: Tumor necrosis factor – α

TRAF6: TNFR-associated factor 6

TRAM: Translocation associated membrane protein

TRIF: TIR-domain-containing adapter-inducing interferon-β

WB: Western Blot

Publications

This thesis summarizes the work carried out by me in the laboratories of Prof. Dr. Gerhard Schratt and Prof. Felix Rosenow at the Philipps University, Marburg, Germany.

The thesis is written as a cumulative dissertation based on two publications and one manuscript in preparation.

Publication 1: A novel animal model of acquired human temporal lobe epilepsy based on the simultaneous administration of kainic acid and lorazepam

Epilepsia, 58(2):222–230, 2017 doi: 10.1111/epi.13579

Friederike Kienzler-Norwood, Lara Costard, **Chinmaya Sadangi**, Philipp Muller, Valentin Neubert, Sebastian Bauer, Felix Rosenow, and Braxton A. Norwood

Publication 2: Validation of Reference Genes for Quantitative Gene Expression Analysis in Experimental Epilepsy

Journal of Neuroscience Research doi: 10.1002/jnr.24089

Chinmaya Sadangi, Felix Rosenow, and Braxton A. Norwood

Publication 3: Role of endosomal toll-like receptors (TLRs) in experimental epilepsy (In preparation)

Chinmaya Sadangi, Stephan Bauer, Felix Rosenow, Philip Yu, and Braxton A. Norwood

Summary

Epilepsy is a common disorder affecting about 60 million people worldwide. The population of epilepsy patients who cannot achieve seizure freedom has remained stubbornly fixed at around 30% despite the introduction of new therapies in recent years. The only way to stop the development of epilepsy is to prevent an injury. Epilepsy is caused by myriad factors and is characterized by recurrent and spontaneous seizures, increased mortality rate, and decreased social interaction and quality of life (Henshall et al. 2016). The harmful effects include disruption of the developmental process and neuronal degeneration (Yehezkel Ben-Ari and Holmes 2006). The most affected region due to epilepsy is the hippocampus, a part of the limbic system. There are no treatments that can prevent epilepsy; hence, there is a clear need for better anti-epileptic remedies.

The Innate immune system acts as the first line of defense against foreign intruders (Akira 2003). Toll-like receptors (TLRs) are a part of the immune system and were first discovered in *Drosophila melanogaster*. TLRs are involved in early host defense against pathogens, and they recognize a pathogen- or damage-associated molecular pattern (PAMPs/DAMPs). TLRs can also identify phagocytes such as neutrophils, macrophages, and dendritic cells (Akira 2003). They play a role in innate immunity, and TLR signaling leads to inflammatory gene expression changes. The first report of TLRs in epilepsy was by Turrin and Rivest (Turrin and Rivest 2004). All studies related to TLRs in epilepsy have been confined to the cell surface TLRs, e.g., TLRs 2 and 4 (Maroso et al. 2010).

TLRs 3, 7, and 9 are expressed intracellularly, whereas TLRs 1, 2, 4 are expressed on the cell surface. TLR3 recognizes double-stranded RNA (dsRNA) and is associated with viral infection. TLR7 recognizes single-stranded RNA virus. TLR9 recognizes unmethylated CpG DNA motifs, characteristics of DNA viruses, and prokaryotic genomes. TLR4 is most well-known for recognizing lipopolysaccharide (LPS), a component present in many bacteria. Only TLRs 2 and 4 have been implicated in both experimental and human epilepsy, and the endosomal TLRs (eTLRs) are yet to be studied.

Our research group recently discovered, serendipitously, that mice lacking certain TLRs have spontaneous seizures. This information led us to hypothesize that TLR deficiency causes epilepsy. This hypothesis was tested by determining: 1) which of these TLRs is/are responsible for epilepsy, and 2) whether TLR activation can prevent epilepsy. In the thesis, I used two different animal models of epilepsy: a) perforant path stimulation (PPS), and b) systemic injection of kainate and lorazepam (KaL).

I found that TLRs are upregulated in the hippocampus during epileptogenesis and chronic epilepsy phases, as validated in both animal models using qPCR. I found upregulation of mRNA in associated cytokines and chemokines. I also showed that the TLR

proteins are upregulated during chronic epilepsy. Lastly, I knocked down the expression of TLRs 3 and 7, and found that TLR3/7 knockdown did not have any effect on seizure reduction.

To summarize, this project revealed that the TLR mRNA and protein expression are upregulated during epileptogenesis and chronic epilepsy. Knocking down the TLRs using siRNA did not have any effect on the development of epilepsy or inactivation of spontaneous seizures. The originality of the work lies in the fact that we are, to the best of our knowledge, the first to use a phenotype-driven approach to elucidate the role of (as yet unexplored) TLRs in epilepsy.

Zusammenfassung

Epilepsie ist eine der häufigsten neurologischen Erkrankungen und betrifft ca. 60 Millionen Menschen weltweit. Trotz neuer Medikamente und Behandlungsmethoden der letzten Jahre kann bei 30% der Patienten keine Anfallsfreiheit erreicht werden. Die Auslöser für die Entstehung einer Epilepsie sind vielfältig, bislang können jedoch nur bereits manifeste Epilepsien erkannt werden. Epilepsien sind durch wiederkehrende, spontane Anfälle gekennzeichnet und führen zu erhöhter Mortalitätsrate, eingeschränkter Lebensqualität und Sozialleben (Henshall et al. 2016). Weiterhin gehören Entwicklungsstörungen und neuronale Degeneration zu den Symptomen (Yehezkel Ben-Ari and Holmes 2006). Der Hippokampus, ein Teil des limbischen Systems, ist die am häufigsten bei Epilepsie betroffene Hirnstruktur. Bisher sind keine Verfahren bekannt, die die Entstehung einer Epilepsie (Epileptogenese) erkennen oder verhindern können, deshalb besteht weiterhin großer Forschungsbedarf zur Pathogenese.

Das angeborene Immunsystem bildet die erste Abwehrlinie gegen eingedrungene Pathogene (Akira 2003). Toll-like-Rezeptoren (TLRs) gehören zum angeborenen Immunsystem und wurden zuerst in Drosophila melanogaster entdeckt. TLRs erkennen als Teil des angeborenen Immunsystems frühzeitig pathogen- oder schadens-assoziierte molekulare Strukturen (PAMPs/DAMPs) und können auch Phagozyten wie Neutrophile, Makrophagen und dendritische Zellen erkennen (Akira 2003). Die Aktivierung der TLR-Signalwege führt zu veränderten Genexpressionen verschiedener Entzündungsreaktionen. Im Zusammenhang mit Epilepsien wurden TLRs zuerst 2004 beschrieben (Turrin and Rivest 2004). Bei den bisher dabei beschriebenen TLRs handelt es sich ausschließlich um TLRs an der Zelloberfläche (z.B. TLRs 2, 4) (Maroso et al. 2010).

TLRs 3, 7 und 9 werden intrazellulär exprimiert, TLRs 1, 2, und 4 dagegen an der Zelloberfläche. TLR3 erkennt doppelsträngige DNA (dsDNA), TLR7 einzelsträngige DNA (ssDNA) jeweils im Rahmen der viralen Abwehr. TLR9 erkennt für DNA-Viren und Prokaryotengenome typische, unmethylierte CpG-DNA-Motive. TLR4 ist bestens für die Erkennung von Lipopolysacchariden (LPS) in Bakterien bekannt. Nur TLR2 und 4 wurden im Zusammenhang mit Epilepsie sowohl im Experiment als auch in Patienten erwähnt. Endosomale TLRs (eTLRs) dagegen sind weitestgehend unbeschrieben.

Mäuse, denen bestimmte TLRs fehlen, zeigten im Labor epilepsie-typisch spontane Anfälle. Ein Zusammenhang zwischen fehlenden TLRs und Epilepsie ist anzunehmen. Deshalb sollten im Rahmen dieser Arbeit folgende Fragen geprüft werden:

1. Welche TLRs sind für die Epilepsie verantwortlich?
2. Kann die Aktivierung von TLRs eine Epilepsie verhindern?

Es wurden zwei Tiermodelle der hippokampalen Epilepsie verwendet:

1. Stimulation des Tractus perforans (PPS)
2. Systemische Injektion von Kainat und Lorazepam (KaL)

Eine Hochregulation von TLR-mRNAs im Hippokampus konnte in der Epileptogenese und der manifesten Epilepsie durch qPCR-Messungen in beiden Modellen gezeigt werden. Die mRNAs assoziierter Zytokine und Chemokine waren ebenfalls hochreguliert. Erhöhte TLR-Proteinkonzentrationen konnten während der manifesten Epilepsie gezeigt werden. Ein Knock-down der Expression von TLR 3/7 hatte keinen Einfluss auf eine Anfalls-Reduktion.

Zusammenfassend konnten in dieser Arbeit Änderungen der TLR-mRNA- und Protein-Expression während der Epileptogenese und der manifesten Epilepsie gezeigt werden. Ein Knock-down mittels siRNA konnte weder die Epileptogenese, noch das Auftreten spontaner Anfälle verhindern.

Da die Zusammenhänge von eTLRs und Epilepsie weitestgehend ungeklärt sind, bieten sich hier viele Möglichkeiten für weitere Untersuchungen, die eine Erkennung und Behandlung der Epileptogenese zum Ziel haben.

1. REVIEW OF THE LITERATURE

1.1.1 Epilepsy

Over 60 million people worldwide are affected by epilepsy, which is a common and chronic neurological disorder (Wijnen et al. 2017; Van de Vel et al. 2013) with a yearly frequency of 50.4 per 100,000 people (Wijnen et al. 2017; Ngugi et al. 2011). In Europe alone, about 6 million people are treated for epilepsy with 14 billion € as an estimated annual cost (Olesen et al. 2011; Henshall et al. 2016). After migraine, stroke, and Alzheimer's disease, epilepsy is considered to be one of the most common disorders (Reddy and Kuruba 2013).

A seizure is defined as "a transient occurrence of signs and/or symptoms due to abnormal, excessive, or synchronous neuronal activity in the brain" (Fisher et al. 2005), and is a result of an imbalance between excitation and inhibition (Fisher et al. 2005). A person is diagnosed with epilepsy after two spontaneous seizures. However, all disorders characterized by a seizure are not epilepsy, for example, febrile or drug-induced seizures (Manford 2017). An epileptic seizure is classified either as a partial seizure, also known as focal seizure, or generalized seizures. A partial seizure affects only one hemisphere of the brain, whereas a generalized seizure affects both the hemispheres, causing loss of consciousness. According to the International League Against Epilepsy (ILAE), epilepsy is defined when one or any of these criteria are met "(i) at least two unprovoked (or reflex) seizures occurring more than 24 hours apart; (ii) one unprovoked (or reflex) seizure and a probability of further seizures similar to the general recurrence risk after two unprovoked seizures (at least 60%) occurring over the next 10 years; and (iii) diagnosis of an epilepsy syndrome (Fisher et al. 2014)". However, a new basis of classification is in place that classifies seizures according to a) the anatomical site of seizure origin, b) awareness level during a seizure, and c) other features of seizures (Fisher, Shafer, and DSouza 2017; Scheffer et al. 2016; Scheffer et al. 2017).

Epilepsy is more common in children compared to adults, as the underdeveloped brain is more inclined to seizure in comparison to the developed brain, due to the imbalance between excitation and inhibition (Holmes and Ben-Ari 2001). The major causes of epilepsy in children and newborns are believed to include malformation of the brain, lack of oxygen during birth, maternal drug use, and seldom brain tumors (Schachter, Shafer, and Sirven 2017). In adults as well as children, brain infection, stroke, brain injury due to accidents, and genetic factors are some of the reasons that can cause epilepsy.

1.1.2 Epileptogenesis

The process by which a normal brain becomes epileptic is known as epileptogenesis, (Giblin and Blumenfeld 2010) and it is characterized by pathological changes which lead to

the epilepsy development and maintenance (Manford 2017). The brain has cellular, molecular, and neuronal network level changes that result in an epileptic phenotype (Pitkaenen and Lukasiuk 2009; Giblin and Blumenfeld 2010; Rakhade and Jensen 2009). The process is slow and can take months to years to complete without any available biomarkers to detect the process of epileptogenesis (Sloviter and Bumanglag 2013). Epileptogenesis has both genetic and acquired mechanisms. A genetic mechanism is where the seizure occurs due to a presumed genetic alteration, whereas an acquired mechanism is where epileptogenesis occurs after a brain injury. The etiology of idiopathic epilepsy (e.g., childhood absence epilepsy) is unknown, and neuronal circuit rewiring after a brain injury is associated with acquired mechanisms. As shown by human and animal studies, there is a progressive neuropathological change related to epileptogenesis, and as this process progresses, the seizures become more frequent (Sillanpää et al. 1998; Kwan and Sander 2004; Shorvon and Luciano 2007).

Epileptogenesis brings about changes in gene expression, inflammation, protein expression, and the neural network and circuits, all of which are possible drug targets (Manford 2017), and this process ends with chronic spontaneous seizures, i.e. epilepsy. It is hard to study the process of epileptogenesis in humans, as obtaining tissues from the patients is difficult, and tissues are typically only obtained at a very advanced stage of their illness. Animal studies (discussed in section 2.2) have proven to be very fruitful to gain knowledge about the process of epileptogenesis after an initial insult (Tanaka et al. 1992; Hellier et al. 1998; Kharatishvili et al. 2006), because the tissues from animals can be collected within a few months of the injury. In humans this process can take several years (French et al. 1993; Mathern et al. 1995). Also, animal studies allow invasive procedures to reveal causative mechanisms, making them preferable to use.

1.1.3 Status Epilepticus

According to ILAE, Status epilepticus (SE) is defined as a seizure or repeated seizures lasting for more than 30 minutes with a loss of consciousness (Knake, Hamer, and Rosenow 2009). SE occurs because of the failure of mechanisms that help stop a seizure (Walker 2016; Betjemann and Lowenstein 2015), and the failure is caused due to loss of inhibitory mechanisms or excessive increase in excitation during a seizure (Betjemann and Lowenstein 2015). SE is characterized by two stages; the first stage is characterized by generalized tonic-clonic seizures, while the second stage is characterized by behavioral symptoms, decline in cerebral blood flow, and rise in intracranial pressure (Levesque, Avoli, and Bernard 2015). SE can also be focal, and a focal status epilepticus can be defined as a condition where the epileptic disturbance is anatomically discrete and continuous, and lasts for more than 1 hr with an apparent neurological behavior (Schomer 2005). SE is a severe medical and life-threatening condition and needs to be treated rapidy and aggressively (Levesque, Avoli, and Bernard 2015). Animal studies have also shown that a permanent neuronal damage and

synaptic reorganization occurs after seizures lasting more than 30 min (Levesque, Avoli, and Bernard 2015; Norwood et al. 2011), which can be followed by chronic epilepsy. In adult animals, SE causes loss of neurons in CA3 and CA1 regions of the hippocampus, the granule cell layer of the dentate gyrus (DG), and the hilar interneurons in the DG (Martin and Pozo 2006). Prolonged seizures can result in synaptic reorganization, sprouting, and formation of new synapses in different parts of the brain, and compared to adult animals; young animals are less prone to such hippocampal cell loss after prolonged seizures (Martin and Pozo 2006).

1.1.4 Temporal lobe epilepsy

The temporal lobe in the brain is the site of origin of TLE (Van Roost et al. 1998) and affects about 80% of focal epilepsy in adults (Hauser, Annegers, and Kurland 1991). The main structures in the temporal lobe are also a part of the limbic system and include the amygdala, parahippocampal gyrus, and the hippocampus (Figure 1).

TLE may be caused by many different factors including traumatic brain injury (TBI), stress (Haut et al. 2007; Koutsogiannopoulos et al. 2009), or drug abuse (Gordon and Devinsky 2001).

Some TLE patients do respond to anti-epileptic drugs (AEDs) without further problems. However, about one-third of the patients fail to respond (Löscher 2005). Surgical removal of the temporal lobe is an alternative form of treatment for those patients who do not respond to AEDs. Treatment of TLE depends on seizure suppression by the use of AEDs, but as many as 75% of these patients are drug resistant (Schmidt and Löscher 2005), and approximately 40% have side effects due to AEDs (Kwan and Brodie 2000).

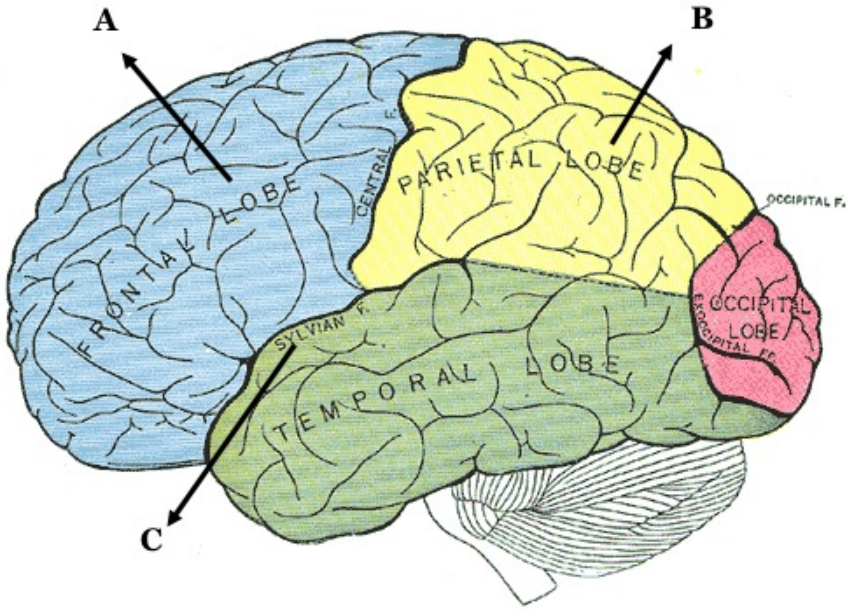

Figure 1: The temporal lobe is located just below the (a) frontal lobe, (b) the parietal lobe, and positioned right underneath the (c) the Sylvian fissure which separates it from a and b. Image accessed from http://webspace.ship.edu/cgboer/lobes.html on 4th April 2017 and used with permission from the author.

Hippocampal sclerosis (HS) is a common neuropathological finding associated with epilepsy (Goldberg and Coulter 2013) and is characterized by the loss of principal neurons in the hippocampus. Astrogliosis and atrophy in the different brain regions such as the amygdala, hippocampus, and the entorhinal cortex are some of the features of HS (Tatum 2012). Mesial TLE (mTLE) appears after damage to entorhinal cortex (Bartolomei et al. 2005), hippocampus (Mathern et al. 2002), and perirhinal cortex (Biagini et al. 2013), as they are significant in spreading limbic seizures. TLE is defined by (i) localization of seizure foci in the limbic system; (ii) an initial precipitating injury that is anticipated before the start of TLE; (iii) a latent period, which is also known as the seizure-free period; and (iv) a hippocampal lesion leading to atrophy which is caused by neuronal loss and gliosis. These characteristics can be reproduced in animal models of TLE, especially in the kindling or SE models, and also in non-SE models like the perforant path stimulation (PPS), the kainate-lorazepam (KaL) or the pilocarpine models. (Section 1.2.3).

1.2 Animal models of epilepsy

Epilepsy can be modeled in animals by different ways depending on the objectives of the experiments and is either induced by chemoconvulsants or electrical stimulation of the brain structures or kindling. Researchers use animal models before any application on humans because of the high anatomical and physiological similarities between animals and humans. Therefore, animal models are important in epilepsy research, and details like the

complex mechanisms of epileptogenesis and seizure generation can be better understood through animal models (Kandratavicius et al. 2014).

1.2.1 Electrical Stimulation models

The advantages of electrical stimulation based models are that they reproduce epileptogenic features in the brain, have low mortality, and better reproducibility as compared to chemoconvulsant methods (Kandratavicius et al. 2014). However, a major limitation of electrical stimulation models are their high costs and labor intensity for chronic epilepsy studies (Pitkänen, Schwartzkroin, and Moshé, 2006; Kandratavicius et al. 2014). The stimulation based models target brain areas prone to epileptogenesis such as the hippocampus (Vicedomini and Nadler 1987), amygdala (Nissinen et al. 2000), and perforant pathway (Sloviter 1983; Norwood et al. 2010). Electrical stimulation results in neuronal damage as well as spontaneous seizures, after a seizure-free period (Nissinen et al. 2000). The latent period is characterized by neuronal degeneration and synaptic reorganization (Nissinen et al. 2000).

1.2.2 Kainic acid

A convulsant is defined as "a substance with demonstrated convulsive effects in vivo" (De Deyn et al. 1992), and it acts by creating an imbalance between excitatory and inhibitory signals (De Deyn et al. 1992). Kainic acid (KA) is a common chemoconvulsant used in animal models of epilepsy and is a cyclic analog of L-glutamate and an agonist at ionotropic KA receptor (Lévesque and Avoli 2013). It was first isolated and extracted in tropical and sub-tropical waters from red algae (*Digenea simplex*) in 1953 (Murakami, Takemoto, and Shimizu 1953). Local application of KA on neurons causes neuronal destruction and pyramidal cell loss in the hippocampus (Nadler, Perry, and Cotman 1978). Some major characteristics of TLE such as depolarization and excitotoxic cell death are activated by KA (Lévesque and Avoli 2013). KA activates KA receptors (KARs), and with a higher concentration of KA α-amino-3-hydroxy-5-methyl-4-isoxazolepropionic acid receptors (AMPARs) can be activated (Lerma et al. 1993). KARs are expressed in different regions of the brain during development (hippocampus, cortex, thalamus, and the cerebellum) (Bahn, Volk, and Wisden 1994) and localize within hippocampal neurons both pre- and post-synaptically (Bloss and Hunter 2010). KA-induced neurodegeneration depends on the concentration of KA and administration route. For example, an intraperitoneal (i.p.) injection damages the CA1 region, whereas intracerebroventricular or intra-amygdala injection damages the CA3 region (Nadler, Perry, and Cotman 1978; SPERK 1994). KA causes SE seizure which lasts for several hours and is characterized by motor convulsion (SPERK et al. 1983). An advantage of the KA model is that it causes injuries restricted only to the hippocampus (Kandratavicius et al. 2014).

1.2.3 Other chemoconvulsant models

Another commonly used chemoconvulsant method is pilocarpine, which is a potent muscarinic Acetylcholine receptor (AChR) agonist and shows sequential behavioral and electrographic changes. Systemic injection of pilocarpine can cause seizure and also develop into limbic SE. Inducing epilepsy using pilocarpine can lead to severe and extensive cell loss in different brain regions (Scorza et al. 2009). A common feature shared by the KA and pilocarpine model is widespread neuronal damage and associated changes like gliosis and neurogenesis within a few days after SE (SPERK et al. 1983), and after a quiet period of 1-3 weeks, spontaneous seizures can be noticed. The significant limitations of the pilocarpine model of SE are its high mortality rate, variable frequency, and severity of spontaneous seizures and neocortical lesions (Kandratavicius et al. 2014). However, if animals are directly injected pilocarpine in the hippocampus, they show reduced mortality rate and similar kind of behaviors and neuropathological characteristics compared to the systemic injection of pilocarpine (Furtado et al. 2002).

Some other chemoconvulsant models induce seizures by blocking inhibitory GABAergic systems (Fisher 1989), and pentylenetetrazole (PTZ) or bicuculline methiodide. They are used as acute seizure models but cannot be used in animal models of epilepsy (Kandratavicius et al. 2014) because they cause less damage to the brain and are not associated with spontaneous seizures (Nehlig and Pereira de Vasconcelos 1996).

Kindling is defined as “the progressive changes that result from repeated electrical stimulation” (Goddard, McIntyre, and Leech 1969). It is a process where repeated stimuli cause an increased seizure susceptibility, and it also is a common chronic model of TLE (Kandratavicius et al. 2014). The animals undergo electrical stimulation daily in the seizure-prone regions of the brain (hippocampus or amygdala) (Rolston et al. 2011). Initially, the stimulation generates low electrical after-discharges that do not cause behavioral seizures. Repeated stimulation eventually causes high-frequency electrical discharges and convulsive seizures (Rolston et al. 2011). Kindled animals typically do not exhibit spontaneous seizures. A major limitation of the kindling model is the associated costs and the time-consumption. However, it can be used for the prevention of epileptogenesis processes and pharmacoresistant epilepsy treatments (Kandratavicius et al. 2014).

1.3 Hippocampus

The hippocampus is located in the temporal lobe of the brain and is an important brain area in the pathophysiology of epilepsy. The hippocampus is susceptible to epileptic seizures, and TLE is considered to be generated in the hippocampus due to observations made by histopathology in TLE patients (Avoli 2007). The hippocampus is more prone to damages caused by epileptic seizures, and CA3 and CA1 sub-regions of the hippocampus are

more susceptible to neuronal damage (Faherty, Xanthoudakis, and Smeyne 1999; W. Liu et al. 2001).

The hippocampus is sub-divided into the following regions – *cornu ammonis* (CA) CA1 - CA4, dentate gyrus (DG), and the subiculum (Figure 2), and these parts vary in sizes and cell types (Amaral and Lavenex 2006). The DG is further subdivided into two layers; a granular cell layer that includes the granule cells, and a molecular layer that includes dendrites of the granular cells and axons projecting from the entorhinal cortex (EC) (also known as the perforant path) (Amaral and Lavenex 2006). The granule cell (mossy fibers) layer axons project towards the CA3 region. Pyramidal cell layers are present in the CA region and have cell bodies of the pyramidal cell types neurons, adjacent to the *stratum oriens,* and *stratum radiatum* (Amaral and Lavenex 2006). The basal dendrites of pyramidal cells are present in the *stratum oriens,* while the apical dendrites are present in the *stratum radiatum*. Axons from the CA3 region (Schaeffer collaterals) first project into the *stratum oriens* and then to *stratum radiatum* of the CA1 region. Finally, the axons from the CA1 region project towards the subiculum and from there they project back to the EC (Amaral and Lavenex 2006).

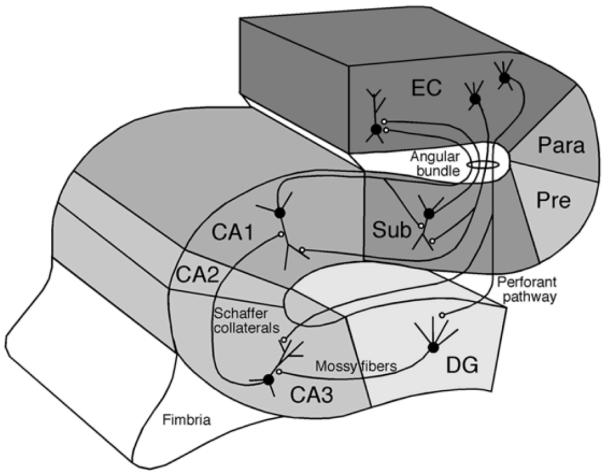

Figure 2: Cross section of the hippocampus. The Hippocampus book (Amaral and Lavenex 2006). The figure has been used with permission from the publisher (Oxford University Press).

The excitatory pathway starts by input from the EC present at the DG and continues from CA3 to CA1 to the subiculum, and then continues back to the EC. Hippocampal neurons mainly consist of excitatory neurons with glutamate as their neurotransmitter; however, a small population, ~ 10% neurons are inhibitory with gamma-aminobutyric acid (GABA) as their neurotransmitter (Freund and Buzsáki 1996). The excitatory activity of the hippocampus is modulated by these interneurons (Freund and Buzsáki 1996).

1.4 Inflammation

Inflammation can be defined as an adaptive response to harmful stimuli such as pathogens or irritants (Medzhitov 2008), and the process of inflammation protects the body against pathogens (Vezzani et al. 2011). During an inflammatory response, molecules are produced by cells of the immune system with proinflammatory or anti-inflammatory properties to heal the site of injury (Vezzani and Rüegg 2011). Invading pathogens (Vezzani and Rüegg 2011) and endogenous "danger signals" released by cells (Bianchi 2007) prompt inflammation.

1.4.1 Brain Inflammation

Neuroinflammation or brain inflammation can be defined as the inflammation of the central nervous system (CNS). Neuroinflammation is characterized by a wide range of pathological phenomena such as glial cell morphological changes and invasion of foreign agents to tissues (Becher, Spath, and Goverman 2016). They have an important role in innate immunity by producing inflammatory mediators like cytokines, chemokines, and leukocytes (Vezzani and Rüegg 2011).

It was assumed in previous studies that the blood-brain-barrier (BBB) protects the CNS from the immune system, preventing the entry of inflammatory cells and molecules. It has also been observed that leukocytes, cytokines, and chemokines can cross the BBB and induce an immune response in microglia and astrocytes (Rivest 2009). After the first signs of inflammation, different mechanisms have been identified to stop detrimental effects on a tissue. Inflammation may become chronic and can last for longer periods to provoke tissue damage or dysfunction when endogenous and regulatory mechanisms fail (Vezzani and Rüegg 2011).

1.4.2 Inflammation and epilepsy

Previous studies have suggested an involvement of inflammation in epileptogenesis and a relation between inflammation and the immune system in different types of seizures (Aarli 2000; Palace 2000; Choi et al. 2009; Vezzani et al. 2011). The role of inflammation and immunity in human epilepsy was first shown by an anticonvulsant activity of adrenocorticotropic hormone (ACTH) (Vezzani and Rüegg 2011). An epileptic condition known as Rasmussen's encephalitis is characterized by severe seizures, encephalitis, and dementia (Rasmussen, Olszewski, and Lloydsmith1958), providing the first evidence of chronic and progressive brain inflammation (Vezzani and Rüegg 2011). There is an activation of the immune system in epileptic patients, which happens by circulation of autoantibodies that recognize intracellular or membrane antigenic neuronal epitopes (Vezzani and Rüegg 2011). It has been observed in animal models that epileptic activity and

brain inflammation are correlated. This emphasizes that inflammation can be a major cause that contributes to epilepsy development after an injury. Recurrent seizures are "potent inducers" in brain inflammation in endothelial cells, neurons, microglia, and the BBB (Vezzani and Rüegg 2011). A correlation between activation of specific inflammatory pathways in the brain and seizure activity has been studied in acute and chronic epilepsy models. For example, anticonvulsant activity has been observed during blocking or activation of proinflammatory cytokines, such as tumor necrosis factor-α (TNF-α) or interleukin-1β (IL-1β) (Vezzani, Balosso, and Ravizza 2008; Heida, Moshé, and Pittman 2009), TLR signaling pathways (Maroso et al. 2010), and cyclooxygenase-2 (COX-2) (Kulkarni and Dhir 2009). In patients who have chronic epilepsy, the level of pro-inflammatory cytokines has been found to be elevated in the cerebrospinal fluid (CSF) and sera. This suggests that neuroinflammation plays a role in epileptogenesis (Babcock et al. 2006; Iliev et al. 2004; Alexopoulou et al. 2001).

1.4.3 Inflammatory mediators

(a) Cytokines

Cytokines can be defined as small peptides or proteins secreted by cells associated with inflammation, immune activation, cell differentiation, or death, and have an effect on interaction and communications among cells. Cytokines are pleiotropic in nature (Becher, Spath, and Goverman 2016) and function either by autocrine action, i.e. acting on cells that secrete them, or by paracrine action, i.e. acting on nearby cells, and are grouped into pro-inflammatory and anti-inflammatory cytokines (Zhang and An 2007). They are upregulated after brain insults and are expressed in immune cells, but are also produced in resident brain cells including glia and neurons (Hedtjärn et al. 2002; T. Liu et al. 1994; Szelényi 2001). After inducing chemoconvulsants, there has been a rapid increase in cytokines in seizure models, both in the developing and mature brain (Jankowsky and Patterson 2001; Ravizza et al. 2005).

In an adult brain, TNF-α is upregulated after ischemia (Ohtaki et al. 2004; Saito et al. 1996) and it induces apoptosis of oligodendrocytes (Selmaj et al. 1991; Cammer 2000). TNF-α acts as a proconvulsant and is important in enhancing PTZ-induced seizures by *Shigella dysenteriae* (Yuhas et al. 2002). In amygdala-kindled rats, TNF-α treatment increased the seizure frequency and caused changes in the EEG pattern (Shandra et al. 2002). Recent studies have found that TNF-α concentration decreased in the hippocampus and piriform cortex 5 h post pilocarpine SE. However, TNF-a levels were elevated in the hippocampus 5 days after SE (Arisi et al. 2015).

Administering IL-1 β can induce white matter damage in neonatal mice, and in neonatal brains with hypoxia-ischemia (HI), IL-1β increased with infection. Deletion of IL-1β didn't protect against HI, but administering IL-1ra, an inhibitor of IL-1β protects the neonatal

brain against HI. Depending on the dosage and concentration, IL-1β can be neuroprotective in nature (Bernardino et al. 2005). IL-1 β is upregulated 2 hr after pilocarpine-induced SE in the piriform cortex, hippocampus and neocortex. However, the concentration returned to basal levels after 5 days (Arisi et al. 2015).

IL-6 is a pro-inflammatory cytokine and has an increased level in the hippocampus, DG, amygdala, and meninges after seizures, however, IL-6 messenger RNA (mRNA) level is limited to the hippocampus (Li et al. 2011). In limbic SE models, it has been found that both IL-6 mRNA and IL-6 protein levels were increased in glial cells 6h after SE (Vezzani et al. 2002). Some studies showed that mice lacking IL-6 develop severe brain injuries, while others showed that mice which overexpressed IL-6 develop neurologic syndromes.

IL-10 acts by inhibition of IL-1, TNF-α, and IL-6, and is an anti-inflammatory cytokine (Ledeboer et al. 2000; Zhai, Futrell, and Chen 1997; Heyen et al. 2000). Studies have shown that IL-10 is neuroprotective against glutamate-induced or HI-induced neuronal death. Li et al have demonstrated that IL-10 has anti-convulsant properties (Li et al. 2011), and another study by Levin and Godukhin has shown that they have protective effects against the development of epileptiform activity (Levin and Godukhin 2007).

(b) Chemokines

They are a family of cytokines but are smaller in size (8-14 kDa) and have chemoattractant properties (Bernardino et al. 2005) that guide them towards the chemokine. They are either pro-inflammatory or homeostatic and are involved in controlling cell migration, proliferation, and differentiation and attract inflammatory cells and leukocytes to the injury spot. They bind to cell surface receptors which are coupled with G-proteins to exert their biological activity (Bernardino et al. 2005). They have recently been described in the CNS and are upregulated during inflammation (Bernardino et al. 2005). Previous studies have shown the involvement of chemokines in epilepsy: (a) there is an increased release of Monocyte Chemokine Protein-1 (MCP-1) by NMDA-induced neuronal death from astrocytes (Minami and Satoh 2003); (b) in pilocarpine-induced seizures, MCP-1 mRNA levels were seen to be upregulated (Turrin and Rivest 2004); and (c) upregulation of CCR5 in neuronal and non-neuronal cell types by kainate-induced seizures (Mennicken, Chabot, and Quirion 2002). In ischemic brain injury, MCP-1 production is reduced. However, increased MCP-1 levels have been associated with brain injury. It has been shown that there is an upregulation of CCL3 and CCL2 in the neocortex, hippocampus, and piriform cortex in pilocarpine-induced seizures (Arisi et al. 2015). CCL5 was also found to be upregulated after 24 hr in the neocortex and piriform cortex in pilocarpine-induced SE (Arisi et al. 2015).

1.5 Toll-like receptors

The immune system is classified into either innate or adaptive immunity. Innate immunity is activated during birth and helps to combat pathogens, while adaptive immunity (acquired immunity) is limited to vertebrates. The innate immune system includes TLRs, which are transmembrane proteins initially discovered in *Drosophila Melanogaster*. It helps in the developmental process and is responsible for controlling functions like synaptogenesis and axon path-finding (Stein et al. 1991; Rose et al. 1997). Pathogen-associated molecular patterns (PAMPs) or damage- (or danger-) associated molecular patterns (DAMPs) activate the TLR signaling pathway. In humans, 11 TLR paralogues have been recognized, while in other mammals 13 TLR paralogues have been recognized (Hopkins and Sriskandan 2005). The presence of TLRs is not just confined to the peripheral immune system where they are abundantly expressed, but also to immunological functions and CNS injuries (Lehnardt 2010; Visser et al. 2006). TLRs are expressed in mammalian immune cell types like B cells, mast cells, dendritic cells, neutrophils, and basophils. Also, they are present in non-immune cells such as epithelial and endothelial cells (Okun, Griffioen, and Mattson 2011).

1.5.1 Toll-like receptor signaling pathway

TLRs are classified according to their cellular distribution. TLRs 1, 2, 4, 5, 6, 8, 9, 11, 12, and 13 are expressed on the cell surface, while TLRs 3, 7, 8, and 9 are present in the intracellular compartments. Pattern recognition factor (PRR) is a primary component of the innate immune system and recognizes both PAMPs and DAMPs. Microbial membrane components like proteins and lipids are identified by TLRs present on the cell surface, whereas bacteria and virus-derived nucleic acids are identified by endosomal TLRs (eTLRs) (Kawasaki and Kawai 2014). TLR3 detects viral double-stranded RNA (dsRNA) formed during the replication process of a positive-stranded RNA virus, small interfering RNAs (siRNAs), and self-RNAs extracted from damaged cells (Kawasaki and Kawai 2014). TLR4 detects lipopolysaccharides (LPS), which are major components of gram-negative bacteria (Maroso et al. 2010). TLR7 recognizes single-stranded RNA (ssRNA) and is expressed in plasmacytoid dendritic cells (DC) (Kawasaki and Kawai 2014). TLR9 recognizes non-methylated CpG-dinucleotides, which are present abundantly in microbial DNA compared to mammalian DNA (Latz et al. 2004). Initially, TLR9 was thought to recognize microbial DNA, but recent research has shown that it can also identify self-DNA as a DAMP and is involved in numerous autoimmune diseases (Matsuda et al. 2015).

All the TLRs bind to adaptor proteins, among which MyD88 and TRIF are the essential adaptor proteins required for activating the intracellular pathway and releasing the inflammatory response in the immune cells. Additionally, there are three other adaptor proteins, Toll-like receptor adaptor molecule 1 (TICAM1), Translocation associated

membrane protein (TRAM), and sterile-alpha and Armadillo motif containing protein (SARM) (Matin et al. 2015).

TLR3 is the only TLR which does not recruit MyD88, while all other TLRs recruit MyD88 followed by Interleukin-1 receptor-associated kinase (IRAK) protein family, thus leading to TNF receptor-associated factor 6 (TRAF6) activation. TRAF6 activates TAK1 by linking k63-linked polyubiquitination, which is followed by activation of Nuclear Factor kappa-light-chain-enhancer of activated B cells (NF-κB) by employing IkB Kinase (IKK) complex or MAP-kinases, respectively. TLR3 uses a TIR-domain-containing adapter-inducing interferon-ß (TRIF) dependent pathway leading to activation of inflammatory cytokines and type-1 interferons by two independent pathways. Whereas the TRIF N-terminal associates with TRAF6, the C-terminal interacts with RIP1 activating transforming growth factor-beta-activated kinase 1 (TAK1). Both these pathways end up enabling NF-κB and help in the expression of inflammatory cytokines. TLR3 activates type-1 Interferons (IFNs) using Interferon regulatory transcription factor (IRF)-3, a phosphorylated protein activated by the IKK-related kinases, and TBK1, which is recruited by TRAF3. The TLR4 signaling pathway is split into MyD88-dependent and -independent pathway. TRAF6 and Interlukin-1 receptor associated kinase-4 (IRAK-4) are essential for the MyD88 dependent pathway while the MyD88 independent pathway employs TRIF, IRF-3, and NF-κB. On the other hand, TLR7 and TLR9 secrete inflammatory cytokines using MyD88, and both of them can also secrete type 1 IFNs by activation of IRF7 (Zhu and Mohan 2010) (Figure 3).

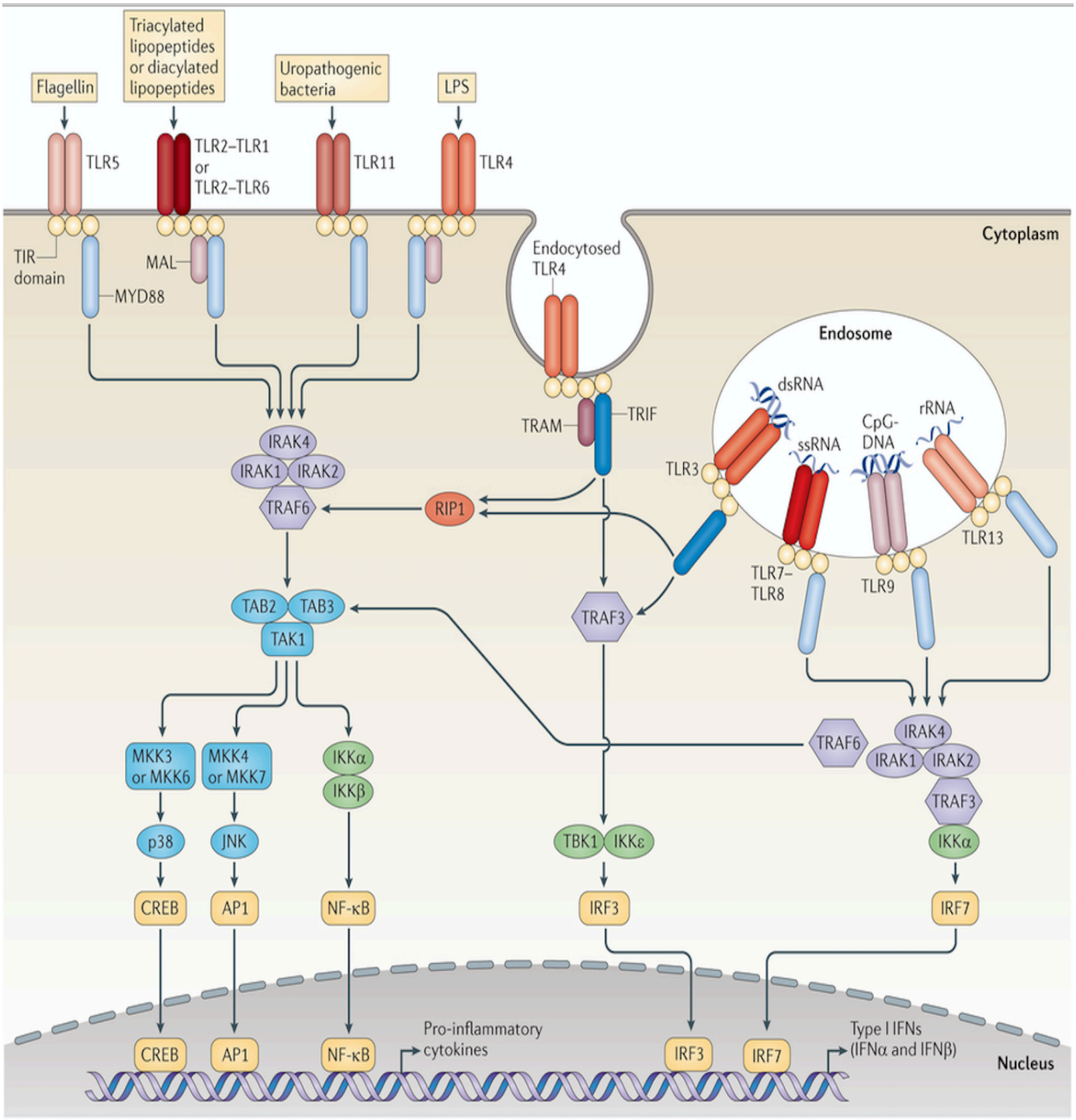

Figure 3: Toll-like receptor signaling pathway. TLR 3, 7, 8 and 9 are endosomal TLRs and bind to microbes or nucleic acids whereas the other TLRs are located on the cell surface and bind to their respective ligands. TLR4 is an exception which localizes both at the plasma membrane and endosomes. Only TLR3 follows a MyD88 independent pathway, whereas other endosomal TLRs follow a MyD88 dependent pathway. The TLRs activate NFkB, CREB, IRFs by using and activating other intermediary pathways. The figure has been adapted from O'Neill, 2013 (O'Neill, Golenbock, and Bowie 2013) with permission from the publishers.

1.5.2 Toll-like receptor function

The adult brain (B. B. Mishra, Mishra, and Teale 2006; Bsibsi et al. 2002), as well as different cell types, express TLRs (Mallard, Wang, and Hagberg 2009). At P0 and P8 embryonic stages TLR3 is highly expressed, but expression decreases at later developmental stages (embryonic, postnatal, and adult stages). TLRs 7 and 9 are strongly expressed during different stages of development, while the other TLRs don't show significant differences during development (Kaul et al. 2012). TLRs 7 and 9 mRNA levels were detected by in-situ hybridization and qPCR in different brain regions of the mouse including the hippocampus and the neocortex (Kaul et al. 2012). TLR7 is increased prenatally in CNS neurons and axons of the developing brain (Kaul et al. 2012). TLR8 is involved in injury and neurite outgrowth (Ma et al. 2006), whereas TLRs 2 and 4 are involved in adult neurogenesis. (Rolls et al. 2007; Okun et al. 2010). TLRs also play a pivotal role in developmental and adult stages of life, for example, TLR3 is involved in inhibiting neural progenitor cell proliferation and regulates axonal growth (Lathia et al. 2008; Cameron et al. 2007).

TLR3 is prevalent in the CNS (Alexopoulou et al. 2001) and is expressed in glial cells (Jack et al. 2005; Farina et al. 2005), neurons, and in neurodegenerative disorders (Préhaud et al. 2005; Jackson, Rossiter, and Lafon 2006). TLR3 is found intracellularly in neuronal cells (Jack et al. 2005; Préhaud et al. 2005; Jackson, Rossiter, and Lafon 2006), whereas in non-neuronal cells (Dendritic or Epithelial Cells) it is found in intracellular compartments (Ménager et al. 2009) or multivesicular bodies (MVBs) (Matsumoto et al. 2003; Jack et al. 2005). The high expression of TLR3 can be associated with neuronal injury or viral infection. TL3 function is not limited to innate immune response, as it inhibits axonal growth in neurons. TLR7 doesn't elicit inflammatory, thermal, mechanical, and neuropathic pain in mice but is expressed in dorsal root ganglion (DRG) neurons, where it induces itch sensation by using non-histamine pruritogens (Okun, Griffioen, and Mattson 2011). They are involved in protection against infections like encephalitis mediated by West Nile Virus and herpes simplex virus (HSV), and also in the pathogenesis of influenza virus. TLR9 doesn't have any effect on neuronal viability (Okun, Griffioen, and Mattson 2011). Activation of TLR9 has an effect on spatial learning and memory, and TLR9 also plays a role in stimulating antiviral activities to protect against HSV (Sørensen et al. 2008) and doesn't play any role in ischemic stroke outcome (Hyakkoku et al. 2010).

1.5.3 Toll-like receptors in epilepsy

TLRs were first reported in epilepsy by Turrin and Rivest (Turrin and Rivest 2004) by studying hippocampal levels of pro-inflammatory transcripts in a mouse model of pilocarpine-induced SE in which increased levels of TLR2 were reported. TLR expression has been found to change during epileptogenesis and chronic epilepsy, but all the literature has been limited to the expression of either TLRs 2 or 4, which are expressed on the cell

membrane. TLR3 is involved in seizures, and its involvement has been shown by the interaction of febrile seizures due to viral infection, and the viral PAMPs interact with TLR 3 (Matin et al. 2015).

In focal cortical dysplasia (FCD), a common cause of medically refractory epilepsy in newborns (Kabat and Król 2012), human specimens have also shown an increase in mRNA expression of TLRs 2 and 4 and also associated with high-mobility group box protein 1 (HMGB1). TLR3 has functions in neurogenesis, neuronal plasticity, immunity, cognition, and embryonic neural progenitor cells, but doesn't play any role in protection against ischemic stroke and neurodegenerative disorders (Okun, Griffioen, and Mattson 2011). According to recent studies, TLR3 deficiency in a pilocarpine mouse model decreases epileptogenesis (Gross et al. 2017).

2. Aims

Previous studies have shown the involvement of TLRs in brain injury, both in response to injurious and non-injurious stimuli. The role of TLRs has also been studied in epilepsy. However, all the data has been limited to TLRs 2 and 4. Only a few studies have shown the role of endosomal TLRs in epilepsy. The overall aim of this thesis was to study the role of endosomal TLRs, associated cytokines and chemokines, and intracellular signaling pathways in epileptogenesis and chronic epilepsy.

Specific aims were:

- To study the expression and regulation of endosomal TLRs in the hippocampus in epileptogenesis and chronic epilepsy.

- To study the expression of associated cytokines, chemokines, and downstream signaling pathways.

- To study the role of activation of endosomal TLRs in preventing epilepsy.

3. Methods

3.1 Animals

Male Sprague-Dawley (SD) rats were used for all the experiments. The animals weighed in the range of 318-344 g. They were housed in an on-site animal facility (21-25°C; 31-47% humidity) and were provided with a 12:12 light/dark cycle with access to ad libitum food and water. The animals were treated in accordance with the guidelines of the European community (EUVD 86/609/EEC). All experiments were approved by the local regulation authority (Regierungspräsidium Gießen (MR 20/15 Nr. 56-2014), Germany).

3.2 Animal models

(a) Perforant Path Stimulation (PPS) model

All surgeries were performed in a stereotaxic apparatus (David Kopf) under anesthesia (3-5% in oxygen). Bipolar stimulating electrodes were implanted bilaterally in the perforant path. The rats were implanted with unipolar recording electrodes and stimulated, whereas the control rats were implanted with electrodes but were not stimulated. After electrode implantation, the rats were transferred to the home cage with access to ad-libitum food and water for a week to recover from surgery. Rats were either stimulated for 8 h or 30 min using the PPS model.

(b) Kainate Lorazepam (KaL) model

Rats were administered 15 mg/kg Kainic acid monohydrate (10 mg/ml in phosphate buffer saline (PBS) Milestone Pharmaceuticals, USA, CM-0100) and 0.25 mg/kg lorazepam (Pfizer, Germany), while the control rats received a single dose of 1 mg/kg lorazepam and PBS, subcutaneously (Kienzler-Norwood et al. 2017). The animals were transferred to the home cage after injections.

3.3 EEG transmitter implantation

EEG data was obtained by screws fitted on top of the cerebrum surface. Reference ground was always a screw located caudal and medial to the recording site and was not over the hippocampus. The wireless transmitters (FT20, Data Science International, USA) were implanted subcutaneously in the rats. Spontaneous EEG activities were recorded using LabChart 7 Software (ADInstruments, New Zealand), and the behavior was recorded using Edimax IC-7110W infrared cameras (Taiwan). Both the EEGs and animal behaviors were recorded continuously (24/7). The EEG activities were stored digitally in 3-hour periods, and the video files were captured at 15 frames/sec and time stamped to match the EEG data using Security Spy Surveillance Software (Ben Software, UK).

3.4 EEG analysis

All EEG files were reviewed manually, and all events with amplitudes >120% of baseline were analyzed.

3.5 Perfusion

Animals were transferred to a transparent box containing Isoflurane and received an overdose of Ketamine (> 100 mg/kg i.p.). The rats were perfused with 0.9% saline, either with or without 4% Paraformaldehyde (PFA). The animals were sacrificed after 4 or 14 days (epileptogenesis group) or 20 weeks (chronic epilepsy group).

(a) Saline perfusion

The animals were perfused through the aorta for 2 min to remove intravascular blood. The Brain was removed from the skull and the hippocampi were microdissected, frozen on dry ice, and stored at -80°C until RNA or protein extraction.

(b) PFA perfusion

The animals were initially perfused with 0.9% saline for 2 min through the aorta to wash off the intravascular blood, followed by 8 min perfusion with PFA. Brain was removed from the skull and transferred to 4 % PFA and stored at 4°C until sectioned on a cryostat.

3.6 RNA extraction and qPCR

RNA was extracted, cDNA was synthesized from the extracted RNA, and qPCR was performed as described in paper II (Sadangi, Rosenow, and Norwood 2017).

3.7 Sample preparation for ELISA

The left hippocampi from the saline perfused rats were homogenized using 1 ml of 1x Phosphate Buffer Saline (PBS) mixed with 10 µl of Halt Proteinase Inhibitor Cocktail (Thermo Scientific, Germany, 87785), using the mechanical pellet pestle. The homogenate was then centrifuged at 13,000g for 20 min at 4°C(Do Young Kim et al. 2012), the supernatant was transferred to a fresh tube, and the pellet was stored at -80°C.

3.8 ELISA

A multi-analyte ELISA was performed using the Qiagen Multi-Analyte ELISArray Kit (Qiagen, Germany, 336161) which analyzed eleven cytokines and one chemokine as described below. Quantitative ELISA was performed for five cytokines and one chemokine using kits from Peprotech, Germany (ELISA Buffer Kit – 900 – M109; IFN γ – 900-M109;

IL6 – 900-M86; IL2- 900-M205; IL1β – 900- M91; and CCL5 – 900- M72). For the quantitative ELISA, the samples were diluted in a 1:5 ratio using the sample buffer provided with the Peprotech kit (Peprotech, Germany).

(a) Multi-Analyte ELISA

The cytokines and chemokines that were detected using this kit were IL1A, IL1B, IL2, IL6, IL10, IL12, IL13, IFN-γ, TNF-α, GM-CSF, and RANTES (CCL5). For the analysis, samples from 4- and 14 days epileptogenesis group were used. On a 96-well pre-coated antigen plate, the upper and lower rows (A & H respectively) were used as negative and positive controls respectively. 50 µl of Assay Buffer was added to the entire plate followed by adding 50 µl of samples to the rows B-G and was incubated for 2 hours. The plate was washed three times, and 100 µl of detection antibody was added and was further incubated for 1 hour. The plate was again washed three times, and 100 µl of Avidin was added, and incubated for 30 min, followed by four washes. 100 µl of development solution was added to the plate and incubated for 15 min in the dark, and 100 µl of stop solution was added to stop the reaction. The plate was read at 450 nm using a Spectral Plate Reader (Thermo Electron, Multiskan, Germany), and raw optical density (OD) values were obtained using the Ascent Software (Thermo Scientific, Germany). All the plate washes were performed using the Wash Buffer provided with the kit, and all incubations were carried out at RT.

(b) Quantitative ELISA

The ELISAs were performed over two days. On day 1, the capture antibody was diluted in PBS, and 100 µl of capture antibody was added to a 96-well plate. The plate was sealed using a sealing film in an aluminum foil, and incubated overnight at RT. On day 2, the capture antibody was aspirated, and the plate was washed four times and was incubated with blocking buffer for 1 hr. The plate was washed four times, and standards were added for either one of the cytokines or chemokine (mentioned above), and then the samples were added to the plate in duplicates along with a positive control. The plate was incubated for 2 hr before adding the detection antibody and further incubated for 2 hr at RT. The Avidin-HRP conjugate was diluted and added to the plate and incubated for 30 min, after which 100 µl of ABTS substrate was added to the wells and incubated at RT until the color changed to green. The plate was read at 405 nm using Spectral Plate Reader, and raw ODs were obtained using the Ascent Software (Thermo Fisher Scientific, Germany).

3.9 Sample preparation for Western Blots

Western Blots were performed to measure TLRs 3 and 7 protein expression changes in chronic epilepsy groups. Animals were perfused with saline, as described before, and the hippocampi were extracted. 1 mL of RIPA buffer was added to the hippocampi, also, to halt protease inhibitor and homogenized using the mechanical pellet pestle. The amount of protein present was measured using a Bicinchoninic acid assay (BCA) kit (Thermo Fisher,

Germany, 23327), and Laemmli buffer was added to the samples in a ratio of 4:1 and heated at 95˚C for 5 min. The samples in Laemmli buffer were stored at -20°C. The samples were re-heated at 95°C for 5 min before loading onto the gel.

3.10 Coomassie staining

Coomassie staining shows the presence of proteins as blue bands on a transparent background. 8-12% gels were prepared, and the samples in Laemmli buffer were loaded onto the gel. An SDS-PAGE was run for the samples for 90-100 min. The gel was then carefully transferred to a container filled with distilled water and washed for 5 min with gentle agitation. The distilled water was then discarded, and fresh staining solution was added. It was then agitated slowly on a shaker for 60 min at RT. This was followed by washing the gel with distilled H_2O briefly, and was further destained with a fast destaining solution for 1-2 hr. The gel was then transferred to a slow destaining solution, and was agitated overnight at RT. The following day the gel was observed for the presence of blue bands on a transparent background. If there was a high background, the gel was further destained in fast destaining solution until the background became transparent. The gel was given a brief wash with distilled H_2O to get rid of the excess destaining solution, and it was packed between plastic membranes and scanned on a flat-bed scanner to obtain a digital copy.

3.11 Western Blots

20µg of samples were loaded onto an 8-12% SDS-PAGE gel. The SDS-PAGE gel was run for 120 minutes, post which it was transferred to a Polyvinylidene fluoride (PVDF) membrane and sandwiched between sponges and filter paper, and was blotted for 90 minutes at 90 V. After disassembling the blot, the membrane was stained with Ponceau staining for 2-3 min, or until the protein bands could be seen. The membrane was then bathed several times with distilled water to wash off the Ponceau staining, followed by blocking with 5% milk in TBS-T at 4°C overnight. TLR3 (Novus Bio, NBP2-24565, Germany, 1:2000), TLR7 (Novus Bio, NBP2-24906, Germany, 1:2000), or ACTB (Sigma-Aldrich, A5316, Germany) primary antibody was added to the membrane and incubated for 1 hr at RT. The primary antibody was collected, and the membrane was washed with TBS-T, followed by incubating the membrane in anti-mouse (Calbiochem, 1: 20,000) or anti-rabbit (Calbiochem, 1: 20,000) secondary antibody for 1 hr. The membrane was washed with TBS-T to wash off the secondary antibody, followed by a short wash with TBS. ECL reagent (GE Healthcare, Amersham, Germany, RPN 2232) was added to the membrane and incubated for 5 min with gentle shaking for TLRs, while a homemade ECL reagent was used to incubate the ACTB membrane for 3 min. The membrane was transferred to a Hypercassete (Amersham, Germany, RPN 1642) and developed in the dark room. Quantification of the blot was done using ImageJ.

3.12 siRNA

Small Interfering RNA (siRNA) was used to knockdown TLR 3 and 7 mRNA. siRNA sequences were ordered from GE Dharmacon, Netherlands.

a) **Pilot study**

A pilot study was conducted to verify the knockdown (KD) effect of TLRs 3 and 7. Rats received an intracerrebellar ventricle (i.c.v.) injection using a single 28-gauge stainless steel injection cannula (define coordinates) of Accell siRNA (5µg/rat) in 5µl of Accell siRNA delivery media (GE Dharmacon, Netherlands, B-005000-100), at a rate of 1 µl/min in a 10 µl microsyringe(Nakajima et al. 2012). The rats received 5 µg of TLRs 3 and 7 in the right and left hippocampi respectively. After the injection, the cannula was left in place for additional 5 min and was removed slowly. The skin was closed using a clip applier (Reflex Clip Applier, USA, 204-1000), and the rats were transferred to the home cage with access to ad-libitum food and water. The animals were sacrificed by saline after 2, 4, and 7 days to assess the maximum knock-down time point. RNA was extracted from the hippocampi and qPCR was performed as described earlier.

b) **TLR 3 and 7 Knockdown**

After concluding the time point at which the TLR KD was maximum, rats were injected bilaterally with 5 µl of either TLRs 3 or 7 in the right and left hippocampi as described above. The rats were implanted with EEG transmitters (as described above) and were transferred to the home cage with access to ad-libitum food and water. After four days, the rats were injected with a dose of kainate and lorazepam (as described earlier) and monitored for seizure activity for three weeks.

3.13 Statistics

All statistical analyses were done using Graphpad Prism, Version 7.0 a (La Jolla, California, USA) for Mac. All data are presented as mean $\pm$ Standard Error of Mean (S.E.M). The t-tests were done using two-tailed tests. * represents $p \leq 0.05$; ** represents $p \leq 0.005$; and *** represents $p \leq 0.0005$. For the ELISA data, raw OD values were entered into GraphPad, and the values were converted to log-format before analyzing, using the Sigmoidal 4PL parameter. The log values were converted back to the base and were multiplied by the dilution factor to get values for the unknown in pg/ml.

4. Summary of papers

4.1 **Paper I:** A novel animal model of acquired human temporal lobe epilepsy based on the simultaneous administration of kainic acid and lorazepam

Friederike Kienzler-Norwood, Lara Costard, ***Chinmaya Sadangi****, Philipp Muller, Valentin Neubert, Sebastian Bauer, Felix Rosenow, and Braxton A. Norwood*

The objective of this paper was to develop a simple animal model of temporal lobe epilepsy (TLE) that avoids caveats associated with traditional models. We used kainic acid (KA) to induce epilepsy and avoid convulsive status epilepticus (cSE). cSE is a condition that can occur with extended or repeated tonic-clonic seizures, and can lead to long-term injuries. cSE is also associated with problems like variability and mortality, and without pharmacological treatment it can be fatal. Kainate, a glutamate agonist, is a commonly used chemoconvulsant to model human TLE in rodents. It initiates seizures by activating kainate receptors (KAR) or AMPA receptors. KA was first used as a model of epilepsy by Ben-Ari and colleagues (Y Ben-Ari et al. 1979), where they did recurrent intra-amygdaloid KA injections to induce seizures. We show a list of different KA models of epilepsy in Table 1 of this publication (Kienzler-Norwood et al. 2017).

In this paper, we described a novel method for inducing epilepsy in the animals by using KA and lorazepam. Lorazepam is a benzodiazepine used to terminate cSE. We injected a single dose of KA subcutaneously with a single lower dose of lorazepam. The lorazepam dose was lower than what is used to stop cSE.

We recorded video-EEGs, which showed that animals that received less lorazepam developed more neurodegeneration and vice versa. A low dose of lorazepam blocked kainate induced convulsive seizures in the animals, but had no effect on the hippocampal seizure activity (Kienzler-Norwood et al. 2017). We also quantified hippocampal neurodegeneration using Fluoro-Jade-B staining, and the mossy fiber sprouting using Timm staining (Figure 2). Mossy fiber sprouting in the dentate gyrus (DG) is a pattern of synaptic reorganization (Dudek and Shao 2004). It develops in human and animal models of TLE.

Our study shows that cSE is blocked by an inadequate dose of lorazepam, but acute hippocampal seizures, neurodegeneration, or epileptogenesis are not blocked by the same. The advantage of this model is its simplicity of use. Previous kainate models required repeated administration; hence the animals needed more attention and care. Our model is based on a single dose of KA and lorazepam, thus avoiding cSE. Therefore, the animals do not need additional or post-operative care. This model shows the same characteristics as acquired mesial TLE, hippocampal sclerosis, and spontaneous hippocampal-onset seizure after a prolonged seizure-free period.

Our study shows that a single dose of KA with a low dose of lorazepam can induce characteristics of mesial TLE in rats while avoiding cSE. In conclusion, this is a simple protocol for inducing epilepsy where acute hippocampal seizures are self-terminating, and there is a lack of morbidity and mortality. Due to the ease of use of this model, it will be useful in studies related to elucidating the mechanisms of epileptogenesis and ictogenesis.

4.2 Paper II: Validation of Reference Genes for Quantitative Gene Expression Analysis in Experimental Epilepsy

***Chinmaya Sadangi**, Felix Rosenow, and Braxton A. Norwood*

The objective of this paper was to identify (novel) reference genes for quantitative real-time polymerase chain reaction (qPCR) data normalization in two different models of epilepsy. Previous studies have used either one or multiple invalidated reference genes for quantifying gene expression normalization. Ours was the first study to systemically evaluate and validate reference genes in experimental epilepsy using rat models in epileptogenesis and chronic epilepsy. In this paper, I described novel reference genes that are more stably expressed (*NONO, RP2*), instead of those that are commonly used (*GAPDH, HPRT1*) in epilepsy studies.

Reference genes play a role in the core maintenance of cellular and molecular structure or function. They are used to determine the expression of the genes of interest (GOI) because they are supposed to be stably expressed across experimental conditions. Normalizing data from gene of interests to reference genes is important to understand the amplification efficiency, cDNA loading differences, and comparison of GOI in different samples. In various experimental models the reference genes vary; therefore, it is crucial to validate them before using them for the normalization of qPCR data.

The first model was a perforant path stimulation (PPS) model, where the animals were stimulated for either 8 h or 30 min. The 8 h stimulation model induced hippocampal sclerosis, and onset of epilepsy that occurred after two to three weeks. The 30 min PPS model did not induce epilepsy or neurodegeneration. The second model used was a Kainate-lorazepam (KaL) model (Kienzler-Norwood et al. 2017), as described in Paper I. All animals were sacrificed after 4- and 14- days post-PPS or KaL injections. An additional group of the KaL animal model was sacrificed 20-weeks post-injection (chronic epilepsy group).

I selected 15 candidate reference genes used in prior epilepsy studies, other rodent disease models and model organisms. In addition, I used some novel reference genes like *NONO*, *RP2*, and *RPLP1,* which were never used earlier in experimental epilepsy studies. I obtained the nucleotide sequences from NCBI and Rat Genome Database (RGD), designed the primers using the online software primer3plus, and verified for secondary structures. The candidate reference genes are given in the paper. Primer sequences for all the candidate reference genes are provided in the Supplementary files of this paper. An r^2 value was obtained for each primer pair to determine its efficiency.

I used four different algorithms to identify the most stable reference genes: geNorm, NormFinder, BestKeeper, and Delta-Ct. These algorithms determine the stability of genes, calculate expression stability, and provide a minimum number of reference genes to be used for normalization. I have provided all the necessary information about the algorithms in this paper and performed all the experiments according to the Minimum Information for Publication of Quantitative Real-time PCR (MIQE) guidelines. These guidelines promote transparency in the experiments and help in facilitating replication of experiments.

I found that each algorithm gave a different set of stable reference genes. To reach a consensus, I calculated a comprehensive ranking by taking the geometric mean of individual ranking provided by the four algorithms. Lastly, I used TLR4 to evaluate the most stable and unstable reference genes in different models of epilepsy (Figure 2).

Reference genes were systematically evaluated in two different animal models of epilepsy, at various time points and using four different algorithms. According to a few previous studies, reference genes can vary between animal models of disease. In addition to confirming this finding, I also show that they can even vary within a model – at different time points. I found that some commonly used reference genes like *GAPDH* and *PPIA* were unstable, and a few novel reference genes like *NONO* and *RPLP1* were stable. Some stable reference genes remained the same within models. For example, *TFRC* was stable in both epileptogenesis and chronic epilepsy groups. I also found that some reference genes were common to multiple models. For example, *NONO* was a stable reference gene for the 8-hr PPS and chronic KaL groups. One limitation of this study was that I did not evaluate potential reference genes in other models of epilepsy, or in other strains or model organisms.

To summarize, I showed that reference genes could vary between different models and different time points in the same model. I also studied the importance of validation of reference genes before using them for qPCR normalization, and found that a few novel reference genes (*NONO*, *RP2*, and *RPLP1*) were more stable compared to commonly used ones (*PPIA*, *GAPDH*, and *HPRT1*).

4.3 Paper III: Role of endosomal toll-like receptors in epilepsy (In preparation)

***Chinmaya Sadangi**, Stephan Bauer, Felix Rosenow, Philip Yu, and Braxton A. Norwood*

In paper III, I determined the endosomal Toll-like receptors (eTLRs) mRNA expression changes in epileptogenesis and chronic epilepsy by using the perforant path stimulation (PPS) and the KaL model. Epilepsy was induced in male Sprague-Dawley rats by using the KaL method described in Paper I (Kienzler-Norwood et al. 2017), or by the PPS model described in Paper II (Sadangi, Rosenow, and Norwood 2017). I measured the gene expression changes of TLRs 3, 7, and 9 by using qPCR. I also measured TLR4, which is upregulated during epileptogenesis (Maroso et al. 2010) in both the animal models. I used the validated reference genes obtained in paper II (Sadangi, Rosenow, and Norwood 2017) to normalize the qPCR data for both animal models. I found that the TLRs (3, 7, and 9) and TLR4 are upregulated during epileptogenesis in both models. I also measured the gene expression changes of the TLRs in chronic epilepsy and found that they remain upregulated during the chronic phase, but with minor divergences from the epileptogenesis phase.

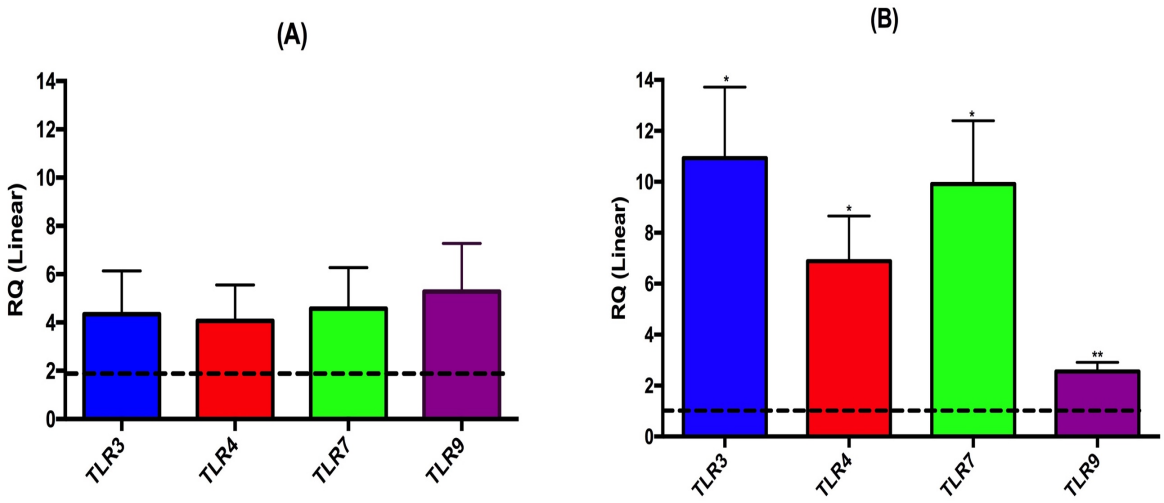

Figure 4: TLR expression during epileptogenesis at (a) 4 days and (b) 14 days post PPS

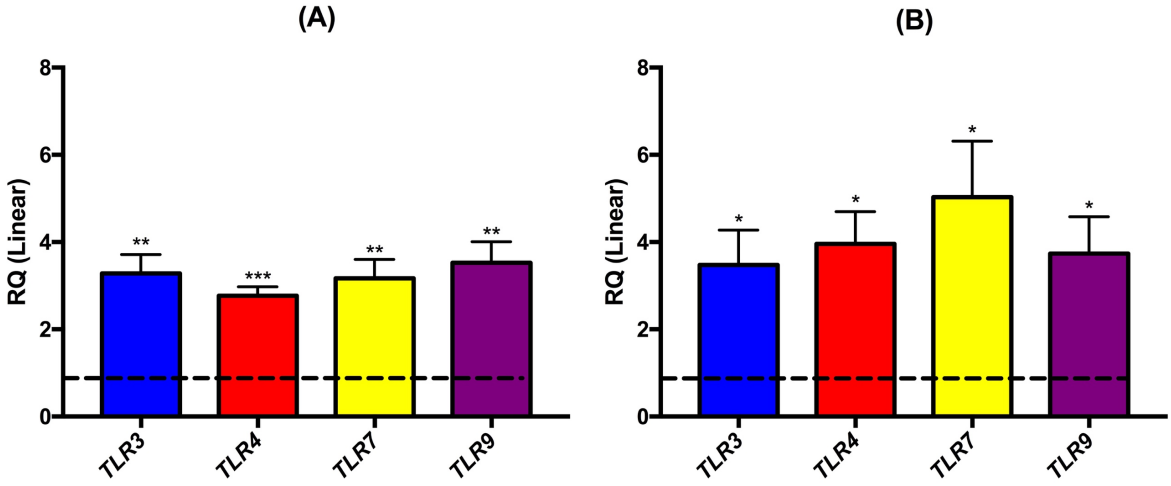

Figure 5: TLR expression during epileptogenesis at (a) 4 days and (b) 14 days in the KaL model

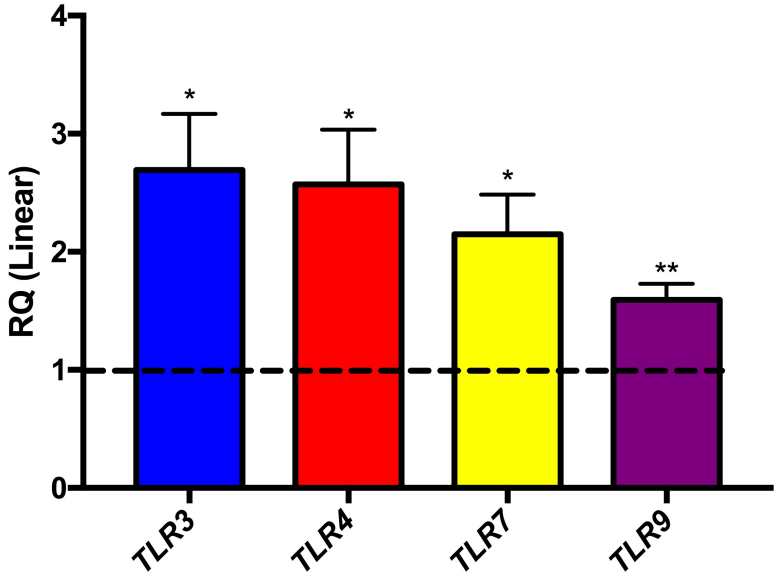

Figure 6: Expression of TLRs post 20 weeks after KaL

In addition, I measured the mRNA expression changes of cytokines and chemokines, which are part of the TLR signaling pathway. IL-1β, IL-2, IL-6, IL-10, and TNFα were measured both during epileptogenesis and chronic epilepsy time points using the KaL model. A difference in gene expression at 4 and 14 days KaL epileptogenesis was found. At 4 days, IL-2 and TNFα were significantly upregulated, but at 14 days they were significantly downregulated compared to the controls. IL-6 which was not expressed at 4 days, but was significantly upregulated at 14 days compared to the controls. IL-1β and IL-10 were not expressed at both time points. In the chronic phase, IL-1β and TNFα were upregulated, and the other cytokines (IL-2, IL-6, and IL-10) were not detectable.

Quantitative and qualitative ELISA was performed for cytokines and chemokines to monitor changes in protein levels during epileptogenesis and chronic epilepsy. A qualitative ELISA was carried out to measure protein expression levels of different cytokines and chemokines, such as IL-2, IL-1β, IL-6, IFN-γ, and CCL5.

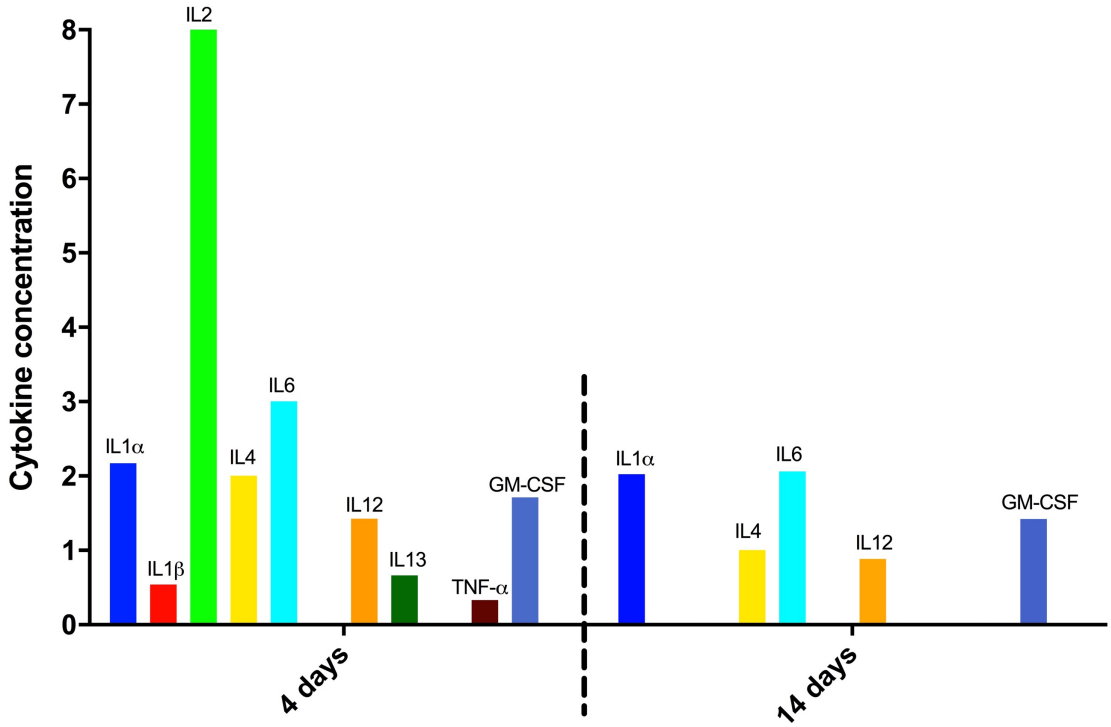

Figure 7: Qualitative analysis of cytokines and chemokines in the KaL model of epilepsy

Protein expression changes of TLRs were measured for the chronic epilepsy model by Western Blot analysis. Protein was extracted from the hippocampi and analyzed for expression changes as described in the methods. The protein expression changes were similar to the mRNA levels of TLRs, i.e. they were upregulated in chronic epilepsy. Immunohistochemistry was also performed for the TLRs to see the expression of TLRs in the hippocampal neurons.

Lastly, I knocked down TLR mRNA using siRNA to study the effect of TLR inactivation on spontaneous seizures. In a pilot study, I determined the optimal time point at which TLR knockdown efficiency was maximal post-siRNA injection by using qPCR. I injected siRNA directly into the hippocampus and sacrificed the animals at three different time points. Then I performed qPCR with RNA obtained from hippocampus, and found that TLR knockdown was maximal at 4 days post siRNA injection. In the treatment group, I injected the siRNA bilaterally, and after 4 days started monitoring the effect of knocking down TLRs on seizure frequency in the KaL model. The animals were observed for 3 weeks, and I found that knocking down the TLRs did not have any effect on epileptogenesis or seizure frequency.

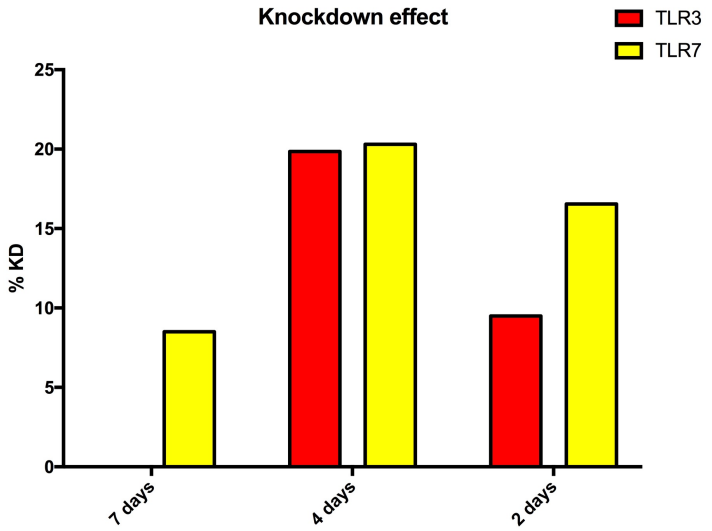

Figure 8: Percentage knockdown using TLR siRNA at 2, 4, and 7 days

To summarize, I showed that the endosomal TLRs are expressed during epileptogenesis and chronic epilepsy and are present in the hippocampus. They are upregulated during epileptogenesis and chronic epilepsy, along with a few associated cytokines and chemokines. However, knocking down the TLRs does not have any effect on seizure frequency, suggesting that they are not functionally involved in epileptogenesis. The reason for this could be that I used siRNA for TLRs knockdown. siRNA has a low knockdown efficiency, and it may be degraded by serum and tissue exonucleases (Lan et al. 2010). The siRNA oligonucleotides are not capable of crossing the blood-brain barrier. However, they can help in achieving enhanced levels of gene silencing, increased in vivo potency, and enhanced plasma stability, with less side effects (Lan et al. 2010).

5. Contribution to the papers and manuscripts

Paper I: A novel animal model of acquired human temporal lobe epilepsy based on the simultaneous administration of kainic acid and lorazepam

Epilepsia, 58(2):222–230, 2017 doi: 10.1111/epi.13579

Friederike Kienzler-Norwood, Lara Costard, **Chinmaya Sadangi**, Philipp Muller, Valentin Neubert, Sebastian Bauer, Felix Rosenow, and Braxton A. Norwood

F.K.N. and B.A.N. designed the experiments, analyzed the data and wrote the first draft of the manuscript. L.C., C.S., P.M., V.N., and S.B. assisted in the EEG analysis. All the authors contributed in editing and proofreading of the manuscript.

Paper II: Validation of Reference Genes for Quantitative Gene Expression Analysis in Experimental Epilepsy

Journal of Neuroscience Research (In press) doi: 10.1002/jnr.24089

Chinmaya Sadangi, Felix Rosenow, and Braxton A. Norwood

C.S. and B.A.N designed the experiments and analyzed the data. All the experiments and data analysis were carried out by C.S. and C.S. wrote the first draft of the manuscript. All the authors contributed in editing and proofreading of the manuscript.

Paper III: Role of endosomal toll-like receptors (TLRs) in experimental epilepsy
In preparation

Chinmaya Sadangi, Stephan Bauer, Felix Rosenow, Philip Yu, and Braxton A. Norwood

C.S. and B.A.N. designed the experiments and analyzed the data. C.S. carried out all the experiment in the rat models. C.S. wrote the first draft of the manuscript. S.B. and P.Y. provided the TLR 379 knockout mice. All the authors contributed in editing and proofreading of the manuscript.

6. References

Aarli, J A. 2000. Epilepsy and the Immune System. *Archives of Neurology* 57 (12): 1689–92.

Akira, Shizuo. 2003. Toll-Like Receptor Signaling. *Journal of Biological Chemistry* 278 (40). 38105–8.

Alexopoulou, L, A C Holt, R Medzhitov, and R A Flavell. 2001. Recognition of Double-Stranded RNA and Activation of NF-kappaB by Toll-Like Receptor 3. *Nature* 413 (6857). 732–38.

Amaral, David, and Pierre Lavenex. 2006. *The Hippocampus Book*. Edited by Per Andersen, Richard Morris, David Amaral, Tim Bliss, and John O Keefe. Oxford University Press.

Arisi, Gabriel M, Maira L Foresti, Khurshed Katki, and Lee A Shapiro. 2015. Increased CCL2, CCL3, CCL5, and IL-1β Cytokine Concentration in Piriform Cortex, Hippocampus, and Neocortex After Pilocarpine-Induced Seizures. *Journal of Neuroinflammation* 12 (1): 129.

Avoli, Massimo. 2007. The Epileptic Hippocampus Revisited: Back to the Future. *Epilepsy Currents* 7 (4). 116–18.

Babcock, Alicia A, Martin Wirenfeldt, Thomas Holm, Helle H Nielsen, Lasse Dissing-Olesen, Henrik Toft-Hansen, Jason M Millward, et al. 2006. Toll-Like Receptor 2 Signaling in Response to Brain Injury: an Innate Bridge to Neuroinflammation. *The Journal of Neuroscience* 26 (49). 12826–37.

Bahn, S, B Volk, and W Wisden. 1994. Kainate Receptor Gene Expression in the Developing Rat Brain. *Journal of Neuroscience* 14 (9): 5525–47.

Bartolomei, Fabrice, Mouhamad Khalil, Fabrice Wendling, Anna Sontheimer, Jean Régis, Jean Phillipe Ranjeva, Maxime Guye, and Patrick Chauvel. 2005. Entorhinal Cortex Involvement in Human Mesial Temporal Lobe Epilepsy: an Electrophysiologic and Volumetric Study. *Epilepsia* 46 (5). 677–87.

Becher, Burkhard, Sabine Spath, and Joan Goverman. 2016. Cytokine Networks in Neuroinflammation. *Nature Reviews Immunology* 17 (1): 49–59.

Ben-Ari, Y, J Lagowska, E Tremblay, and G Le Gal La Salle. 1979. A New Model of Focal Status Epilepticus: Intra-Amygdaloid Application of Kainic Acid Elicits Repetitive Secondarily Generalized Convulsive Seizures. *Brain Research* 163 (1). 176–79.

Ben-Ari, Yehezkel, and Gregory L Holmes. 2006. Effects of Seizures on Developmental Processes in the Immature Brain. *The Lancet. Neurology* 5 (12).

1055–63.

Bernardino, L, R Ferreira, A J Cristóvao, F Sales, and J O Malva. 2005. Inflammation and Neurogenesis in Temporal Lobe Epilepsy. *Current Drug Targets*. 4 (4): 349–60.

Betjemann, John P, and Daniel H Lowenstein. 2015. Status Epilepticus in Adults. *The Lancet. Neurology* 14 (6). 615–24.

Biagini, Giuseppe, Margherita D'Antuono, Ruba Benini, Philip de Guzman, Daniela Longo, and Massimo Avoli. 2013. Perirhinal Cortex and Temporal Lobe Epilepsy. *Frontiers in Cellular Neuroscience* 7 (August). 130.

Bianchi, Marco E. 2007. DAMPs, PAMPs and Alarmins: All We Need to Know About Danger. *Journal of Leukocyte Biology* 81 (1). 1–5.

Bloss, Erik B, and Richard G Hunter. 2010. Hippocampal Kainate Receptors. *Vitamins and Hormones* 82. 167–84.

Bsibsi, Malika, Rivka Ravid, Djordje Gveric, and Johannes M van Noort. 2002. Broad Expression of Toll-Like Receptors in the Human Central Nervous System. *Journal of Neuropathology & Experimental Neurology* 61 (11): 1013–21.

Cameron, Jill S, Lena Alexopoulou, Jacob A Sloane, Allitia B DiBernardo, Yinghua Ma, Bela Kosaras, Richard Flavell, et al. 2007. Toll-Like Receptor 3 Is a Potent Negative Regulator of Axonal Growth in Mammals. *The Journal of Neuroscience*. 13033–41.

Cammer, W. 2000. Effects of TNFalpha on Immature and Mature Oligodendrocytes and Their Progenitors in Vitro. *Brain Research* 864 (2): 213–19.

Choi, Jieun, Douglas R Nordli, Tord D Alden, Arthur DiPatri, Linda Laux, Kent Kelley, Joshua Rosenow, Stephan U Schuele, Veena Rajaram, and Sookyong Koh. 2009. Cellular Injury and Neuroinflammation in Children with Chronic Intractable Epilepsy. *Journal of Neuroinflammation* 6 (1). 38.

De Deyn, P P, R D'Hooge, B Marescau, and Y Q Pei. 1992. Chemical Models of Epilepsy with Some Reference to Their Applicability in the Development of Anticonvulsants. *Epilepsy Research* 12 (2). 87–110.

Do Young Kim, Junwei Hao, Ruolan Liu, Gregory Turner, Fu-Dong Shi, and Jong M Rho. 2012. Inflammation-Mediated Memory Dysfunction and Effects of a Ketogenic Diet in a Murine Model of Multiple Sclerosis. Edited by Pablo Villoslada. *PLoS One* 7 (5). e35476.

Dudek, F Edward, and Li-Rong Shao. 2004. Mossy Fiber Sprouting and Recurrent Excitation: Direct Electrophysiologic Evidence and Potential Implications. *Epilepsy Currents* 4 (5). 184–87.

Faherty, C J, S Xanthoudakis, and R J Smeyne. 1999. Caspase-3-Dependent Neuronal Death in the Hippocampus Following Kainic Acid Treatment. *Brain Research. Molecular Brain Research* 70 (1): 159–63.

Farina, Cinthia, Markus Krumbholz, Thomas Giese, Gunther Hartmann, Francesca Aloisi, and Edgar Meinl. 2005. Preferential Expression and Function of Toll-Like Receptor 3 in Human Astrocytes. *Journal of Neuroimmunology* 159 (1-2). 12–19.

Fisher, Robert S. 1989. Animal Models of the Epilepsies. *Brain Research Reviews* 14 (3): 245–78.

Fisher, Robert S, Carlos Acevedo, Alexis Arzimanoglou, Alicia Bogacz, J Helen Cross, Christian E Elger, Jerome Engel Jr, et al. 2014. ILAE Official Report: a Practical Clinical Definition of Epilepsy. *Epilepsia* 55 (4): 475–82.

Fisher, Robert S, P O Shafer, and C DSouza. 2017. 2017 Revised Classification of Seizures. Accessed March. http://www.epilepsy.com/article/2016/12/2017-revised-classification-seizures.

Fisher, Robert S, Walter van Emde Boas, Warren Blume, Christian Elger, Pierre Genton, Phillip Lee, and Jerome Engel. 2005. Epileptic Seizures and Epilepsy: Definitions Proposed by the International League Against Epilepsy (ILAE) and the International Bureau for Epilepsy (IBE). *Epilepsia* 46 (4). 470–72.

French, J A, P D Williamson, V M Thadani, T M Darcey, R H Mattson, S S Spencer, and D D Spencer. 1993. Characteristics of Medial Temporal Lobe Epilepsy: I. Results of History and Physical Examination. *Annals of Neurology* 34 (6). 774–80.

Freund, T F, and G Buzsáki. 1996. Interneurons of the Hippocampus. *Hippocampus* 6 (4). 347–470.

Furtado, Marcio de A, Glaucia K Braga, José A C Oliveira, Flavio Del Vecchio, and Norberto Garcia-Cairasco. 2002. Behavioral, Morphologic, and Electroencephalographic Evaluation of Seizures Induced by Intrahippocampal Microinjection of Pilocarpine. 37–39.

Giblin, Kathryn A, and Hal Blumenfeld. 2010. Is Epilepsy a Preventable Disorder? New Evidence From Animal Models. *Neuroscientist* 16 (3). 253–75.

Goddard, G V, D C McIntyre, and C K Leech. 1969. A Permanent Change in Brain Function Resulting From Daily Electrical Stimulation. *Experimental Neurology* 25 (3): 295–330.

Goldberg, Ethan M, and Douglas A Coulter. 2013. Mechanisms of Epileptogenesis: a Convergence on Neural Circuit Dysfunction. *Nature Reviews Neuroscience* 14 (5). 337–49.

Gordon, E, and O Devinsky. 2001. Alcohol and Marijuana: Effects on Epilepsy and Use by Patients with Epilepsy. *Epilepsia* 42 (10): 1266–72.

Gross, Adi, Felix Benninger, Ravit Madar, Tomer Illouz, Kathleen Griffioen, Israel Steiner, Daniel Offen, and Eitan Okun. 2017. Toll-Like Receptor 3 Deficiency Decreases Epileptogenesis in a Pilocarpine Model of SE-Induced Epilepsy in Mice. *Epilepsia* 7 (Suppl 2): 31.

Hauser, W A, J F Annegers, and L T Kurland. 1991. Prevalence of Epilepsy in Rochester, Minnesota: 1940-1980. *Epilepsia* 32 (4): 429–45.

Haut, Sheryl R, Charles B Hall, Jonathan Masur, and Richard B Lipton. 2007. Seizure Occurrence: Precipitants and Prediction. *Neurology* 69 (20): 1905–10.

Hedtjärn, Maj, Anna-Lena Leverin, Kristina Eriksson, Klas Blomgren, Carina Mallard, and Henrik Hagberg. 2002. Interleukin-18 Involvement in Hypoxic-Ischemic Brain Injury. *The Journal of Neuroscience.*22 (14): 5910–19.

Heida, James G, Solomon L Moshé, and Quentin J Pittman. 2009. The Role of Interleukin-1β in Febrile Seizures. *Brain and Development* 31 (5). 388–93.

Hellier, Jennifer L, Peter R Patrylo, Paul S Buckmaster, and F Edward Dudek. 1998. Recurrent Spontaneous Motor Seizures After Repeated Low-Dose Systemic Treatment with Kainate: Assessment of a Rat Model of Temporal Lobe Epilepsy. *Epilepsy Research* 31 (1): 73–84.

Henshall, David C, Hajo M Hamer, R Jeroen Pasterkamp, David B Goldstein, Jørgen Kjems, Jochen H M Prehn, Stephanie Schorge, Kai Lamottke, and Felix Rosenow. 2016. MicroRNAs in Epilepsy: Pathophysiology and Clinical Utility. *The Lancet. Neurology* 15 (13): 1368–76.

Heyen, Jonathan R R, Shi-ming Ye, Brian N Finck, and Rodney W Johnson. 2000. Interleukin (IL)-10 Inhibits IL-6 Production in Microglia by Preventing Activation of NF-κB. *Molecular Brain Research* 77 (1): 138–47.

Holmes, Gregory L, and Yehezkiel Ben-Ari. 2001. The Neurobiology and Consequences of Epilepsy in the Developing Brain. *Pediatric Research* 49 (3). 320–25.

Hopkins, P A, and S Sriskandan. 2005. Mammalian Toll-Like Receptors: to Immunity and Beyond. *Clinical and Experimental Immunology* 140 (3). 395–407.

Hyakkoku, K, J Hamanaka, K Tsuruma, M Shimazawa, H Tanaka, S Uematsu, S

Akira, N Inagaki, H Nagai, and H Hara. 2010. Toll-Like Receptor 4 (TLR4), but Not TLR3 or TLR9, Knock-Out Mice Have Neuroprotective Effects Against Focal Cerebral Ischemia. *Neuroscience* 171 (1): 258–67.

Iliev, Asparouh I, Argyrios K Stringaris, Roland Nau, and Harald Neumann. 2004. Neuronal Injury Mediated via Stimulation of Microglial Toll-Like Receptor-9 (TLR9). *FASEB Journal* 18 (2): 412–14.

Jack, Carolyn S, Nathalie Arbour, Joshua Manusow, Vivianne Montgrain, Manon Blain, Ellie McCrea, Aaron Shapiro, and Jack P Antel. 2005. TLR Signaling Tailors Innate Immune Responses in Human Microglia and Astrocytes. *The Journal of Immunology* 175 (7): 4320–30.

Jackson, Alan C, John P Rossiter, and Monique Lafon. 2006. Expression of Toll-Like Receptor 3 in the Human Cerebellar Cortex in Rabies, Herpes Simplex Encephalitis, and Other Neurological Diseases. *Journal of Neurovirology* 12 (3). 229–34.

Jankowsky, J L, and P H Patterson. 2001. The Role of Cytokines and Growth Factors in Seizures and their Sequelae. *Progress in Neurobiology* 63 (2): 125–49.

Kabat, Joanna, and Przemysław Król. 2012. Focal Cortical Dysplasia - Review. *Polish Journal of Radiology* 77 (2): 35–43.

Kandratavicius, Ludmyla, Priscila Alves Balista, Cleiton Lopes-Aguiar, Rafael Naime Ruggiero, Eduardo Henrique Umeoka, Norberto Garcia-Cairasco, Lezio Soares Bueno-Junior, and Joao Pereira Leite. 2014. Animal Models of Epilepsy: Use and Limitations. *Neuropsychiatric Disease and Treatment* 10. Dove Press: 1693–1705.

Kaul, David, Piet Habbel, Katja Derkow, Christina Krüger, Eleonora Franzoni, F Gregory Wulczyn, Stefan Bereswill, et al. 2012. Expression of Toll-Like Receptors in the Developing Brain. Edited by Lena Alexopoulou. *PLoS One* 7 (5). e37767.

Kawasaki, Takumi, and Taro Kawai. 2014. Toll-Like Receptor Signaling Pathways. *Frontiers in Immunology* 5 (September). 197.

Kharatishvili, I, J P Nissinen, T K McIntosh, and A Pitkänen. 2006. A Model of Posttraumatic Epilepsy Induced by Lateral Fluid-Percussion Brain Injury in Rats. *Neuroscience* 140 (2): 685–97.

Kienzler-Norwood, Friederike, Lara Costard, Chinmaya Sadangi, Philipp Müller, Valentin Neubert, Sebastian Bauer, Felix Rosenow, and Braxton A Norwood. 2017. A Novel Animal Model of Acquired Human Temporal Lobe Epilepsy Based on the Simultaneous Administration of Kainic Acid and Lorazepam. *Epilepsia* 58 (2): 222–30.

Knake, Susanne, Hajo M Hamer, and Felix Rosenow. 2009. Status Epilepticus: a Critical Review. *Epilepsy & Behavior : E&B* 15 (1): 10–14.

Koutsogiannopoulos, Sheila, Francine Adelson, Virginia Lee, and Frederick Andermann. 2009. Stressors at the Onset of Adult Epilepsy: Implications for Practice. *Epileptic Disorders :* 11 (1): 42–47.

Kulkarni, S K, and Ashish Dhir. 2009. Cyclooxygenase in Epilepsy: From Perception to Application. *Drugs of Today (Barcelona, Spain : 1998)* 45 (2): 135–54.

Kwan, P, and J W Sander. 2004. The Natural History of Epilepsy: an Epidemiological View. *Journal of Neurology, Neurosurgery & Psychiatry* 75 (10): 1376–81.

Kwan, P, and M J Brodie. 2000. Epilepsy After the First Drug Fails: Substitution or Add-on? *Seizure: European Journal of Epilepsy* 9 (7). 464–68.

Lan, L.S., Yang, J.P., Wang, L.N., Jiang M., Qiu, Q.C., Ma Z.N., Liu L., Li C.F., Ren C.G., Zhou J., and Li, W. Downregulation of Toll-like receptor 4 gene expression by short interfering RNA attenuates bone cancer pain in a rat model. Molecular Pain, 2010, 6:2. 10.1186/1744-8069-6-2

Lathia, Justin D, Eitan Okun, Sung-Chun Tang, Kathleen Griffioen, Aiwu Cheng, Mohamed R Mughal, Gloria Laryea, et al. 2008. Toll-Like Receptor 3 Is a Negative Regulator of Embryonic Neural Progenitor Cell Proliferation. *The Journal of Neuroscience.* 28 (51). 13978–84.

Latz, E, A Visintin, T Espevik, and D T Golenbock. 2004. Mechanisms of TLR9 Activation. *Journal of Endotoxin Research* 10 (6). 406–12.

Ledeboer, A, J J Brevé, S Poole, F J Tilders, and A M Van Dam. 2000. Interleukin-10, Interleukin-4, and Transforming Growth Factor-Beta Differentially Regulate Lipopolysaccharide-Induced Production of Pro-Inflammatory Cytokines and Nitric Oxide in Co-Cultures of Rat Astroglial and Microglial Cells. *Glia* 30 (2): 134–42.

Lehnardt, Seija. 2010. Innate Immunity and Neuroinflammation in the CNS: the Role of Microglia in Toll-Like Receptor-Mediated Neuronal Injury. *Glia* 58 (3). 253–63.

Lerma, J, A V Paternain, J R Naranjo, and B Mellström. 1993. Functional Kainate-Selective Glutamate Receptors in Cultured Hippocampal Neurons. *Proceedings of the National Academy of Sciences* 90 (24). 11688–92.

Levin, S G, and O V Godukhin. 2007. Protective Effects of Interleukin-10 on the Development of Epileptiform Activity Evoked by Transient Episodes of Hypoxia in Rat Hippocampal Slices. *Neuroscience and Behavioral Physiology* 37 (5). 467–70.

Lévesque, Maxime, and Massimo Avoli. 2013. The Kainic Acid Model of Temporal Lobe Epilepsy. *Neuroscience & Biobehavioral Reviews* 37 (10): 2887–99.

Lévesque, Maxime, Massimo Avoli, and Christophe Bernard. 2015. Animal Models of Temporal Lobe Epilepsy Following Systemic Chemoconvulsant Administration. *Journal of Neuroscience Methods*.

Li, Gang, Sebastian Bauer, Mareike Nowak, Braxton Norwood, Bjoern Tackenberg, Felix Rosenow, Susanne Knake, Wolfgang H Oertel, and Hajo M Hamer. 2011. Cytokines and Epilepsy. *Seizure:* 20 (3): 249–56.

Liu, T, R K Clark, P C McDonnell, P R Young, R F White, F C Barone, and G Z Feuerstein. 1994. Tumor Necrosis Factor-Alpha Expression in Ischemic Neurons. *Stroke* 25 (7): 1481–88.

Liu, W, R Liu, J T Chun, R Bi, W Hoe, S S Schreiber, and M Baudry. 2001. Kainate Excitotoxicity in Organotypic Hippocampal Slice Cultures: Evidence for Multiple Apoptotic Pathways. *Brain Research* 916 (1-2): 239–48.

Löscher, Wolfgang. 2005. How to Explain Multidrug Resistance in Epilepsy? *Epilepsy Currents* 5 (3). 107–12.

Ma, Yinghua, Jianxue Li, Isaac Chiu, Yawen Wang, Jacob A Sloane, Jining Lü, Bela Kosaras, Richard L Sidman, Joseph J Volpe, and Timothy Vartanian. 2006. Toll-Like Receptor 8 Functions as a Negative Regulator of Neurite Outgrowth and Inducer of Neuronal Apoptosis. *Journal of Cell Biology* 175 (2): 209–15.

Mallard, Carina, Xiaoyang Wang, and Henrik Hagberg. 2009. The Role of Toll-Like Receptors in Perinatal Brain Injury. *Clinics in Perinatology* 36 (4): 763–72–v–vi.

Manford, Mark. 2017. Recent Advances in Epilepsy. *Journal of Neurology*, January. Springer. 1–14.

Maroso, Mattia, Silvia Balosso, Teresa Ravizza, Jaron Liu, Eleonora Aronica, Anand M Iyer, Carlo Rossetti, et al. 2010. Toll-Like Receptor 4 and High-Mobility Group Box-1 Are Involved in Ictogenesis and Can Be Targeted to Reduce Seizures. *Nature Medicine* 16 (4). 413–19.

Martín, Ed, and Ma Pozo. 2006. Animal Models for the Development of New Neuropharmacological Therapeutics in the Status Epilepticus. *Current Neuropharmacology* 4 (1). 33–40.

Mathern, Gary W, P David Adelson, Leslie D Cahan, and Joao P Leite. 2002. Hippocampal Neuron Damage in Human Epilepsy: Meyer's Hypothesis Revisited. In *Do Seizures Damage the Brain*, 135:237–51. Progress in Brain Research.

Mathern, Gary W, Thomas L Babb, Barbara G Vickrey, Maria Melendez, and JAMES K PRETORIUS. 1995. The Clinical-Pathogenic Mechanisms of Hippocampal Neuron Loss and Surgical Outcomes in Temporal Lobe Epilepsy. *Brain:* 118 (1): 105–18.

Matin, Nassim, Omidreza Tabatabaie, Raffaele Falsaperla, Riccardo Lubrano, Piero Pavone, Fahad Mahmood, Melissa Gullotta, et al. 2015. Epilepsy and Innate Immune System: a Possible Immunogenic Predisposition and Related Therapeutic Implications. *Human Vaccines & Immunotherapeutics* 11 (8). 2021–29.

Matsuda, Taito, Naoya Murao, Yuki Katano, Berry Juliandi, Jun Kohyama, Shizuo Akira, Taro Kawai, and Kinichi Nakashima. 2015. TLR9 Signalling in Microglia Attenuates Seizure-Induced Aberrant Neurogenesis in the Adult Hippocampus 6 (March). Nature Communication: 6514.

Matsumoto, Misako, Kenji Funami, Masako Tanabe, Hiroyuki Oshiumi, Masashi Shingai, Yoshiyuki Seto, Akitsugu Yamamoto, and Tsukasa Seya. 2003. Subcellular Localization of Toll-Like Receptor 3 in Human Dendritic Cells. *The Journal of Immunology* 171 (6): 3154–62.

Medzhitov, Ruslan. 2008. Origin and Physiological Roles of Inflammation. *Nature* 454 (7203): 428–35.

Mennicken, Françoise, Jean Guy Chabot, and Rémi Quirion. 2002. Systemic Administration of Kainic Acid in Adult Rat Stimulates Expression of the Chemokine Receptor CCR5 in the Forebrain. *Glia* 37 (2): 124–38.

Ménager, Pauline, Pascal Roux, Françoise Mégret, Jean-Pierre Bourgeois, Anne-Marie Le Sourd, Anne Danckaert, Mireille Lafage, Christophe Préhaud, and Monique Lafon. 2009. Toll-Like Receptor 3 (TLR3) Plays a Major Role in the Formation of Rabies Virus Negri Bodies. *PLoS Pathogens* 5 (2): e1000315.

Minami, Masabumi, and Masamichi Satoh. 2003. Chemokines and Their Receptors in the Brain: Pathophysiological Roles in Ischemic Brain Injury. *Life Sciences* 74 (2-3): 321–27.

Mishra, Bibhuti B, Pramod K Mishra, and Judy M Teale. 2006. Expression and Distribution of Toll-Like Receptors in the Brain During Murine Neurocysticercosis. *Journal of Neuroimmunology* 181 (1-2). 46–56.

Murakami, S, T Takemoto, and S Shimizu. 1953. Studies on the Effective Principles of *Diagenea Simplex* Aq. I Separation of the Effective Fraction by Liquid Chromatography. *Yakugaku Zasshi* 73 (9). 1026–28.

Nadler, J V, B W Perry, and C W Cotman. 1978. Intraventricular Kainic Acid Preferentially Destroys Hippocampal Pyramidal Cells. *Nature* 271 (5646): 676–77.

Nakajima, Hidemitsu, Takeya Kubo, Yuko Semi, Masanori Itakura, Mitsuru Kuwamura, Takeshi Izawa, Yasu-Taka Azuma, and Tadayoshi Takeuchi. 2012. A Rapid, Targeted, Neuron-Selective, in Vivo Knockdown Following a Single Intracerebroventricular Injection of a Novel Chemically Modified siRNA in the Adult Rat Brain. *Journal of Biotechnology* 157 (2): 326–33.

Nehlig, A, and A Pereira de Vasconcelos. 1996. The Model of Pentylenetetrazol-Induced Status Epilepticus in the Immature Rat: Short- and Long-Term Effects. *Epilepsy Research* 26 (1): 93–103.

Ngugi, Anthony K, S M Kariuki, C Bottomley, I Kleinschmidt, J W Sander, and C R Newton. 2011. Incidence of Epilepsy: a Systematic Review and Meta-Analysis. *Neurology* 77 (10): 1005–12.

Nissinen, J, T Halonen, E Koivisto, and A Pitkänen. 2000. A New Model of Chronic Temporal Lobe Epilepsy Induced by Electrical Stimulation of the Amygdala in Rat. *Epilepsy Research* 38 (2-3): 177–205.

Norwood, Braxton A, Argyle V Bumanglag, Francesco Osculati, Andrea Sbarbati, Pasquina Marzola, Elena Nicolato, Paolo F Fabene, and Robert S Sloviter. 2010. Classic Hippocampal Sclerosis and Hippocampal-Onset Epilepsy Produced by a Single 'Cryptic' Episode of Focal Hippocampal Excitation in Awake Rats. *The Journal of Comparative Neurology* 518 (16). 3381–3407.

Norwood, Braxton A, Sebastian Bauer, Sven Wegner, Hajo M Hamer, Wolfgang H Oertel, Robert S Sloviter, and Felix Rosenow. 2011. Electrical Stimulation-Induced Seizures in Rats: a 'Dose-Response' Study on Resultant Neurodegeneration. *Epilepsia* 52 (9). e109–12.

Ohtaki, Hirokazu, Li Yin, Tomoya Nakamachi, Kenji Dohi, Yoshifumi Kudo, Reiko Makino, and Seiji Shioda. 2004. Expression of Tumor Necrosis Factor Alpha in Nerve Fibers and Oligodendrocytes After Transient Focal Ischemia in Mice. *Neuroscience Letters* 368 (2): 162–66.

Okun, Eitan, Kathleen Griffioen, Boaz Barak, Nicholas J Roberts, Kamilah Castro, Mario A Pita, Aiwu Cheng, et al. 2010. Toll-Like Receptor 3 Inhibits Memory Retention and Constrains Adult Hippocampal Neurogenesis. *Proceedings of the National Academy of Sciences*. 107 (35). 15625–30.

Okun, Eitan, Kathleen J Griffioen, and Mark P Mattson. 2011. Toll-Like Receptor Signaling in Neural Plasticity and Disease. *Trends in Neurosciences* 34 (5): 269–81.

Olesen, J, A Gustavsson, M Svensson, H U Wittchen, B Jönsson, on behalf of the CDBE2010 study group, the European Brain Council. 2011. The Economic Cost of Brain Disorders in Europe. *European Journal of Neurology* 19 (1). 155–62.

O'Neill, Luke A J, Douglas Golenbock, and Andrew G Bowie. 2013. The History of Toll-Like Receptors - Redefining Innate Immunity. *Nature Reviews Immunology* 13 (6). Nature Research: 453–60.

Palace, J. 2000. Epilepsy: an Autoimmune Disease? *Journal of Neurology, Neurosurgery & Psychiatry* 69 (6): 711–14.

Pitkaenen, Asla, and Katarzyna Lukasiuk. 2009. Molecular and Cellular Basis of Epileptogenesis in Symptomatic Epilepsy. *Epilepsy & Behavior* 14 (1): 16–25.

Pitkänen, A, A P Schwartzkroin, and Solomon L Moshé, eds. 2006 *Models of Seizure and Epilepsy*. Elsevier.

Préhaud, Christophe, Françoise Mégret, Mireille Lafage, and Monique Lafon. 2005. Virus Infection Switches TLR-3-Positive Human Neurons to Become Strong Producers of Beta Interferon. *Journal of Virology* 79 (20): 12893–904.

Rakhade, Sanjay N, and Frances E Jensen. 2009. Epileptogenesis in the Immature Brain: Emerging Mechanisms. *Nature Reviews. Neurology* 5 (7): 380–91.

Rasmussen, T, J Olszewski, and D Lloydsmith. 1958. Focal Seizures Due to Chronic Localized Encephalitis. *Neurology* 8 (6): 435–45.

Ravizza, Teresa, Massimo Rizzi, Carlo Perego, Cristina Richichi, Jana Velísková, Solomon L Moshé, M Grazia De Simoni, and Annamaria Vezzani. 2005. Inflammatory Response and Glia Activation in Developing Rat Hippocampus After Status Epilepticus. *Epilepsia* 46 Suppl 5 (s5). 113–17.

Reddy, Doodipala Samba, and Ramkumar Kuruba. 2013. Experimental Models of Status Epilepticus and Neuronal Injury for Evaluation of Therapeutic Interventions. *International Journal of Molecular Sciences* 14 (9). 18284–318.

Rivest, Serge. 2009. Regulation of Innate Immune Responses in the Brain. *Nature Reviews Immunology* 9 (6): 429–39.

Rolls, Asya, Ravid Shechter, Anat London, Yaniv Ziv, Ayal Ronen, Rinat Levy, and Michal Schwartz. 2007. Toll-Like Receptors Modulate Adult Hippocampal Neurogenesis. *Nature Cell Biology* 9 (9): 1081–88.

Rolston, John D, Sharanya Arcot Desai, Nealen G Laxpati, and Robert E Gross. 2011. Electrical Stimulation for Epilepsy: Experimental Approaches. *Neurosurgery Clinics of North America* 22 (4): 425–42–v.

Rose, D, X Zhu, H Kose, B Hoang, J Cho, and A Chiba. 1997. Toll, a Muscle Cell Surface Molecule, Locally Inhibits Synaptic Initiation of the RP3 Motoneuron Growth Cone in Drosophila. *Development* 124 (8): 1561–71.

Sadangi, C., Rosenow F., and Norwood BA. 2017. Validation of Reference Genes for Quantitative Gene Expression Analysis in Experimental Epilepsy. *Journal of Neuroscience Research*. 10:1002/jnr.24089

Saito, Kuniaki, Kazuhiko Suyama, Keiji Nishida, Yoshitatsu Sei, and Anthony S Basile. 1996. Early Increases in TNF-A, IL-6 and IL-1β Levels Following Transient Cerebral Ischemia in Gerbil Brain. *Neuroscience Letters* 206 (2-3): 149–52.

Schachter, S C, P O Shafer, and J I Sirven. 2017. What Causes Epilepsy and Seizures? Accessed March. http://www.epilepsy.com/learn/epilepsy-101/what-causes-epilepsy-and-seizures.

Scheffer, Ingrid E, Jacqueline French, Edouard Hirsch, Satish Jain, Gary W Mathern, Solomon L Moshé, Emilio Perucca, et al. 2016. Classification of the Epilepsies: New Concepts for Discussion and Debate-Special Report of the ILAE Classification Task Force of the Commission for Classification and Terminology. *Epilepsia Open* 1 (1-2): 37–44.

Scheffer, Ingrid E, Samuel Berkovic, Giuseppe Capovilla, Mary B Connolly, Jacqueline French, Laura Guilhoto, Edouard Hirsch, et al. 2017. ILAE Classification of the Epilepsies: Position Paper of the ILAE Commission for Classification and Terminology. *Epilepsia* 58 (4): 512–21.

Schmidt, Dieter, and Wolfgang Löscher. 2005. Drug Resistance in Epilepsy: Putative Neurobiologic and Clinical Mechanisms. *Epilepsia* 46 (6). 858–77.

Schomer, Donald L. 2005. Focal Status Epilepticus. 143–57. Totowa, NJ: Humana Press.

Scorza, Fulvio A, Ricardo M Arida, Maria da Graça Naffah-Mazzacoratti, Débora A Scerni, Lineu Calderazzo, and Esper A Cavalheiro. 2009. The Pilocarpine Model of Epilepsy: What Have We Learned? 81 (3). Academia Brasileira de Ciências: 345–65.

Selmaj, K, C S Raine, M Farooq, W T Norton, and C F Brosnan. 1991. Cytokine Cytotoxicity Against Oligodendrocytes. Apoptosis Induced by Lymphotoxin. *The Journal of Immunology* 147 (5): 1522–29.

Shandra, A A, L S Godlevsky, R S Vastyanov, A A Oleinik, V L Konovalenko, E N Rapoport, and N N Korobka. 2002. The Role of TNF-Alpha in Amygdala Kindled Rats. *Neuroscience Research* 42 (2): 147–53.

Shorvon, Simon, and Anna Lisa Luciano. 2007. Prognosis of Chronic and Newly Diagnosed Epilepsy: Revisiting Temporal Aspects. *Current Opinion in Neurology* 20 (2): 208–12.

Sillanpää, Matti, Merja Jalava, Olli Kaleva, and Shlomo Shinnar. 1998. Long-Term Prognosis of Seizures with Onset in Childhood. *The New England Journal of*

Medicine 338 (24). 1715–22.

Sloviter, R S. 1983. 'Epileptic' Brain Damage in Rats Induced by Sustained Electrical Stimulation of the Perforant Path. I. Acute Electrophysiological and Light Microscopic Studies. *Brain Research Bulletin* 10 (5): 675–97.

Sloviter, Robert S, and Argyle V Bumanglag. 2013. Defining "Epileptogenesis" and Identifying 'Antiepileptogenic Targets' in Animal Models of Acquired Temporal Lobe Epilepsy Is Not as Simple as It Might Seem. *Neuropharmacology* 69 (June): 3–15.

Sperk, G. 1994. Kainic Acid Seizures in the Rat. *Progress in Neurobiology* 42 (1): 1–32.

Sperk, G., Lassmann, H., Baran H., Kish S.J., Seitelberger F., and Hornykiewicz O. 1983. Kainic Acid Induced Seizures: Neurochemical and Histopathological Changes. *Neuroscience* 10 (4): 1301–15.

Stein, D, S Roth, E Vogelsang, and C Nüsslein-Volhard. 1991. The Polarity of the Dorsoventral Axis in the Drosophila Embryo Is Defined by an Extracellular Signal. *Cell* 65 (5): 725–35.

Szelényi, Judith. 2001. Cytokines and the Central Nervous System. *Brain Research Bulletin* 54 (4): 329–38.

Sørensen, Louise N, Line S Reinert, Lene Malmgaard, Christina Bartholdy, Allan R Thomsen, and Søren R Paludan. 2008. TLR2 and TLR9 Synergistically Control Herpes Simplex Virus Infection in the Brain. *Journal of Immunology*. 181 (12): 8604–12.

Tanaka, Tatsuya, Shigeya Tanaka, Tsutomu Fujita, Katsunobu Takano, Hiroshi Fukuda, Kazuhiro Sako, and Yukichi Yonemasu. 1992. Experimental Complex Partial Seizures Induced by a Microinjection of Kainic Acid Into Limbic Structures. *Progress in Neurobiology* 38 (3): 317–34.

Tatum, William O. 2012. Mesial Temporal Lobe Epilepsy. *Journal of Clinical Neurophysiology*. 29 (5): 356–65.

Turrin, N P, and S Rivest. 2004. Innate Immune Reaction in Response to Seizures: Implications for the Neuropathology Associated with Epilepsy. *Neurobiology of Disease* 16 (2): 321–34.

Van de Vel, Anouk, Kris Cuppens, Bert Bonroy, Milica Milosevic, Katrien Jansen, Sabine Van Huffel, Bart Vanrumste, Lieven Lagae, and Berten Ceulemans. 2013. Non-EEG Seizure-Detection Systems and Potential SUDEP Prevention: State of the Art. *Seizure* 22 (5): 345–55.

Van Roost, D, L Solymosi, J Schramm, B van Oosterwyck, and C E Elger. 1998.

Depth Electrode Implantation in the Length Axis of the Hippocampus for the Presurgical Evaluation of Medial Temporal Lobe Epilepsy: a Computed Tomography-Based Stereotactic Insertion Technique and Its Accuracy. *Neurosurgery* 43 (4): 819–26–discussion826–7.

Vezzani, Annamaria, and Stephan Rüegg. 2011. The Pivotal Role of Immunity and Inflammatory Processes in Epilepsy Is Increasingly Recognized: Introduction. *Epilepsia* 52 Suppl 3 (s3). 1–4.

Vezzani, Annamaria, Daniela Moneta, Cristina Richichi, Marisa Aliprandi, Stephanie J Burrows, Teresa Ravizza, Carlo Perego, and M Grazia De Simoni. 2002. Functional Role of Inflammatory Cytokines and Antiinflammatory Molecules in Seizures and Epileptogenesis. *Epilepsia* 43 Suppl 5: 30–35.

Vezzani, Annamaria, Jacqueline French, Tamas Bartfai, and Tallie Z Baram. 2011. The Role of Inflammation in Epilepsy. *Nature Reviews. Neurology* 7 (1): 31–40.

Vezzani, Annamaria, Silvia Balosso, and Teresa Ravizza. 2008. The Role of Cytokines in the Pathophysiology of Epilepsy. *Brain, Behavior, and Immunity* 22 (6): 797–803.

Vicedomini, J P, and J V Nadler. 1987. A Model of Status Epilepticus Based on Electrical Stimulation of Hippocampal Afferent Pathways. *Experimental Neurology* 96 (3): 681–91.

Visser, Lizette, Marie-José Melief, Debby van Riel, Marjan van Meurs, Ella A Sick, Seiichi Inamura, Jeffrey J Bajramovic, et al. 2006. Phagocytes Containing a Disease-Promoting Toll-Like Receptor/Nod Ligand Are Present in the Brain During Demyelinating Disease in Primates. *The American Journal of Pathology* 169 (5). 1671–85.

Walker, Matthew C. 2016. Pathophysiology of Status Epilepticus. *Neuroscience Letters*, December.

Wijnen, Ben F M, Ghislaine A P G van Mastrigt, Silvia M A A Evers, Olga Gershuni, Danielle A J E Lambrechts, Marian H J M Majoie, Debby Postulart, Bert A P Aldenkamp, and Reina J A de Kinderen. 2017. A Systematic Review of Economic Evaluations of Treatments for Patients with Epilepsy. *Epilepsia*, 2017 May;58(5):706-726.

Yuhas, Yael, Yehuda Nofech-Mozes, Abraham Weizman, and Shai Ashkenazi. 2002. Enhancement of Pentylenetetrazole-Induced Seizures by Shigella Dysenteriae in LPS-Resistant C3H/HeJ Mice: Role of the Host Response. *Medical Microbiology and Immunology* 190 (4): 173–78.

Zhai, Q H, N Futrell, and F J Chen. 1997. Gene Expression of IL-10 in Relationship to TNF-Alpha, IL-1beta and IL-2 in the Rat Brain Following Middle Cerebral Artery

Occlusion. *Journal of the Neurological Sciences* 152 (2): 119–24.

Zhang, Jun-Ming, and Jianxiong An. 2007. Cytokines, Inflammation, and Pain. *International Anesthesiology Clinics* 45 (2): 27–37.

Zhu, Jiankun, and Chandra Mohan. 2010. Toll-Like Receptor Signaling Pathways--Therapeutic Opportunities. *Mediators of Inflammation* 2010 (8). 781235–37.

7. REPRINTS OF ORIGNIAL PUBLICATION

7.1 A novel model of acquired human temporal lobe epilepsy based on simultaneous administration of kainic acid and lorazepam

Epilepsia, 58(2):222–230, 2017 doi: 10.1111/epi.13579

Friederike Kienzler-Norwood, Lara Costard, **Chinmaya Sadangi**, Philipp Muller, Valentin Neubert, Sebastian Bauer, Felix Rosenow, and Braxton A. Norwood

FULL-LENGTH ORIGINAL RESEARCH

A novel animal model of acquired human temporal lobe epilepsy based on the simultaneous administration of kainic acid and lorazepam

*†‡Friederike Kienzler-Norwood, *Lara Costard, *Chinmaya Sadangi, *Philipp Müller, *Valentin Neubert, *†Sebastian Bauer, *†Felix Rosenow, and *†‡Braxton A. Norwood

Epilepsia, 58(2):222–230, 2017
doi: 10.1111/epi.13579

Friederike Kienzler-Norwood is a physician-scientist with interests in clinical and basic science epilepsy research.

Summary

Objective: **Kainic acid (KA) is a potent glutamate analog that is used to induce neurodegeneration and model temporal lobe epilepsy (TLE) in rodents. KA reliably induces severe, prolonged seizures, that is, convulsive status epilepticus (cSE), which is typically fatal without pharmacologic intervention. Although the use of KA to model human epilepsy has proven unquestionably valuable for >30 years, significant variability and mortality continue to confound results. These issues are probably the consequence of cSE, an all-or-nothing response that is inherently capricious and uncontrollable. The relevance of cSE to the human condition is dubious, however, as most patients with epilepsy never experienced it. We sought to develop a simple, KA-based animal model of TLE that avoids cSE and its confounds.**

Methods: **Adult, male Sprague-Dawley rats received coincident subcutaneous injections of KA (5 mg) and lorazepam (0.25 mg), approximately 15.0 and 0.75 mg/kg, respectively. Continuous video–electroencephalography (EEG) was used to monitor acute seizure activity and detect spontaneous seizures. Immunocytochemistry, Fluoro-Jade B staining, and Timm staining were used to characterize both acute and chronic neuropathology.**

Results: **Acutely, focal hippocampal seizures were induced, which began after about 30 min and were self-terminating after a few hours. Widespread hippocampal neurodegeneration was detected after 4 days. Spontaneous, focal hippocampal seizures began after an average of 12 days in all animals. Classic hippocampal sclerosis and mossy fiber sprouting characterized the long-term neuropathology. Morbidity and mortality rates were both 0%.**

Significance: **We show here that the effects of systemic KA can be limited to the hippocampus simply with coadministration of a benzodiazepine at a low dose. This means that lorazepam can block convulsive seizures without truly stopping seizure activity. This novel, cSE-free animal model reliably mimics the defining characteristics of acquired mesial TLE: hippocampal sclerosis and spontaneous hippocampal-onset seizures after a prolonged seizure-free period, without significant morbidity, mortality, or nonresponders.**

KEY WORDS: **Nonconvulsive status epilepticus, Benzodiazepine, Hippocampal sclerosis.**

Accepted September 7, 2016.

*Department of Neurology, Epilepsy Center-Marburg, Philipps University, Marburg, Germany; †Department of Neurology, Epilepsy Center-Frankfurt Rhein-Main, Goethe University, Frankfurt am Main, Germany; and ‡Expesicor LLC, Kalispell, Montana, U.S.A.

Address correspondence to Braxton A. Norwood, Karl-von-Frisch-Str. 1, Marburg 35043, Germany. E-mail: braxton.norwood@gmail.com

Key Points

- Simultaneous administration of kainic acid and lorazepam reliably models TLE with hippocampal sclerosis in rats
- Spontaneous, hippocampal seizures arise in this model after 10–15 days
- Lorazepam can block cSE without stopping electrographic seizures

Epilepsy is a chronic neurologic condition that is characterized by recurrent, unprovoked seizures.[1] It is the most common neurologic disorder, affecting approximately 1% of the world population (approximately 65 million), with ~2.4 million new diagnoses annually.[2–4] Temporal lobe epilepsy (TLE), where seizures originate in the temporal lobe, is the most common epilepsy syndrome, is often refractory to treatment, and is thought to be caused by a brain insult.[3] TLE is characterized by pronounced hippocampal atrophy and limited extrahippocampal damage,[3,5] as well as seizures that originate in the hippocampus and/or closely related structures.[6]

Kainic acid (KA) is a glutamate analog that is used to induce acute seizures and neurodegeneration, and to model human TLE in animals, most commonly rodents.[7] KA was first isolated from red algae (*Digenea simplex*) found in tropical and subtropical waters.[8] It evokes seizures through activation of kainate receptors, a type of ionotropic glutamate receptor, and also through activation of AMPA receptors, for which it is a partial agonist.[9] The original KA model of epilepsy was developed by Ben-Ari and colleagues.[10,11] In these initial studies, intraamygdaloid injections of KA were found to induce behavioral seizures and neurodegeneration in the dorsal hippocampus, primarily in the CA3 region. Since then, several KA-based models of epilepsy have been developed (Table 1). The crux of these models is the induction of a period of severe, prolonged seizures, that is, convulsive status epilepticus (cSE), which is typically fatal without pharmacologic intervention.[12] Various protocols have been developed with the goal of reducing variability and mortality without preventing cSE and later epilepsy, such as repeated low doses, which have been somewhat successful[13] (Table 1).

Despite the value of KA-based epilepsy models, which have unequivocally contributed greatly to our understanding of epilepsy, substantial drawbacks persist: high mortality (up to 50%), variable neuropathology, erratic latency to spontaneous epilepsy (first seizures can occur weeks apart in age-matched animals that received identical treatment), and nonresponders (up to 50% of surviving animals never exhibit spontaneous seizures).[7,12] Rather than attempt to incrementally increase either the reliability or survivability of cSE, we approached the problem from a different angle. Our aim was to develop a simple, robust animal model of acquired TLE, based on KA, which closely and reliably mimics the human condition, while avoiding cSE and its complications. Herein we introduce a novel method, which comprises a single dose of KA administered concurrently with a single low-dose of lorazepam—a benzodiazepine that is a first-line treatment for cSE[14]—to adult Sprague-Dawley rats.

Methods

Animals

Male Sprague-Dawley rats (Harlan-Winkelmann, Borchen, Germany), weighing approximately 330 g (range 318–344 g), were treated in accordance with the guidelines of the European community (EUVD 86/609/EEC). All experiments were approved by the local regulation authority (Regierungspräsidium Gießen). Rats were housed in an on-site animal facility (21–25°C; 31–47% humidity) under a 12:12 light/dark cycle with ad libitum access to food and water.

Kainate + lorazepam administration

Single subcutaneous injections of 5 mg (equivalent to 14.5–15.7 mg/kg, depending on animal weight) kainic acid monohydrate (K0250, 10 mg/ml in phosphate-buffered saline; Sigma-Aldrich, Germany) and 0.25–1.5 mg (approximately 0.75–4.5 mg/kg) lorazepam (2 mg/ml; Pfizer, Germany) were administered under isoflurane sedation. Rats were placed in an acrylic box containing 5% isoflurane in oxygen until sedation was achieved (15–30 s), then removed and placed on a clean table where the injections were given. If electrodes and/or electroencephalography (EEG) transmitters were implanted (see below), injections were given after a recovery period of at least 4 days. Following injections, rats were housed in clear acrylic boxes allowing free movement and visual observation.

Seizure monitoring (continuous video-EEG)

EEG data were acquired via either (1) recording electrodes with tips located in the dentate gyrus (approximate coordinates 2 mm lateral, 3 mm caudal to bregma, and 3.5 mm below the brain surface) or (2) screws with tips on the brain surface. Reference ground was always a screw located caudal and medial to the recording site and was not dorsal to the hippocampus. Electrodes and ground screws were connected to miniature wireless transmitters (FT20; Data Sciences International, U.S.A.) that were implanted subcutaneously on the animal's flank. All surgeries were performed in a stereotaxic apparatus (David Kopf) under isoflurane anesthesia (3–5% in oxygen). Spontaneous activity was recorded continuously (24/7) and stored digitally and automatically in 3-h epochs using LabChart 7 software (ADInstruments, New Zealand) as described previously.[15,16] All files were evaluated by at least two

Epilepsia, 58(2):222–230, 2017
doi: 10.1111/epi.13579

Table 1. Common kainic acid (KA)-based epilepsy models

Model	Advantages	Disadvantages	References
Intracerebral KA			
Intrahippocampal	Induces severe hippocampal sclerosis and spontaneous seizures	Causes convulsive SE that requires pharmacologic termination (e.g., benzodiazepine, ketamine) Hippocampal injury is variable; extensive damage to extrahippocampal regions High nonresponder rate Highly variable seizure rate Elaborate and costly implementation Results tend to be unique to each lab	24–28
Intraamygdaloid	Induces mild hippocampal sclerosis and spontaneous seizures Low nonresponder rate	Causes convulsive SE that requires pharmacologic termination (e.g., benzodiazepine, ketamine) Hippocampal injury is variable; extensive damage to extrahippocampal regions (dose dependent) Mortality ± 55% Elaborate and costly implementation Results tend to be unique to the lab	29–36
Systemic KA injection			
Intraperitoneal or subcutaneous Single injection	No surgical procedures No brain damage, e.g., from cannulas High throughput Low costs (no expensive laboratory equipment is necessary, e.g., stereotaxic) Induces hippocampal sclerosis and spontaneous seizures	No control over bioavailability of KA in the brain Amount of KA varies between animals Causes convulsive SE that needs to be terminated medically (diazepam, ketamine) If SE is successfully induced, massive extrahippocampal neuron loss occurs as well as extensive bilateral gliosis, brain edema and neuron loss in the piriform and entorhinal cortices, olfactory bulb, substantia nigra, thalamus, and mesencephalon High variability in neuropathology Up to 30% mortality Nonresponders: 20–40% of surviving animals	30,37–43
Intraperitoneal Multiple low-dose injections	No surgical procedures No brain damage, e.g., from cannulas Low nonresponder rate Medium throughput Low costs (no expensive laboratory equipment is necessary, e.g., stereotaxic) Induces hippocampal sclerosis and spontaneous seizures	No control over bioavailability of KA in the brain Amount of KA varies between animals Doses are given over several hours and the amount of KA has to be tailored to each animal, which requires close monitoring Mortality ± 15%	13,46

experienced reviewers; at least one reviewer was blinded to the treatment. Recordings were assessed visually, and all events with amplitudes obviously larger than baseline were analyzed. Simultaneous video monitoring used Edimax IC-7110W infrared cameras (Taiwan). Video files were captured at 15 frames/s and time-stamped for integration with the EEG data using SecuritySpy surveillance software (Ben Software, United Kingdom) and stored digitally. Seizures were scored according to the Racine scale.[17]

Perfusion fixation

Rats received an overdose of ketamine (>100 mg/kg, i.p.) and xylazine (10 mg/kg, i.p.) and were then perfused through the aorta with 0.9% saline for 90 s to remove intravascular blood. This was followed by 8 min of aortal perfusion with paraformaldehyde (4%) in 0.1 M phosphate buffer (pH 7.4). Brains were immediately removed from the skull and placed in 4% paraformaldehyde solution for at least 48 h before being sectioned (30 μm) on a freezing microtome.

Fluorescence and light microscopy

Nissl staining, Fluoro-Jade B staining, Timm staining, and neuronal nuclear antigen (NeuN) immunocytochemistry were performed on the resultant sections as described previously.[15] Images were acquired with a DMI6000B microscope equipped with a DCF360FX camera (Leica, Germany). Figures were made with Photoshop CS6 software (Adobe, U.S.A.), which was used to optimize contrast and brightness, but not to change the image content.

Quantification of neurodegeneration

Fluoro-Jade B–positive neurons were counted in matching Fluoro-Jade B–stained sections from the dorsal

hippocampus (one section per animal) using the Count Tool in Adobe Photoshop CS6.

Quantification of hippocampal area

The area of five matching, nonadjacent NeuN-immunostained or Nissl-stained sections from throughout the dorsal hippocampus was measured using the Adobe Photoshop CS6 Extended Measurement feature to calculate the area bounded by an irregular border, as described previously.[9] Values were obtained for the entire hippocampus (excluding the fimbria), dentate gyrus, and cornu ammonis. Group means were compared using Student's *t*-test.

Quantification of mossy fiber sprouting, that is, Timm staining

Five Timm-stained sections, equally distributed throughout the dorsal hippocampus, were evaluated using the Adobe Photoshop CS6 Histogram feature, which calculates the mean gray value for a selected area. Color images were converted to grayscale and inverted. The mean gray values for 64 pixel^2 squares in the intermolecular layer were recorded and averaged. Background was calculated from a cell-free area in stratum radiatum and subtracted from the intermolecular layer values. Group means were compared using Student's *t*-test.

Results

Smaller lorazepam doses increase hippocampal neurodegeneration

Various doses of lorazepam were evaluated (0.25–1.5 mg/animal; approximately 0.75–4.5 mg/kg), whereas the KA dose was kept constant (5 mg/animal; equivalent to 14.5–15.7 mg/kg, depending on weight) ($n \geq 4$ per group, $n = 33$ total). These doses of lorazepam are far below what is typically used to terminate experimental SE in rodents (6–8 mg/kg). Although acute hippocampal seizures were induced by KA at lorazepam doses of 1 mg ($n = 8$) and 1.5 mg/animal ($n = 5$), neither neurodegeneration nor later spontaneous seizures was detected. Animals that received less lorazepam had more neurodegeneration and vice versa (Fig. 1). By systematically reducing the lorazepam dose, we found the optimal amount to be 0.25 mg/animal (approximately 0.75 mg/kg). An average of 565.4 ± (standard deviation) 43.7 Fluoro-Jade B–positive neurons were counted in dorsal hippocampus sections from animals that were sacrificed 4 days after receiving 5 mg KA and 0.25 mg lorazepam ($n = 8$), compared with 0.0 ± 0.0 in animals that received 5 mg KA and 1.0 mg lorazepam ($n = 8$). Broken down into hippocampal subfields, the mean values were 255.4 ± 31.7 for CA1, 273.0 ± 29.1 for CA3, and 37 ± 7.7 for the hilus. During the 24 h immediately following KA and lorazepam administration, as determined by continuous video-EEG monitoring, not a single animal in any group exhibited any convulsive seizures, let alone cSE ($n = 33$ total). At no time did any animal exhibit signs of morbidity; the survival rate was 100%.

Low-dose lorazepam blocks kainate-induced convulsive seizures, but not hippocampal seizure activity

Following simultaneous, subcutaneous administration of 5 mg KA and 0.25 mg lorazepam ($n = 8$), aberrant electrographic activity was detected within minutes and the first hippocampal seizures after 30–40 min, as determined with electrodes located in the dorsal dentate gyrus. Epileptiform discharging of hippocampal granule cells (Fig. 2) persisted for at least 3 h in all animals, with an average of 3.3 ± 0.4 h. During the treatment, seizure behavior was limited to occasional wet dog shakes, which were observed in some, but not all, rats. As seizures were self-terminating, no additional lorazepam was administered. On the 3 days following treatment, animals appeared and behaved normally. None presented with any sign of morbidity, for example, ≥10% weight loss, jumpiness, or reduced mobility. Consequently, none required palliative care. Animals that received 5 mg KA and 1.0 mg lorazepam exhibited an average of 12 ± 7 min of hippocampal seizures ($n = 5$).

Spontaneous hippocampal seizures arise after a discrete latent period

Continuous video-EEG monitoring revealed the first spontaneous seizures, which were nonconvulsive, to occur an average of 12.1 days after administration of 5 mg KA and 0.25 mg lorazepam ($n = 5$; range 10–15 days) (Fig. 3A, video). Spontaneous seizures were detected in all animals, were typically 45–60 s long (Fig. 2A), and occurred at a frequency of 7.8 per animal per day during the first two weeks of spontaneous epilepsy (Fig. 3B). Seventy-two percent of seizures occurred during the light phase (6:00 a.m. to 5:59 p.m.) (Fig. 3C). Intracerebral recordings obtained from the dentate gyrus demonstrated hippocampal involvement, for example, epileptiform discharging of granule cells (Fig. 2B). The corresponding, time-stamped video files revealed no overt seizure-like behavior, rather only freezing/staring. Later spontaneous seizures (≥3 weeks post-treatment) also included behavioral manifestation, for example, mastication and forepaw clonus, corresponding to stages 3–5 on the Racine scale[17] (Videos S1 and S2). No spontaneous seizures were detected in any rats that received 5 mg KA and 1.0 mg lorazepam ($n = 4$, 4 weeks continuous video-EEG monitoring).

Neuropathology resembles (refractory) mesial TLE with hippocampal sclerosis

Hippocampal neuropathology in this model closely mimics that seen in a subset of patients with mesial TLE whose seizures are refractory to drug treatment (International League Against Epilepsy [ILAE] Type 1[18]). In fact, ILAE Type I is the most common TLE pathology.

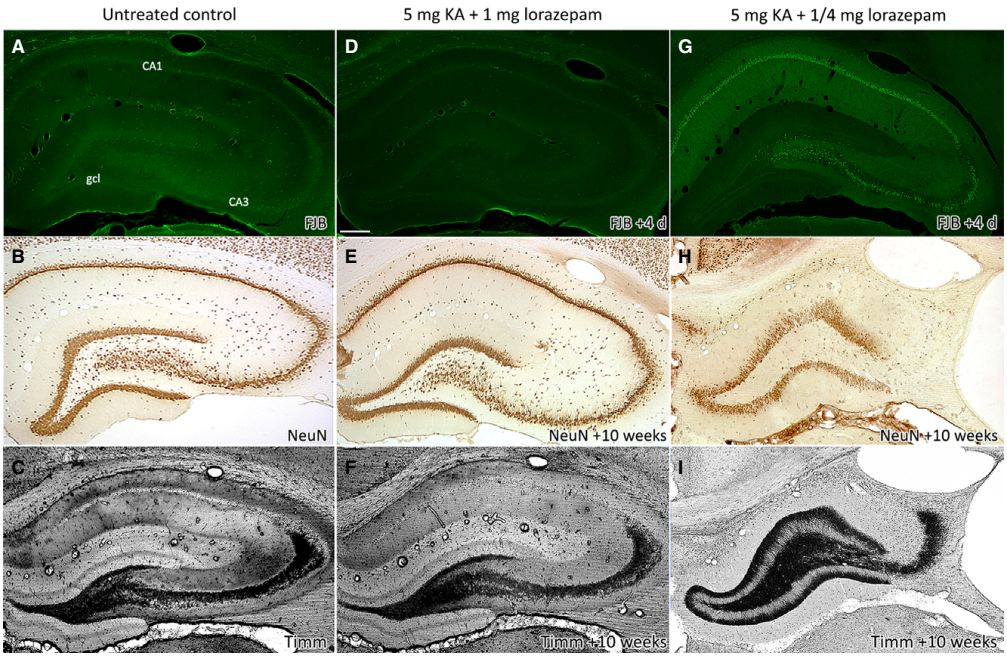

Figure 1.
Acute and chronic hippocampal neuropathology after systemic, concurrent administration of 5 mg kainate (KA) and lorazepam at either 1 or 1/4 mg. (**A**) Fluoro-Jade B (FJB) staining, (**B**) NeuN immunoreactivity, and (**C**) Timm staining in the dorsal hippocampus from an untreated control rat, demonstrating normal neuroanatomy. (**D**) FJB staining 4 days posttreatment (1 mg lorazepam) showing no apparent neurodegeneration. (**E**) NeuN-immunostaining 10 weeks posttreatment (1 mg lorazepam) exhibiting apparently normal neuroanatomy. (**F**) Timm staining 10 weeks posttreatment (1 mg lorazepam) confirms normal granule cell efferents, that is, lack of mossy fiber sprouting. (**G**) FJB staining 4 days posttreatment (1/4 mg lorazepam) showing widespread neurodegeneration in the dentate hilus, CA3, and CA1. (**H**) NeuN-immunostaining 10 weeks posttreatment (1/4 mg lorazepam) reveals extensive neuron loss in the dentate hilus, CA3, and CA1, that is, classic hippocampal sclerosis. (**I**) Timm staining 10 weeks posttreatment (1/4 mg lorazepam), demonstrating aberrant reorganization of granule cell axons, that is, mossy fiber sprouting. Scale bar: 200 μm.

Acutely, following administration of 5 mg KA and 0.25 mg lorazepam, pyramidal neurons in areas CA3 and CA1 were virtually wiped out, as were many neurons in the dentate hilus (Fig. 1B). Long-term histology (≥2 months) revealed hallmarks of mesial TLE, such as classic hippocampal sclerosis (Figs. 1D and 4A) and mossy fiber sprouting (Figs. 1F and 4B). Compared with control samples, atrophy was pronounced in the hippocampus overall ($-40.0 \pm 9.6\%$ mm^2), specifically the hippocampus proper ($-74.3 \pm 7.6\%$ mm^2), whereas the dentate gyrus was enlarged by at least 34% in three of four samples (all n's = 4, all p-values ≤ 0.01). Although the thickness of the granule cell layer was consistently enlarged ($124.7 \pm 25.0\%$ of control), a phenomenon called "granule dispersion," this expansion does not seem to drive the overall enlargement seen in the molecular layer (Fig. 1D).

Discussion

The present results demonstrate that a single dose of KA administered concurrently with a low dose of lorazepam can be used to dependably reproduce fundamental characteristics of acquired human TLE in rats, while avoiding cSE and its associated problems, for example, significant variability and mortality. The protocol is simple. Animals receive single, simultaneous, subcutaneous injections of KA and lorazepam and require no additional treatment or care. This is unlike cSE-based models that often require multiple injections and/or substantial palliative care.[7,12] The former is an effort to maximize the number of animals that experience cSE and the latter to reduce mortality. The present results suggest that the crux of animal models should not be the induction of cSE, but rather of prolonged electrographic seizure activity, since seizures do not always have a significant

Epilepsia, 58(2):222–230, 2017
doi: 10.1111/epi.13579

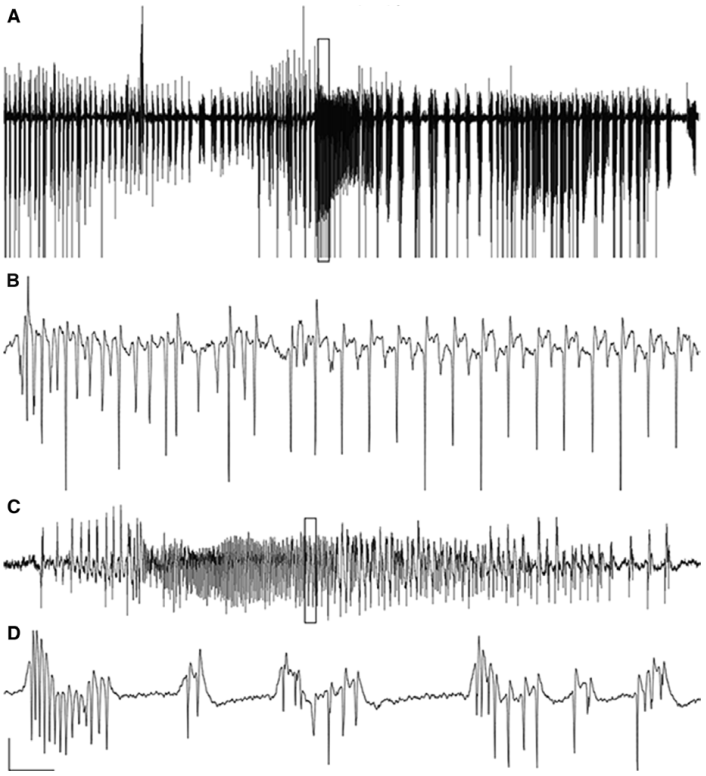

Figure 2.
Hippocampal seizures, kainate-induced and spontaneous, recorded from the dentate gyrus in freely moving Sprague-Dawley rats. (**A**) Fifty-eight seconds of activity, recorded 44 min after kainate and lorazepam administration (5 mg and 1/4 mg, respectively). (**B**) Eight hundred milliseconds extract from panel **A**, demonstrating epileptiform discharging of hippocampal granule cells. (**C**) A rat's first spontaneous (focal) seizure 10 days post-kainate (5 mg) and lorazepam (1/4 mg) administration (see also Video S1). Trace represents 58 s of spontaneous activity. (**D**) Eight hundred milliseconds extract from panel **C**, showing epileptiform discharging of hippocampal granule cells. Behavior during the spontaneous seizure was limited to staring; a few wet dog shakes were seen after the EEG signal returned to baseline. Calibration bar: 2 mV in all panels; 4 s in Panels **A** and **C**, 55 msec in Panels **B** and **D**; sampling rate 2 kHz.

behavioral component. In fact, human status epilepticus is often nonconvulsive.[19] Along these lines, terminating SE, both in the laboratory and clinic, requires both adequate treatment and EEG confirmation that seizures have stopped. We have shown here that an "inadequate" dose of lorazepam can block cSE, but not acute hippocampal seizures, neurodegeneration, or epileptogenesis.

A comparison to the present study is the repeated low-dose KA model, which was thoroughly characterized by Williams et al.[20] Although that model is apparently robust and reliable, the one presented here has some clear advantages; the first is simplicity. Repeated administration requires constant attention for several hours, each animal needs individualized treatment, and much care must be taken to ensure that animals are not overdosed. Because our approach is based on a single administration of KA, which was effective in all animals, no additional attention is necessary, and there is no need to titrate dosing for each individual animal. This ease of use, coupled with a lack of significant variability, should facilitate the present model's implementation in experimental epilepsy studies.

The second advantage is a lack of cSE, which is actually the crux of the low-dose model. Essentially, repeated doses of KA are given until cSE is induced, which is then allowed to persist for 3 h. Animals that survive cSE often require significant care posttreatment. A recovery period of several days is common, during which time animals may not eat or drink normally. The present model avoids cSE

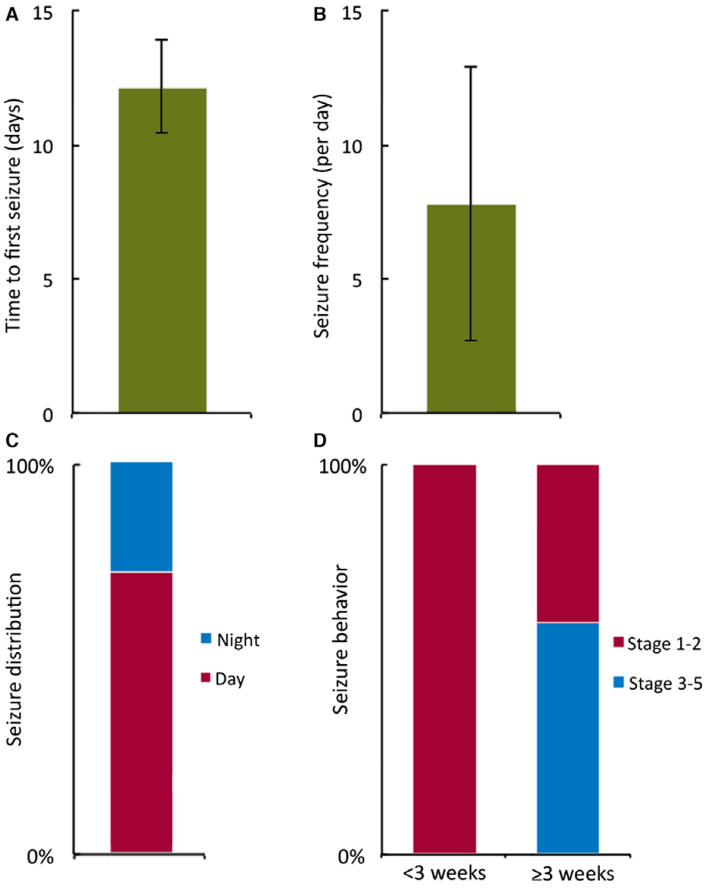

Figure 3.
Characteristics of spontaneous seizures after systemic, concurrent administration of 5 mg kainate and 1/4 mg lorazepam. (**A**) Latency from treatment to the first spontaneous seizure as determined by continuous video-EEG recording with electrodes located in the dorsal dentate gyrus. The mean time to epilepsy was 12.1 ± (standard deviation) 1.7 days. (**B**) Frequency of spontaneous seizures. Animals exhibited an average of 7.8 ± 5.1 seizures per day during the first 2 weeks of spontaneous epilepsy. (**C**) Distribution of seizures during the day (6:00–17:59) and night (18:00–5:59). A majority of seizures (72%) occurred during the day. (**D**) Seizure behavior. All spontaneous seizures that occurred during the first 2 weeks posttreatment were nonconvulsive. Starting at week 3, convulsive motor seizures were seen. Data are presented as mean ± SEM; stages in (**B**) are according to the Racine scale,[17] n's = 5.
Epilepsia © ILAE

and its confounds, for example, morbidity and mortality, nevertheless inducing hippocampal seizures lasting 3–4 h. Presumably because cSE is avoided, animals do not require any palliative care.

That later spontaneous seizures, but not the first, were convulsive, could be indicative of progressing neuronal network reorganization, for example, mossy fiber sprouting, which takes weeks or months to complete.[15,16,21] Such reorganization could provide an aberrant pathway through which early "sequestered" seizure activity can exit the hippocampus and propagate to other brain regions. This might explain why, despite the fact that all seizures involved granule cell discharging, only later seizures generalized.

Finally, there is an urgent need to implement novel models of epilepsy in order to (1) reveal new and different targets for intervention and (2) discover treatments that exploit these novel mechanisms. Despite the advantages of newer antiseizure drugs in the management of epilepsy, such as fewer adverse drug interactions or hypersensitivity reactions,[22,23] their efficacy and tolerability has not improved much over the last 25 years.[23] Consequently, ~30% of patients with epilepsy do not respond satisfactorily to drug therapy, a figure that has also not budged during this time.[23] One reason for this persistent problem is that, with very few exceptions, the same animal models have discovered all antiseizure drugs.[23] Therefore, we propose to include novel animal models in the drug-screening repertoire, in an effort to discover substances targeting novel epileptogenic and ictogenic mechanisms. The present model could be of particular use in drug discovery efforts focused on refractory TLE. Although the pronounced hippocampal sclerosis exhibited by this model is seen in but a minority of patients with TLE, this pattern of injury is strongly correlated with drug-refractory epilepsy.

In summary, the present results demonstrate that a single dose of KA administered concurrently with a low dose of lorazepam can be used to dependably reproduce fundamental characteristics of acquired mesial TLE in rats, while

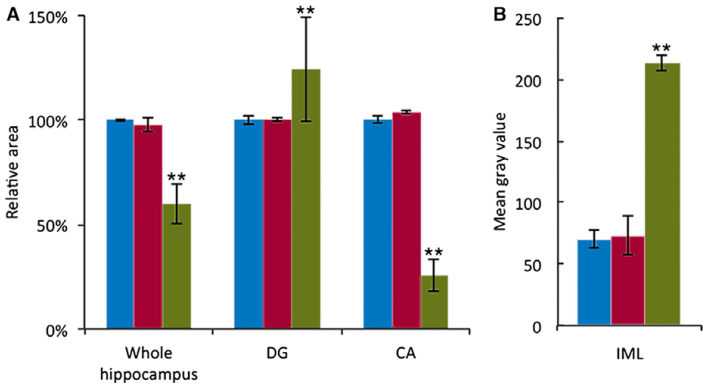

Figure 4.
Quantification of morphologic changes in the hippocampus at least 10 weeks after 5 mg kainate and lorazepam at either 1 mg (red bars) or 1/4 mg (green bars), compared with age-matched naive rats (blue bars). (**A**) Hippocampal area, also subdivided into DG and CA subfields, relative to control, obtained from NeuN-immunostained or Nissl-stained sections as described in the Methods section. Three of four hippocampi in the 1/4 mg group exhibited DG hypertrophy. (**B**) Mean gray values obtained from the IML in Timm-stained brain sections as described in the Methods section. Larger numbers indicate darker gray values, that is, more mossy fiber sprouting into the IML. DG, dentate gyrus; CA, cornu ammonis; IML, inner molecular layer; error bars ± SEM; Student's *t*-test; n = 18–20 sections total from four brains for each group; all p-values ≤ 0.01.

avoiding cSE and its inherent problems. The main features of the "KaL model" are the following: a simple protocol, acute hippocampal seizures that persist for 3–4 h and are self-terminating, substantial hippocampal neurodegeneration, spontaneous hippocampal seizures after a 10–15 day seizure-free period, and a lack of both morbidity and mortality. Due to this model's reliability and ease of use, it is expected to prove useful in studies on mechanisms of epileptogenesis (the development of epilepsy) and ictogenesis (manifestation of individual, spontaneous seizures), as well as drug discovery efforts focused on refractory epilepsy.

Acknowledgments

We thank S. Caspari for excellent technical support along with D. Henshall for useful discussions and helpful suggestions. This work was supported by grants from the European Commission (FP7-602130, S.B., L.C., F.K.N., B.A.N., and F.R.V.N.) and Citizens United for Research in Epilepsy (B.A.N. and C.S.)

Disclosure

None of the authors has any conflict of interest to disclose. We confirm that we have read the Journal's position on issues involved in ethical publication and affirm that this report is consistent with those guidelines.

References

1. Fisher RS, Acevedo C, Arzimanoglou A, et al. ILAE official report: a practical clinical definition of epilepsy. *Epilepsia* 2014;55:475–482.
2. Chang BS, Lowenstein DH. Epilepsy. *N Engl J Med* 2003;349:1257–1266.
3. Margerison JH, Corsellis JA. Epilepsy and the temporal lobes. A clinical, electroencephalographic and neuropathological study of the brain in epilepsy, with particular reference to the temporal lobes. *Brain* 1966;89:499–530.
4. Thurman DJ, Beghi E, Begley CE, et al. Standards for epidemiologic studies and surveillance of epilepsy. *Epilepsia* 2011;52:2–26.
5. De Lanerolle NC, Kim JH, Williamson A, et al. A retrospective analysis of hippocampal pathology in human temporal lobe epilepsy: evidence for distinctive patient subcategories. *Epilepsia* 2003;44:677–687.
6. Spencer SS, Spencer DD. Entorhinal-hippocampal interactions in medial temporal lobe epilepsy. *Epilepsia* 1994;35:721–727.
7. Lévesque M, Avoli M. The kainic acid model of temporal lobe epilepsy. *Neurosci Biobehav Rev* 2013;37:2887–2899.
8. Murakami S, Takemoto T. On the effective principles of digenea-simplex aq. 1. Separation of the effective fraction by liquid chromatography. Yakugaku; 1953.
9. Watkins JC, Evans RH. Excitatory amino acid transmitters. *Annu Rev Pharmacol Toxicol* 1981;21:165–204.
10. Ben-Ari Y, Lagowska J. Epileptogenic action of intra-amygdaloid injection of kainic acid. *C R Acad Sci Hebd Seances Acad Sci D* 1978;287:813–816.
11. Ben-Ari Y, Lagowska J, Tremblay E, et al. A new model of focal status epilepticus: intra-amygdaloid application of kainic acid elicits repetitive secondarily generalized convulsive seizures. *Brain Res* 1979;163:176–179.
12. Lévesque M, Avoli M, Bernard C. Animal models of temporal lobe epilepsy following systemic chemoconvulsant administration. *J Neurosci Methods* 2015;260:45–52.
13. Hellier JL, Dudek FE. Chemoconvulsant model of chronic spontaneous seizures. *Curr Protoc Neurosci* 2005; doi: 10.1002/0471142301.ns0919s31.
14. Alldredge BK, Gelb AM, Isaacs SM, et al. A comparison of lorazepam, diazepam, and placebo for the treatment of out-of-hospital status epilepticus. *N Engl J Med* 2001;345:631–637.
15. Norwood BA, Bumanglag AV, Osculati F, et al. Classic hippocampal sclerosis and hippocampal-onset epilepsy produced by a single

"cryptic" episode of focal hippocampal excitation in awake rats. *J Comp Neurol* 2010;518:3381–3407.
16. Harvey BD, Sloviter RS. Hippocampal granule cell activity and c-Fos expression during spontaneous seizures in awake, chronically epileptic, pilocarpine-treated rats: implications for hippocampal epileptogenesis. *J Comp Neurol* 2005;488:442–463.
17. Racine RJ. Modification of seizure activity by electrical stimulation: II. Motor seizure. *Electroencephalogr Clin Neurophysiol* 1972;32:281–294.
18. Blümcke I, Thom M, Aronica E, et al. International consensus classification of hippocampal sclerosis in temporal lobe epilepsy: a Task Force report from the ILAE Commission on Diagnostic Methods. *Epilepsia* 2013;54:1315–1329.
19. Trinka E, Cock H, Hesdorffer D, et al. A definition and classification of status epilepticus – report of the ILAE Task Force on Classification of Status Epilepticus. *Epilepsia* 2015;56:1515–1523.
20. Williams PA, White AM, Clark S, et al. Development of spontaneous recurrent seizures after kainate-induced status epilepticus. *J Neurosci* 2009;29:2103–2112.
21. Deller T, Frotscher M, Nitsch R. Morphological evidence for the sprouting of inhibitory commissural fibers in response to the lesion of the excitatory entorhinal input to the rat dentate gyrus. *J Neurosci* 1995;15:6868–6878.
22. Elger CE, Schmidt D. Modern management of epilepsy: a practical approach. *Epilepsy Behav* 2008;12:501–539.
23. Löscher W, Schmidt D. Modern antiepileptic drug development has failed to deliver: ways out of the current dilemma. *Epilepsia* 2011;52:657–678.
24. Arabadzisz D, Antal K, Parpan F, et al. Epileptogenesis and chronic seizures in a mouse model of temporal lobe epilepsy are associated with distinct EEG patterns and selective neurochemical alterations in the contralateral hippocampus. *Exp Neurol* 2005;194:76–90.
25. Carriero G, Arcieri S, Cattalini A, et al. A guinea pig model of mesial temporal lobe epilepsy following nonconvulsive status epilepticus induced by unilateral intrahippocampal injection of kainic acid. *Epilepsia* 2012;53:1917–1927.
26. Daniels WMU, Jaffer A, Engelbrecht AH, et al. The effect of intrahippocampal injection of kainic acid on corticosterone release in rats. *Neurochem Res* 1990;15:495–499.
27. Victor Nadler J, Cuthbertson GJ. Kainic acid neurotoxicity toward hippocampal formation: dependence on specific excitatory pathways. *Brain Res* 1980;195:47–56.
28. Raedt R, Van Dycke A, Van Melkebeke D, et al. Seizures in the intrahippocampal kainic acid epilepsy model: characterization using long-term video-EEG monitoring in the rat. *Acta Neurol Scand* 2009;119:293–303.
29. Araki T, Simon RP, Taki W, et al. Characterization of neuronal death induced by focally evoked limbic seizures in the C57BL/6 mouse. *J Neurosci Res* 2002;69:614–621.
30. Ben-Ari Y, Tremblay E, Ottersen OP. Injections of kainic acid into the amygdaloid complex of the rat: an electrographic, clinical and histological study in relation to the pathology of epilepsy. *Neuroscience* 1980;5:515–528.
31. Cavalheiro EA, Riche DA, Le Gal La Salle G. Long-term effects of intrahippocampal kainic acid injection in rats: a method for inducing spontaneous recurrent seizures. *Electroencephalogr Clin Neurophysiol* 1982;53:581–589.
32. Dunleavy M, Shinoda S, Schindler C, et al. Experimental neonatal status epilepticus and the development of temporal lobe epilepsy with unilateral hippocampal sclerosis. *Am J Pathol* 2010;176:330–342.
33. Gurbanova AA, Aker RG, Sirvanci S, et al. Intra-amygdaloid injection of kainic acid in rats with genetic absence epilepsy: the relationship of typical absence epilepsy and temporal lobe epilepsy. *J Neurosci* 2008;28:7828–7836.
34. Jimenez-Mateos EM, Engel T, Merino-Serrais P, et al. Silencing microRNA-134 produces neuroprotective and prolonged seizure-suppressive effects. *Nat Med* 2012;18:1087–1094.
35. Mouri G, Jimenez-Mateos E, Engel T, et al. Unilateral hippocampal CA3-predominant damage and short latency epileptogenesis after intra-amygdala microinjection of kainic acid in mice. *Brain Res* 2008;1213:140–151.
36. Represa A, Tremblay E, Ben-Ari Y. Kainate binding sites in the hippocampal mossy fibers: localization and plasticity. *Neuroscience* 1987;20:739–748.
37. Drexel M, Preidt AP, Sperk G. Sequel of spontaneous seizures after kainic acid-induced status epilepticus and associated neuropathological changes in the subiculum and entorhinal cortex. *Neuropharmacology* 2012;63:806–817.
38. Haas KZ, Sperber EF, Opanashuk LA, et al. Resistance of immature hippocampus to morphologic and physiologic alterations following status epilepticus or kindling. *Hippocampus* 2001;11:615–625.
39. Heggli DE, Malthesorenssen D. Systemic injection of kainic acid - effect on neurotransmitter markers in piriform cortex, amygdaloid complex and hippocampus and protection by cortical lesioning and anticonvulsants. *Neuroscience* 1982;7:1257–1264.
40. Kar S, Seto D, Doré S, et al. Systemic administration of kainic acid induces selective time dependent decrease in [125I]insulin-like growth factor I, [125I]insulin-like growth factor II and [125I]insulin receptor binding sites in adult rat hippocampal formation. *Neuroscience* 1997;80:1041–1055.
41. Sperk G, Lassmann H, Baran H, et al. Kainic acid-induced seizures – dose-relationship of behavioral, neurochemical and histopathological changes. *Brain Res* 1985;338:289–295.
42. Sloviter RS, Damiano BP. Sustained electrical stimulation of the perforant path duplicates kainate-induced electrophysiological effects and hippocampal damage in rats. *Neurosci Lett* 1981;24:279–284.
43. Strain SM, Tasker R. Hippocampal damage produced by systemic injections of domoic acid in mice. *Neuroscience* 1991;44:343–352.
44. Suarez LM, Cid E, Gal B, et al. Systemic injection of kainic acid differently affects LTP magnitude depending on its epileptogenic efficiency. *PLoS ONE* 2012;7:e48128.
45. Zhang X, Cui SS, Wallace AE, et al. Relations between brain pathology and temporal lobe epilepsy. *J Neurosci* 2002;22:6052–6061.
46. Hellier JL, Patrylo PR, Buckmaster PS, et al. Recurrent spontaneous motor seizures after repeated low-dose systemic treatment with kainate: assessment of a rat model of temporal lobe epilepsy. *Epilepsy Res* 1998;31:73–84.

Supporting Information

Additional Supporting Information may be found in the online version of this article:

Video S1. Spontaneous, nonconvulsive hippocampal seizure (video-EEG).

Video S2. Spontaneous convulsive seizure (video-EEG).

7.2 Validation of Reference Genes for Quantitative Gene Expression Analysis in Experimental Epilepsy

Journal of Neuroscience Research, doi: 10.1002/jnr.24089

Chinmaya Sadangi, Felix Rosenow, and Braxton A. Norwood

Received: 9 March 2017 | Revised: 27 April 2017 | Accepted: 4 May 2017

DOI: 10.1002/jnr.24089

RESEARCH ARTICLE

WILEY

Validation of reference genes for quantitative gene expression analysis in experimental epilepsy

Chinmaya Sadangi[1] | Felix Rosenow[1,2] | Braxton A. Norwood[1,2,3]

[1]Department of Neurology, Philipps University, Marburg, Germany

[2]Epilepsy Center Frankfurt Rhine-Main, Department of Neurology, Goethe University, Frankfurt am Main, Germany

[3]Expesicor LLC, Neuroscience Division, Kalispell, Montana

Correspondence
Braxton A. Norwood, Department of Neurology, Philipps University, Karl-von-Frisch Str. 1, 35043 Marburg, Marburg, Germany.
Email: braxton.norwood@gmail.com

Funding Information
This work was supported by grants from the European Commission (FP7602130, B. A.N., F.R) and Citizens United for Research in Epilepsy (B.A.N., C.S.).

Abstract

To grasp the molecular mechanisms and pathophysiology underlying epilepsy development (epileptogenesis) and epilepsy itself, it is important to understand the gene expression changes that occur during these phases. Quantitative real-time polymerase chain reaction (qPCR) is a technique that rapidly and accurately determines gene expression changes. It is crucial, however, that stable reference genes are selected for each experimental condition to ensure that accurate values are obtained for genes of interest. If reference genes are unstably expressed, this can lead to inaccurate data and erroneous conclusions. To date, epilepsy studies have used mostly single, nonvalidated reference genes. This is the first study to systematically evaluate reference genes in male Sprague–Dawley rat models of epilepsy. We assessed 15 potential reference genes in hippocampal tissue obtained from 2 different models during epileptogenesis, 1 model during chronic epilepsy, and a model of noninjurious seizures. Reference gene ranking varied between models and also differed between epileptogenesis and chronic epilepsy time points. There was also some variance between the four mathematical models used to rank reference genes. Notably, we found novel reference genes to be more stably expressed than those most often used in experimental epilepsy studies. The consequence of these findings is that reference genes suitable for one epilepsy model may not be appropriate for others and that reference genes can change over time. It is, therefore, critically important to validate potential reference genes before using them as normalizing factors in expression analysis in order to ensure accurate, valid results. © 2017 Wiley Periodicals, Inc.

KEYWORDS

reference gene expression, experimental epilepsy, hippocampus, animal model, qPCR

1 | INTRODUCTION

Epilepsy is a chronic neurological condition that is characterized by recurrent, unprovoked seizures (Thurman et al., 2011). It is one of the world's most common neurological disorders, affecting approximately 1% of the world population (~65 million) with around 2.4 million new diagnoses annually (Thurman et al., 2011). Temporal lobe epilepsy (TLE), where seizures originate in the temporal lobe, is the most common epilepsy syndrome, often refractory to treatment, and is thought to be caused by a brain insult (Chang & Lowenstein, 2003). TLE is characterized by hippocampal atrophy and limited extrahippocampal damage as well as seizures that originate in the hippocampus and/or closely related structures (Spencer & Spencer, 1994). TLE is most commonly modeled in rats by one of three methods: electrical stimulation (Norwood et al., 2010; Sloviter & Damiano, 1981), systemic administration of kainic acid (Ben-Ari & Lagowska, 1978; Ben-Ari, Lagowska, Tremblay, & Le Gal La Salle, 1979), or systemic administration of pilocarpine (Turski, Cavalheiro, et al., 1983; Turski, Czuczwar, Kleinrok, & Turski, 1983).

Significance

This is the first study on systemic evaluation and validation of reference genes in experimental epilepsy. We present novel reference genes that are more stably expressed than those most often used. We also show that stable, appropriate reference genes can vary between animal models and even within the same animal model (at different time points). We also demonstrate that a minimum of two reference genes should be used for normalization; most studies have used only one.

Gene expression analysis is a standard approach for studying the regulation of biological mechanisms under normal and diseased conditions. A better understanding of the molecular mechanisms at play in epilepsy is crucial for the development of novel therapeutics that correct culpable dysfunction. Quantitative real-time polymerase chain reaction (qPCR) is the gold standard for gene expression analysis in small quantities of tissue. Appropriate reference genes (formerly known as housekeeping genes) are required in order to precisely and accurately determine the expression of genes of interest (GOIs) (Bustin et al., 2009). The purpose of normalizing data to one or more reference genes is to account for differences in the amount of cDNA (McCulloch, Ashwell, O'Nan, & Mente, 2012) and efficiency of amplification (Vandesompele et al., 2002), and to compare GOIs among different samples. Reference genes are typically involved in the basic maintenance of cellular structure and/or function. Irrespective of its role, reference gene mRNA should express at a constant level in all conditions, regardless of cell cycle stage or age (Eisenberg & Levanon, 2013; Radonić et al., 2004). Reference genes vary widely across diseases and experimental models (Bademci et al., 2010) but can be considered suitable if several criteria are met (Chervoneva et al., 2010), the most important criterion being stable expression. The expression of a reference gene cannot be influenced by experimental conditions (Kozera & Rapacz, 2013).

Reference genes have been proposed in a few studies on human and experimental epilepsy (Maurer-Morelli et al., 2012; Pernot, Dorandeu, Beaup, & Peinnequin, 2010). There has, however, not been a systematic evaluation or validation of potential reference genes in any experimental epilepsy model. The aim of this study was to discover reference genes for two rat models of epilepsy: 8-hr perforant pathway stimulation (PPS) (Norwood et al., 2010) and systemic kainate-lorazepam (KaL) during epileptogenesis and/or chronic epilepsy, and after acute, noninjurious seizures (30-min PPS) (Norwood et al., 2010). The mRNA expression levels of 15 (Kienzler-Norwood et al., 2017) potential reference genes were determined in hippocampi from treated and control animals. Four different validated and established methods to determine expression stability were used: geNorm (Vandesompele et al., 2002), NormFinder (Andersen, Jensen, & Ørntoft, 2004), BestKeeper (Pfaffl, Tichopad, Prgomet, & Neuvians, 2004), and Delta-Ct (ΔCt) (Silver, Best, Jiang, & Thein, 2006).

The 15 candidate genes used in this study are actin beta (*ACTB*), beta-2-microglobulin (*B2M*), glyceraldehyde 3-phosphate dehydrogenase (*GAPDH*), hypoxanthine phosphoribosyl-transferase 1 (*HPRT1*), lactate dehydrogenase (*LDHA*), non-POU domain containing octamer-binding (*NONO*), peptidylprolyl isomerase A (*PPIA*), peptidylprolyl isomerase B (*PPIB*), retinitis pigmentosa 2 (*RP2*), ribosomal protein large P1 (*RPLP1*), TATA box binding protein (*TBP*), transferrin receptor (*TFRC*), ubiquitin C (*UBC*), tyrosine-3-monooxygenase (*YWHAZ*), and 18s ribosomal RNA (*18s*). Toll-like receptor 4 (*TLR4*) was used as a GOI to evaluate potential reference genes since it is known to upregulate in experimental and human epilepsy. The candidate reference genes were selected based on previous epilepsy studies, use in other rodent disease models, or use in other model organisms. For example, *TBP* has been determined to be a stable reference gene in a febrile seizure model used in male Sprague–Dawley rat pups (Swijsen, Nelissen, Janssen, Rigo, & Hoogland, 2012); *NONO* has been validated as a stable reference gene in a mouse model of colitis (Eissa, Kermarrec, Hussein, Bernstein, & Ghia, 2017) and adipocyte cell differentiation (Arsenijevic, Grégoire, Delforge, Delporte, & Perret, 2012); *HPRT1* and *TBP* have been described as stable genes in the intrahippocampal kainic acid mouse model (Pernot et al., 2010); and *YWHAZ*, *ACTB*, and *GAPDH* in a nonhuman primate model of Alzheimer disease (Park et al., 2013). Some of our candidate reference genes (*GAPDH*, *HPRT*, *TBP*, *ACTB*, *UBC*, *B2M*) have been used in human epilepsy studies (Wierschke et al., 2010).

2 | METHODS

2.1 | Animals

Male Sprague–Dawley rats ($n = 32$) (Harlan-Winkelmann, Borchen, Germany, weight range: 318–344 g) were used in this study. Animals were treated in accordance with the guidelines of the European community (EUVD 86/609/EEC) and were housed in an on-site animal facility (21 °–25 °C; 45%–60% humidity) under a 12:12 light/dark cycle with ad libitum access to food and water. All experiments were approved by the local regulation authority (Regierungspräsidium Gießen, Germany). All animals were housed in groups (at least two per cage); none were excluded from the study.

2.2 | Animal models

2.2.1 | PPS

The 8-hr PPS model is characterized by hippocampal sclerosis and hippocampal-onset epilepsy after 2 to 3 weeks (Norwood et al., 2010), whereas 30-min PPS does not induce either neurodegeneration or epilepsy (Norwood et al., 2011). Briefly, rats were implanted bilaterally with bipolar stimulating electrodes in the perforant pathway and unipolar recording electrodes in the dorsal hippocampus, then stimulated for 30 min or 8 hr as described previously (Norwood et al., 2010, 2011). Control animals were implanted with electrodes, but not stimulated.

2.2.2 | KaL

The KaL model also recapitulates essential characteristics of human TLE, such as hippocampal sclerosis and hippocampal-onset epilepsy after a discreet seizure-free period (Kienzler-Norwood et al., 2017). Animals received 15 mg/kg kainic acid monohydrate (10 mg/ml in phosphate-buffered saline, K0250, Sigma-Aldrich, Germany) and 0.75 mg/kg lorazepam (2 mg/ml, Pfizer, Germany) that was administered subcutaneously, while the control animals received 15 mg/kg kainic acid monohydrate and 3 mg/kg lorazepam. The controls received a higher dose of lorazepam that blocks neurodegeneration and epilepsy (Kienzler-Norwood et al., 2017).

Animals were not video-EEG monitored to confirm epilepsy. In previous studies (Kienzler-Norwood et al., 2017; Norwood et al., 2010), we found that all animals that were EEG monitored developed epilepsy. In this study, a few animals from the 14-day and 20-week

groups ($n = 3$ for both PPS and KaL models) were video monitored, however, to confirm epilepsy. All six animals exhibited spontaneous convulsive seizures.

2.3 | Tissue harvesting

Rats were sacrificed after 4 days, 14 days, or 20 weeks ($n = 4$ per group). The 30-min PPS, 8-hr PPS, and KaL animals were sacrificed after 4 and 14 days. An additional group of KaL rats was sacrificed after 20 weeks. All animals received an overdose of ketamine (> 100 mg/kg i.p.) and xylazine (10 mg/kg i.p.) and were then perfused through the aorta with 0.9% saline for 90 s to remove intravascular blood. Brains were removed from the skull and the hippocampi were microdissected, frozen on dry ice, and stored at −80 °C.

2.4 | RNA extraction and cDNA synthesis

RNA was extracted using the Quick-RNA Miniprep Kit (R1054, Zymo Research, Germany) according to the manufacturer's protocol. Briefly, hippocampi were weighed and then homogenized using a pellet pestle (Z359971-1EA, Sigma-Aldrich, Germany) in 600 µl of lysis buffer with 0.5% v/v of reagent DX (19088, Qiagen, Germany) to prevent froth formation. RNA was eluted with 30 µl of water and analyzed on a NanoDrop spectrophotometer (2000c, Thermo Scientific, Germany) to obtain the yield and determine purity by 260/280 and 260/230 ratios (Supplementary Figure 1). gDNA was removed by use of the Turbo DNA-free kit (AM1907, Ambion, Life Technologies, Germany) following the manufacturer's instructions. cDNA was synthesized in a 20-µl reaction by using Maxima First Strand cDNA synthesis kit for RT-qPCR (k1641, Thermo Scientific, Germany) using 1 µg of RNA per sample and random hexamer primers. cDNA was aliquoted and stored at −20 °C until further use.

2.5 | qPCR

This was performed on a StepOnePlus Real-Time PCR system (Applied Biosystems, Germany). Each reaction contained 5 µl of 2X Maxima SYBR Green/ROX qPCR Master Mix (K0222, Thermo Scientific, Germany), 2 µl of the cDNA corresponding to 100 ng of RNA, and 0.6 µM forward and reverse primers in a total reaction volume of 10 µl. A two-step protocol was used for amplification with an initial denaturation for 10 min at 95 °C, followed by 40 cycles of 15 s at 95 °C and 60 s at 60 °C in a 96-well reaction plate. The specificity of PCRs was verified by melt curve analysis for each sample after 40 cycles by raising the temperature from 60 °C to 95 °C at a rate of 1 °C per minute. qPCR was performed in triplicate (technical replicates) along with a no-template control (NTC) to rule out contamination. In the NTC well, template RNA was substituted with nuclease-free water; otherwise, the protocol was identical.

2.6 | Primer design

Gene sequences were obtained from the Rat Genome Database (RGD) (RRID: SSCLBR_RGD13063) (http://www.rgd.mcw.edu/wg/home) and NCBI (http://www.ncbi.nlm.nih.gov). Primers were designed using the web interface Primer3Plus (RRID: SCR_003081) (http://primer3plus.com/cgi-bin/dev/primer3plus.cgi). The presence of secondary structures was excluded by the online oligo evaluator from Sigma-Aldrich (http://www.oligoevaulator.com/ShwoToolservlet?TYPE=ANALYSIS), and primers were synthesized at 100 nm (Sigma-Aldrich, Germany). The primer sequences for all of the candidate reference genes and the GOI are shown in Supplementary Table 1.

2.7 | Primer efficiency

Primer efficiency was calculated based on standard curve slope and r^2 value. Standard curves were obtained and analyzed on a StepOnePlus system, using the StepOnePlus software (RRID: SCR_014281) (Applied Biosystems, Version 2.3, Germany). A pair of primers was considered valid if its efficiency was between 90% and 110% (Robledo et al., 2014; Sepúlveda, Bohle, Labra, Grothusen, & Marshall, 2013). The primer pair efficiency ranged between 98% and 102% for all reference genes and GOIs (Supplementary Table 1).

2.8 | Determination of endogenous control stability

We used geNorm (RRID: SCR_006763), NormFinder (RRID: SCR_003387), BestKeeper (RRID: SCR_003380), and the ΔCt method to determine gene expression stability in common samples.

2.8.1 | geNorm

This method determines both the relative stability of genes and the minimum number of reference genes necessary for GOI normalization. Reference gene stability is determined by average expression stability (M) value. The geNorm algorithm has been integrated into a qBase software package (http://biogazelle.com/qbaseplus) and is no longer freely available. A Microsoft Office–compatible version of the original spreadsheet is available at http://ulozto.net/xsFueHSA/geNorm-v3-zip. geNorm converts the raw Cq values to relative quantities by using the ΔCt equation (Equation 2); the highest expression level is set to 1.

$$Q = E^{\text{Delta Ct}} \tag{1}$$

$$Q = E^{(\min \text{Ct} - \text{sample Ct})} \tag{2}$$

where,

Q = sample quantity relative to sample with the highest expression

E = PCR amplification efficiency (2 = 100%) calculated from the standard curve min Ct = lowest Ct value among all genes analyzedsample Ct = Ct value for the current gene geNorm defines the number of genes required for normalization of GOIs by determining an M value that describes the stability of expression of the respective gene (Equation 3). The M value is defined as the mean pairwise variation for a given gene compared with other genes, with a cutoff value of 1.5 (Vandesompele et al., 2002), where lower values indicate greater stability.

$$M_j = \frac{\sum_{k=1}^{n} V_{jk}}{n-1} \tag{3}$$

where,

TABLE 1 Most stable reference genes for the 8-hr PPS model according to the four different algorithms

Algorithm	Stable genes	*M* value/stability value/ Pearson coefficient value
geNorm	*LDHA* and *NONO*	0.2
NormFinder	*ACTB* and *LDHA*	0.198
	ACTB	0.341
BestKeeper	*YWHAZ*	0.987
	UBC	0.987
Delta-Ct	*UBC*	0.73
	LDHA	0.79

Note: LDHA = lactate dehydrogenase; *NONO* = non-POU domain containing octamer-binding; *PPIA* = peptidylprolyl isomerase A; *RP2* = retinitis pigmentosa 2; *TBP* = TATA box binding protein; *TFRC* = transferrin receptor; *UBC* = ubiquitin C.

M_j = gene stability measure

V_{jk} = pairwise variation

n = total number of genes geNorm also calculates a pairwise variation value that determines the minimum number of reference genes required for normalization with a cutoff value of 0.15 (Vandesompele et al., 2002). Values above 0.15 mean additional reference genes are required. Similar to the *M* value, a lower pairwise variation value indicates a more stable combination.

2.8.2 | NormFinder

NormFinder also calculates expression stability values for potential reference genes (Kozera & Rapacz, 2013) and suggests the best candidate gene pairs. It evaluates candidate genes based on expression stability values along with inter- and intragroup variation by direct comparison of genes (Hildyard & Wells, 2014). NormFinder is available as a Microsoft Excel plugin (http://moma.dk/normfinder-software). It accepts *Q* values as input (Equation 2) and ranks genes according to expression and stability value, which is a measure of expression variation. As with geNorm, smaller values mean greater stability.

2.8.3 | BestKeeper

This is a tool for the selection of reference genes based on pairwise correlation analysis and generation of a normalization factor (known as the BestKeeper index). BestKeeper is available as a Microsoft Excel spreadsheet file (http://genequantification.de/bestkeeper.html). It assesses the stability of each gene by comparing the standard deviation of Cq values with the genes and averages these values. Descriptive statistics for individual genes such as coefficient of variance, Pearson correlation coefficient (*r*) values, arithmetic mean (average), and geometric mean are obtained. Genes with high *r* values are considered to be more stable compared with genes with lower *r* values. BestKeeper uses a different algorithm than geNorm and NormFinder; raw Cq values are used to calculate expression variation for candidate reference genes.

2.8.4 | ΔCt method

This is perhaps the simplest way of determining gene expression stability. It can be performed either by using a Microsoft Excel spreadsheet or by input of raw Cq values in RefFinder (RRID: SCR_000472) (http://fulxie.0fees.us). The concept and goal of ΔCt analysis are similar to those of geNorm, but ΔCt is not a unique algorithm. Like geNorm, ΔCt calculations are based on pairs of genes, but it ignores the need to accurately quantify input RNA and instead compares ΔCt values between genes (Silver et al., 2006). The ΔCt method ranks genes according to calculations based on standard deviation and pairwise comparison with other genes.

2.9 | Minimum Information for Publication of Quantitative Real-Time PCR Experiments guidelines

All experiments were performed in accordance with Minimum Information for Publication of Quantitative Real-Time PCR Experiments (MIQE) guidelines (Bustin et al., 2009).

2.10 | Statistics

Statistical analysis was performed using Graphpad Prism 7.0(a) (Graphpad Software, Inc., La Jolla, CA). Data were presented as the mean ± standard error of mean. Student's *t*-test was used for the chronic KaL group (unpaired, two-tailed), and for the remaining groups one-way ANOVA, followed by Tukey method for multiple comparison, was used. *P* values $< .05$ were considered statistically significant.

3 | RESULTS

3.1 | qPCR

Cq values between 15 and 35 cycles were considered valid; mean Cq values are shown in Supplementary Figure 2. A single peak was observed in the dissociation curve for all primer pairs, demonstrating that only specific target products were amplified. The NTC showed no synthesis of any products, thereby indicating that reactions were contamination-free.

3.2 | 8-hr PPS model (epileptogenesis)

3.2.1 | geNorm

LDHA and *NONO* were the most stable genes, whereas *PPIA* and *HPRT1* were the least stable (Table 1). The pairwise variation value for the combination of *LDHA* and *NONO* was 0.13, suggesting that these reference genes were adequate for normalization. The *M* values for all candidate reference genes are shown in Supplementary Figure 3A, and the pairwise variation values are shown in Supplementary Figure 4A.

3.2.2 | NormFinder

ACTB and *LDHA* were ranked as the most stable combination (*ACTB* was the most stable gene), while *PPIA* and *HPRT1* showed the lowest expression stability (Table 1). The expression stability values are shown in Supplementary Figure 3B.

TABLE 2 Most stable reference genes for the 30-min PPS model according to the four different algorithms

Algorithm	Stable genes	*M* value/stability value/ Pearson coefficient value
geNorm	*UBC* and *TBP*	0.16
NormFinder	*PPIB and RPLP1*	0.242
	RPLP1	0.274
BestKeeper	*TBP*	0.993
	UBC	0.972
Delta-Ct	*TBP*	1.19
	UBC	1.21

Note: *ACTB* = actin beta; *GAPDH* = glyceraldehyde 3-phosphate dehydrogenase; *LDHA* = lactate dehydrogenase; *PPIA* = peptidylprolyl isomerase A; *PPIB* = peptidylprolyl isomerase B; *RPLP1* = ribosomal protein large P1.

3.2.3 | BestKeeper

YWHAZ was ranked the most stable gene, followed by *UBC*, while *RPLP1* and *GAPDH* were the least stable (Table 1). Pearson correlation coefficient (*r*) values for the candidate reference genes are shown in Supplementary Figure 3C.

3.2.4 | ΔCt

UBC and *LDHA* were the most stable genes, while *GAPDH* and *HPRT1* were the least stable (Table 1). The stability values for all candidate reference genes are shown in Supplementary Figure 3D.

3.3 | 30-min PPS model (acute phase)

3.3.1 | geNorm

UBC and *TBP* were the most stable combination, while *B2M* and *HPRT1* were the least stable genes (Table 2). The pairwise variation value for a combination of *UBC* and *TBP* was 0.10, suggesting that this combination of these reference genes was suitable for normalization of GOIs. The *M* values for all candidate reference genes are shown in Supplementary Figure 5a, and the pairwise variation values are shown in Supplementary Figure 4B.

3.3.2 | NormFinder

PPIB and *RPLP1* were ranked the most stable combination (*RPLP1* was the most stable gene), while *B2M* and *HPRT1* were the least stable genes (Table 2). The expression stability values are shown in Supplementary Figure 5B.

3.3.3 | Bestkeeper

TBP was the most stable gene, followed by *UBC*, while *PPIA* and *HPRT1* were ranked the least stable (Table 2). Pearson correlation coefficient (*r*) values for all candidate reference genes are shown in Supplementary Figure 5C.

3.3.4 | ΔCt

TBP and *UBC* were ranked most stable, and *B2M* and *HPRT1* were the least stable genes (Table 2). The stability values for all candidate reference genes are shown in Supplementary Figure 5D.

3.4 | KaL (epileptogenesis)

3.4.1 | geNorm

PPIA and *RP2* were found to be the most stable combination, whereas *TBP* and *YWHAZ* were ranked as the least stable genes (Table 3). The pairwise variation value for the combination of *PPIA* and *RP2* was 0.14, suggesting that these reference genes were suitable for normalization. The *M* values for all candidate reference genes are shown in Supplementary Figure 6a, and the pairwise variation values are shown in Supplementary Figure 4C.

3.4.2 | NormFinder

ACTB and *PPIA* were considered the best pairing (*ACTB* was ranked highest for stability), while *TBP* and *YWHAZ* were the least stable genes (Table 3). The expression stability values are shown in Supplementary Figure 6B.

3.4.3 | BestKeeper

ACTB and *YWHAZ* were ranked the most stable genes; *B2M* and *RPLP1* were the least stable genes (Table 3). Pearson correlation coefficient (*r*) values for the candidate reference genes are shown in Supplementary Figure 6C.

3.4.4 | ΔCt

ACTB and *PPIA* were the most stable genes, and *TBP* and *YWHAZ* were the least stable genes (Table 3). The stability values for all candidate reference genes are shown in Supplementary Figure 6D.

TABLE 3 Most stable reference genes for the KaL epileptogenesis group according to the different algorithms

Algorithm	Stable genes	*M* value/stability value/ Pearson coefficient value
geNorm	*PPIA* and *RP2*	0.32
NormFinder	*ACTB* and *PPIA*	0.053
	ACTB	0.066
BestKeeper	*ACTB*	0.929
	YWHAZ	0.781
Delta-Ct	*ACTB*	0.78
	PPIA	0.79

Note: *ACTB* = actin beta; *GAPDH* = glyceraldehyde 3-phosphate dehydrogenase; *LDHA* = lactate dehydrogenase; *PPIA* = peptidylprolyl isomerase A; *PPIB* = peptidylprolyl isomerase B; *RPLP1* = ribosomal protein large P1.

TABLE 4 Most stable reference genes for the KaL chronic epilepsy group according to the different algorithms

Algorithm	Stable genes	*M* value/stability value/ Pearson coefficient value
geNorm	*NONO* and *TFRC*	0.1
NormFinder	*RPLP1* and *GAPDH*	0.045
	GAPDH	0.070
BestKeeper	*UBC*	0.98
	RPLP1	0.963
Delta-Ct	*GAPDH*	0.37
	RPLP1	0.39

Note: *ACTB* = actin beta; *GAPDH* = glyceraldehyde 3-phosphate dehydrogenase; *LDHA* = lactate dehydrogenase; *PPIA* = peptidylprolyl isomerase A; *PPIB* = peptidylprolyl isomerase B; *RPLP1* = ribosomal protein large P1.

3.5 | KaL (chronic epilepsy)

3.5.1 | geNorm

The most stable combination was *NONO* and *TFRC*, whereas *UBC* and *PPIB* showed the lowest expression stability (Table 4). The pairwise variation value of *NONO* and *GAPDH* was 0.07, demonstrating adequate stability for this pair. The *M* values for all candidate reference genes are shown in Supplementary Figure 7A, and the pairwise variation values are shown in Supplementary Figure 4D.

3.5.2 | NormFinder

The combination of *RPLP1* and *GAPDH* was the most stable gene pair (*GAPDH* was the most stable gene), while *B2M* and *ACTB* were the least stable genes (Table 4). The expression stability values are shown in Supplementary Figure 7B.

3.5.3 | BestKeeper

UBC and *RPLP1* were ranked the most stable genes for the chronic group, while *ACTB* and *B2M* were the least stable (Table 4). Pearson correlation coefficient (*r*) values for the candidate reference genes are shown in Supplementary Figure 7C.

3.5.4 | ΔCt

GAPDH and *NONO* were the most stable genes, while *UBC* and *PPIB* were the least stable genes (Table 4). The stability values for all candidate reference genes are shown in Supplementary Figure 7D.

3.6 | Comprehensive ranking of reference genes

Each algorithm ranked potential reference gene (pairs) differently. To reach an objective and unbiased consensus, an overall ranking was obtained by calculating the geometric mean (Chen, Pan, Xiao, Farwell, & Zhang, 2011) of the individual rankings from the four algorithms (Figure 1). The comprehensive ranking showed that *LDHA*, *UBC*, and *NONO* were the overall most stable reference genes for the 8-hr PPS model, and *TBP*, *UBC*, and *PPIB* were the most stable reference genes for the 30-min PPS model. Similarly, for the KaL model, *ACTB*, *PPIA*, and *RP2* were identified as the most stable reference genes during the epileptogenesis phase; *GAPDH*, *NONO*, and *RPLP1* were the most stable during the chronic phase.

3.7 | Validation of reference genes

The expression of *TLR4* is known to be enhanced in both TLE patients and epilepsy models (Maroso et al., 2010). We determined *TLR4* expression in each of the four treatment groups using both the three most stable and two most unstable reference genes (Figure 2). This was done to illustrate how apparent gene expression can change when reference genes of varying stability are used.

For the 8-hr PPS model, *TLR4* expression was found to be 4.6-fold and 4.2-fold higher than control at 4 and 14 days, respectively, when the most stable genes were used. When the two most unstable genes were used (*HPRT1* and *PPIA*), *TLR4* expression was only 1-fold and 1.1-fold at the same time points.

In the 30-min PPS model, *TLR4* expression was 1.3-fold higher than control at 4 days and slightly downregulated at 14 days when using the most stable reference genes. Conversely, the most unstable genes (*HPRT1* and *B2M*) showed *TLR4* expression to be downregulated in the 4-day group and upregulated 1.1-fold in the 14-day group.

In the KaL model, *TLR4* expression was 1.4-fold and 3.4-fold that of control at 4 and 14 days, respectively, when the most stable reference genes were used. The use of *YWHAZ* and *TBP*, the most unstable genes, resulted in increased *TLR4* expression in the 4- and 14- day groups to be enhanced 2.5-fold and 7.2-fold, respectively.

In the chronic KaL group, apparent *TLR4* expression was 3-fold higher than control when the most stable reference genes were used. The combination of *ACTB* and *LDHA*, the most unstable genes, showed a 4.8-fold expression increase.

4 | DISCUSSION

This study systematically evaluated reference genes at various time points and with several algorithms in two different animal models of epilepsy. We found a few novel reference genes, which to our knowledge had not previously been used in experimental epilepsy studies (*NONO*, *RP2*, and *RPLP1*), to be more stable than others that are commonly used, such as *PPIA* (Grabenstatter et al., 2014) and *GAPDH* (Matsuda et al., 2015).

Previous studies have shown that appropriate reference genes can vary between animal models of the same disease (Suzuki, Higgins, & Crawford, 2000; Thellin et al., 1999). We show here that they can even vary within a model—for instance, at different time points. In the KaL model, only one of the five most stable genes was shared between the epileptogenesis and chronic epilepsy groups: *TFRC* (Figure 1). Interestingly, overall reference gene stability increased over time in the KaL model. During epileptogenesis, only 4 genes were sufficiently stable (Supplementary Figure 6A), whereas in the chronic epilepsy phase, all 15 genes were below the stability cutoff (Supplementary Figure 7A). Pairwise variation during the chronic phase was also substantially lower

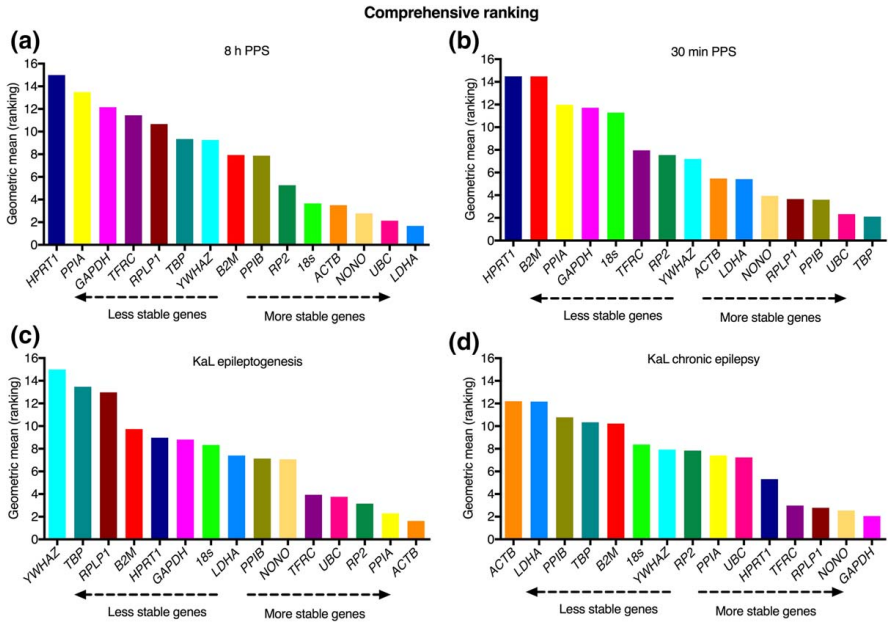

FIGURE 1 Comprehensive reference gene ranking for (A) 8-hr PPS, (B) 30-min PPS, (C) KaL epileptogenesis, and (D) KaL chronic epilepsy groups. The *y* axis represents the geometric mean, which was used to calculate the comprehensive ranking of the genes from the different algorithms. Geometric mean is defined as the nth root of the product of *n* values. The *x* axis represents the genes ranked in order from the least to the most stable genes. Gene colors are consistent in all panels. *ACTB* = actin beta; *B2M* = beta-2-microglobulin; *GAPDH* = glyceraldehyde 3-phosphate dehydrogenase; *HPRT1* = hypoxanthine phosphoribosyl-transferase 1; *LDHA* = lactate dehydrogenase; *NONO* = non-POU domain containing octamer-binding; *PPIA* = peptidylprolyl isomerase A; *PPIB* = peptidylprolyl isomerase B; *RP2* = retinitis pigmentosa 2; *RPLP1* = ribosomal protein large P1; *TBP* = TATA box binding protein; *TFRC* = transferrin receptor; *UBC* = ubiquitin C; *YWHAZ* = tyrosine-3-monooxygenase; *18s* = 18s ribosomal RNA.

for all gene combinations (Supplementary Figure 4, Panel C and D). A potential explanation for this phenomenon is that the brain is seriously perturbed by an epilepsy-inducing event and many genes/pathways are temporarily dysregulated, which affects the expression of reference genes. In fact, a recent study showed that more genes are dysregulated during epileptogenesis than chronic epilepsy in the pilocarpine rat model (Hansen, Sakamoto, Pelz, Impey, & Obrietan, 2014).

We did find that some reference genes are common to multiple models/groups as seen in the comprehensive ranking (Figure 1). *NONO* was a stable reference gene for the 8-hr PPS and chronic KaL groups;

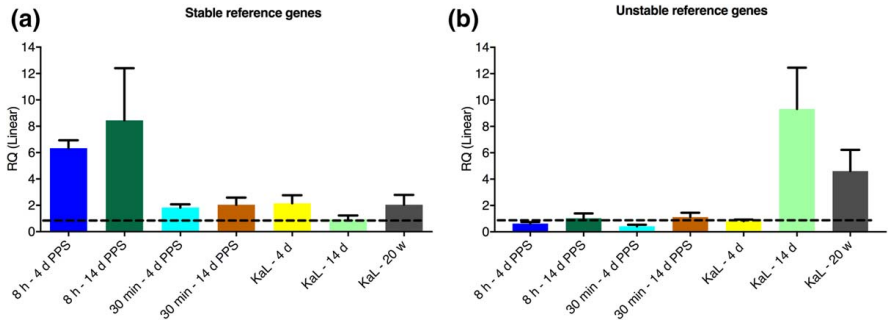

FIGURE 2 Evaluation of reference genes using Toll-like receptor 4 (*TLR4*) (A) with the three most stable reference genes and (B) two most unstable reference genes. Please refer to Figure 1 for the reference gene list.

UBC was common to the 8-hr and 30-min PPS models. We also found genes unique to particular models and time points. *LDHA* (8-hr PPS); *TBP* (30-min PPS); *PPIA*, *ACTB*, *and RP2* (KaL epileptogenesis); and *GAPDH* and *RPLP1* (chronic KaL) were not common to the top three of any other group.

Comprehensive ranking for the PPS models differed significantly. In fact, only two of the top five genes were shared between the 8-hr and 30-min models (*NONO* and *UBC*). This could be because 8-hr PPS induces substantial neuronal injury and epilepsy, whereas 30-min PPS is noninjurious (Norwood et al., 2010, 2011). It is possible that some of the candidate reference genes are influenced by processes involved in neurodegeneration or glial proliferation; both of these phenomena are characteristic of the 8-hr model, but not the 30-min model (Norwood et al., 2010). This would help explain differences in the top candidate reference genes between the two PPS paradigms.

We also found that apparent gene stability varied somewhat between the different evaluation methods. This is, of course, due to subtle differences between the four algorithms. Along these lines, in previous studies evaluating reference genes, minor divergences in geNorm and NormFinder have been reported (Cruz et al., 2009; Pellino, Sharbel, Mau, Amiteye, & Corral, 2011), which leads to slight differences in candidate gene ranking, as we also found in the present study.

A limitation of the present study is that we did not evaluate potential reference genes in other epilepsy models (e.g., pilocarpine or intra-amygdala kainate), in other strains, or in other model organisms. Previous studies have, however, validated some of the same reference genes both in human epilepsy samples (Wierschke et al., 2010) and in the pilocarpine rat model of epilepsy using male Wistar rats (Marques et al., 2013). Regarding the former, *TBP*, *ACTB*, and *UBC* were found to be suitable reference genes in human samples; we show here that they are appropriate for use in the 8-hr and 30-min PPS models. Regarding the latter, *TBP* is a stable reference gene in the pilocarpine model and was ranked first overall for the 30-min PPS group (Figure 1B). The same study showed *ACTB* and *GAPDH* to be stable reference genes; these were ranked first in the KaL epileptogenesis and chronic epilepsy groups, respectively (Figure 1, Panel C and D). Marques and colleagues also found *RPLP1* to be another stable reference gene in the pilocarpine model (Marques et al., 2013); it was ranked among the top four for both the 30-min PPS and chronic KaL groups (Figure 1, Panel B and D).

Unsurprisingly, the use of inappropriate reference genes can lead to erroneous gene expression values (Dheda et al., 2005). An example of this is seen in Figure 2. Apparent expression values are significantly skewed for all groups when unstable reference genes are used. Vandesompele et al. strongly recommend employing multiple reference genes, as the use of a single reference gene might result in higher gene-specific variation and errors in normalization (Vandesompele et al., 2002). It is also prudent to use the geometric mean of multiple reference genes to normalize GOI expression (Equation 4) (Vandesompele et al., 2002) to control for potential outliers.

$$\text{Geometric mean} = \sqrt[n]{x1, x2, x3 \ldots .xn} \quad (4)$$

We suggest using the geNorm algorithm to evaluate reference genes because it ranks the potential genes according to their stability and also determines the minimum number of reference genes required for normalization. Although NormFinder calculates stability values for each gene and BestKeeper ranks the genes according to *r* values, these algorithms do not determine the minimum number of reference genes required for normalization (Kozera & Rapacz, 2013).

Our geNorm data suggest that two reference genes are suitable for normalization as the pairwise variation values for all the animal models were below the 0.15 threshold. Although our data show that just two reference genes can be used for accurate normalization, it is not advisable to rely on these data without validation. The minimum number of reference genes required for normalization should always be determined for each experimental setting.

In summary, we present here validated stable reference genes for two different models of epilepsy and one model of acute, noninjurious seizures. These data show that suitable reference genes vary between models and can also differ between time points in the same model. We found several novel reference genes to be more stably expressed than others that are commonly used in experimental epilepsy studies. These findings demonstrate the importance of validating potential reference genes before using them as normalizing factors in expression analysis. The use of inappropriate (i.e., unstable) reference genes can inadvertently skew data and lead to erroneous conclusions.

ACKNOWLEDGMENTS

The authors would like to thank Dr. Svenja Heischmann and Dr. Deepak Modi for their helpful insight and discussions.

CONFLICT OF INTEREST

The authors declare no conflicts of interest.

AUTHOR CONTRIBUTIONS

C.S. and B.A.N. designed the experiments and analyzed the data. C. S. performed the experiments. C.S., F.R., and B.A.N. wrote the manuscript.

REFERENCES

Andersen, C. L., Jensen, J. L., & Ørntoft, T. F. (2004). Normalization of real-time quantitative reverse transcription-PCR data: A model-based variance estimation approach to identify genes suited for normalization, applied to bladder and colon cancer data sets. *Cancer Research*, *64*, 5245–5250.

Arsenijevic, T., Grégoire, F., Delforge, V., Delporte, C., & Perret, J. (2012). Murine 3T3-L1 adipocyte cell differentiation model: Validated reference genes for qPCR gene expression analysis. *PLoS One*, *7*, e37517.

Bademci, G., Edwards, T. L., Torres, A. L., Scott, W. K., Züchner, S., Martin, E. R., … Wang, L. (2010). A rare novel deletion of the tyrosine hydroxylase gene in Parkinson disease. *Human Mutation*, *31*, E1767–E1771.

Ben-Ari, Y., & Lagowska, J. (1978). Epileptogenic action of intra-amygdaloid injection of kainic acid. *Comptes Rendus Hebdomadaires Des Séances De l'Académie Des Sciences. Série D: Sciences Naturelles*, *287*, 813–816.

Swijsen, A., Nelissen, K., Janssen, D., Rigo, J.-M., & Hoogland, G. (2012). Validation of reference genes for quantitative real-time PCR studies in the dentate gyrus after experimental febrile seizures. *BMC Research Notes*, *5*, 685.

Thellin, O., Zorzi, W., Lakaye, B., De Borman, B., Coumans, B., Hennen, G., ... Heinen, E. (1999). Housekeeping genes as internal standards: Use and limits. *Journal of Biotechnology*, *75*, 291–295.

Thurman, D. J., Beghi, E., Begley, C. E., Berg, A. T., Buchhalter, J. R., Ding, D., ... Wiebe, S; ILAE Commission on Epidemiology. (2011). Standards for epidemiologic studies and surveillance of epilepsy. *Epilepsia*, *52*(Suppl. 7), 2–26.

Turski, W. A., Cavalheiro, E. A., Schwarz, M., Czuczwar, S. J., Kleinrok, Z., & Turski, L. (1983). Limbic seizures produced by pilocarpine in rats: Behavioural, electroencephalographic and neuropathological study. *Behavioural Brain Research*, *9*, 315–335.

Turski, W. A., Czuczwar, S. J., Kleinrok, Z., & Turski, L. (1983). Cholinomimetics produce seizures and brain damage in rats. *Experientia*, *39*, 1408–1411.

Vandesompele, J., De Preter, K., Pattyn, F., Poppe, B., Van Roy, N., De Paepe, A., & Speleman, F. (2002). Accurate normalization of real-time quantitative RT-PCR data by geometric averaging of multiple internal control genes. *Genome Biology*, *3*, research0034.

Wierschke, S., Gigout, S., Horn, P., Lehmann, T.-N., Dehnicke, C., Bräuer, A. U., & Deisz, R. A. (2010). Evaluating reference genes to normalize gene expression in human epileptogenic brain tissues. *Biochemical and Biophysical Research Communications*, *403*, 385–390.

SUPPORTING INFORMATION

Additional Supporting Information may be found online in the supporting information tab for this article.

How to cite this article: Sadangi C, Rosenow F, Norwood BA. Validation of reference genes for quantitative gene expression analysis in experimental epilepsy. *J Neuro Res*. 2017;00:1–10. https://doi.org/10.1002/jnr.24089

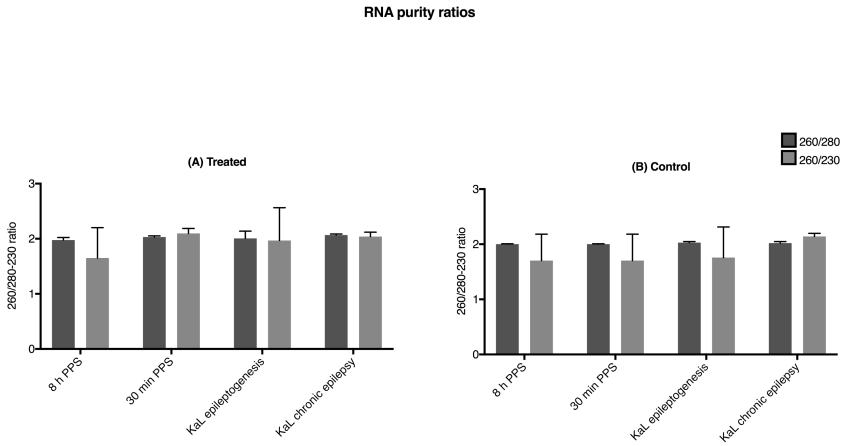

Supplementary Figure 1: RNA purity ratios for (A) treated and (B) control groups for the four animal models. The 260/280 ratio is labeled in blue and the 260/230 ratio is labeled in red in both the panels. The 260/280 ratio is used to evaluate purity and a value of around 2.0 is considered to be adequate. The 260/230 absorbance ratio is a secondary assessment of purity and a value of around 2.0 – 2.2 is considered appropriate.

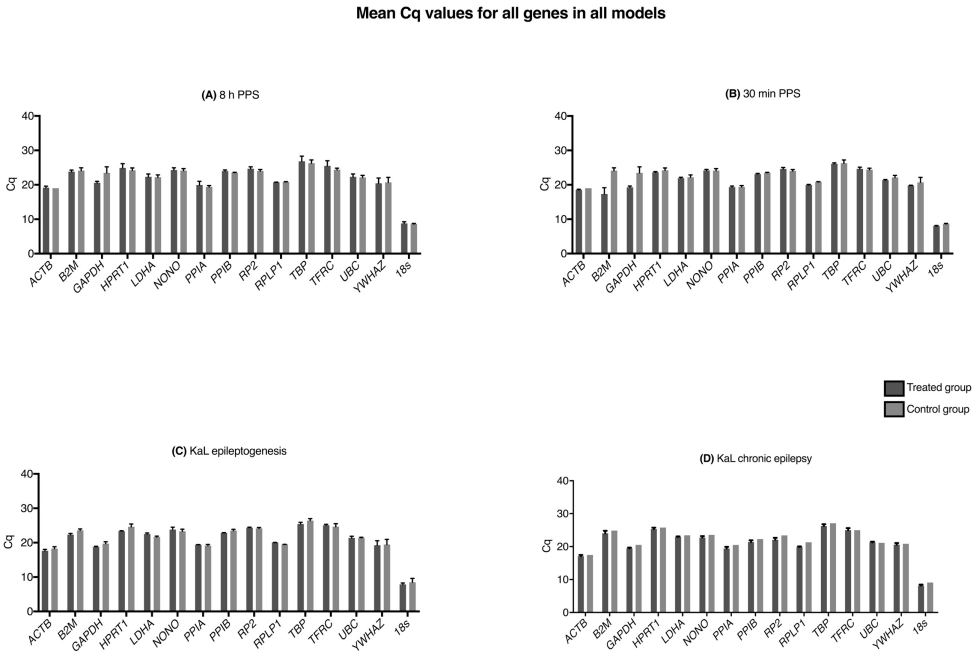

Supplementary Figure 2: Mean Cq values for (A) 8 h PPS, (B) 30 min PPS, (C) KaL epileptogenesis, and (D) KaL chronic epilepsy groups. The four panels in Figure 1 show

the average Cq values for candidate reference genes for treated and control groups. The treated groups are shown in blue and the control groups are red in all panels. The mean Cq values are represented on the y-axis and the candidate reference genes are shown on the x-axis.

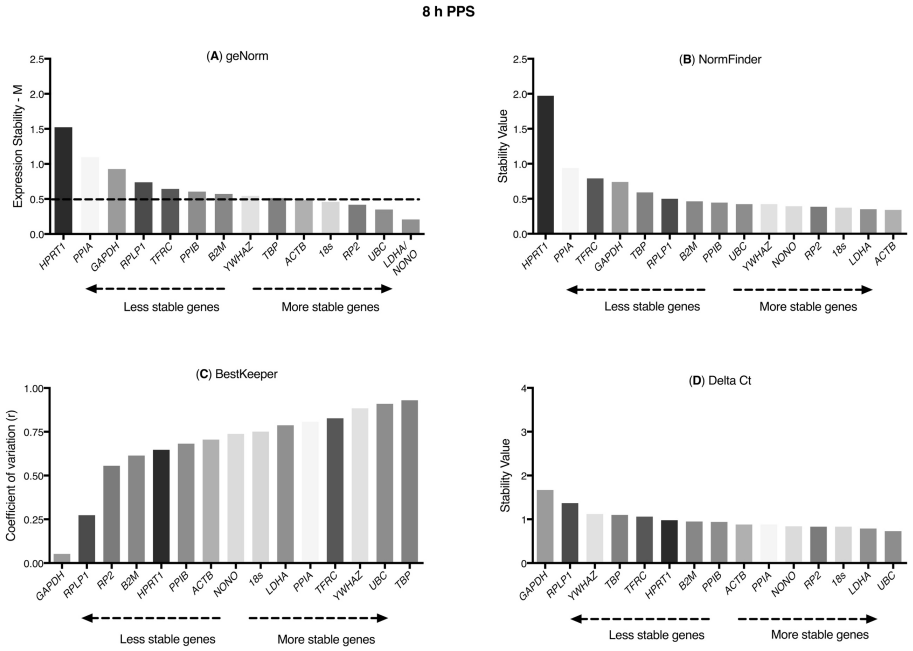

Supplementary Figure 3: Ranking of candidate reference genes for the 8 h PPS model according to (A) geNorm, (B) NormFinder, (C) BestKeeper, and (D) Delta Ct. Panel A shows ranking based on geNorm, where the y-axis represents the average expression stability (M) value, and candidate reference genes are ranked from least to most stable on the x-axis. The dashed line represents the cut-off value of 0.5, below which genes are considered sufficiently stable. Panel B represents ranking based on NormFinder, where the y-axis represents the stability value and the x-axis shows the ranking of reference genes. Panel C represents BestKeeper, where the y-axis represents the co-efficient of variation (r) values, and the x-axis shows the ranking of least to most stable reference genes. Panel D represents the ranking based on Delta Ct method, where the y-axis represents stability values and the x-axis represents the candidate reference gene ranking. All colors are consistent in all panels in all figures, e.g. HPRT1 is always dark blue.

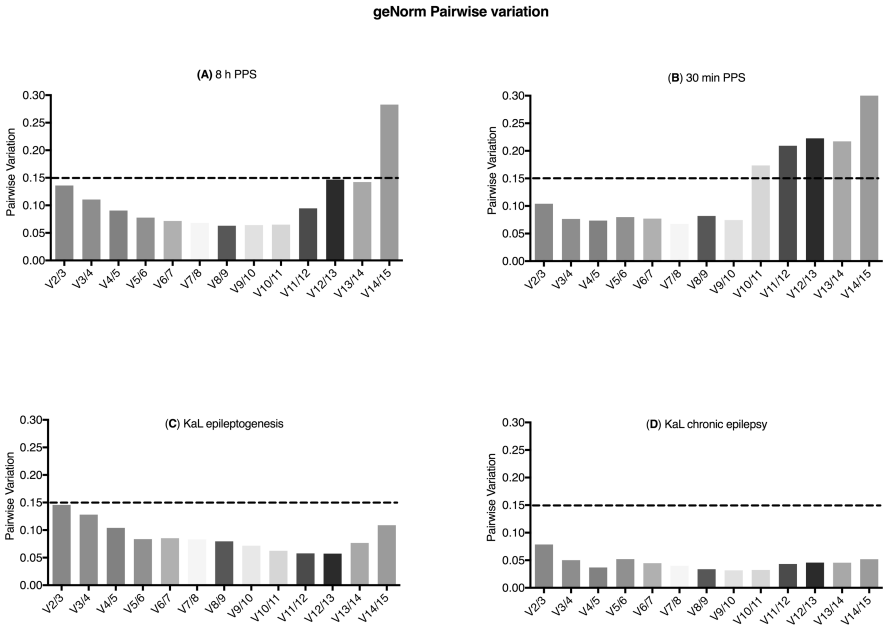

Supplementary Figure 4: geNorm pairwise variation ranking for (A) 8 h PPS, (B) 30 min PPS, (C) KaL epileptogenesis, and (D) KaL chronic epilepsy groups. The y-axis represents the pairwise variation values, whereas the x-axis shows an increasing number of genes, e.g. V14/15 means the addition of a 15th gene. The dashed line represents the cut-off value of 0.15, below which combinations are considered to be sufficiently stable. Note that the addition of a 15th reference gene in Panel A (HPRT1) substantially decreases stability.

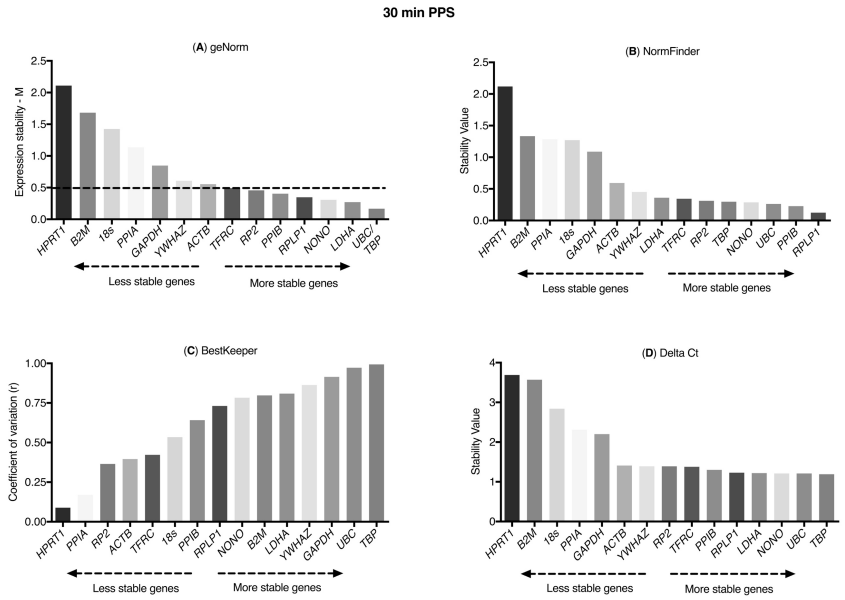

Supplementary Figure 5: Ranking of candidate reference genes for the 30 min PPS model according to (A) geNorm, (B) NormFinder, (C) BestKeeper, and (D) Delta Ct. Panel A shows ranking based on geNorm where the y-axis represents the average expression stability (M) value. Candidate reference genes are ranked from the least to the most stable on the x-axis. The dashed line represents the cut-off value of 0.5, below which genes are considered sufficiently stable. Panel B represents ranking based on NormFinder, where y-axis represents the stability value and the x-axis represents the ranking of reference genes. Panel C represents BestKeeper, where y-axis represents the co-efficient of variation (r) values and the x-axis shows the ranking of least to most stable reference genes. Panel D represents the ranking based on Delta Ct method, where y-axis represents the stability value and x-axis represents the ranking of candidate reference genes. All colors are consistent in all panels in all figures, e.g. HPRT1 is always dark blue.

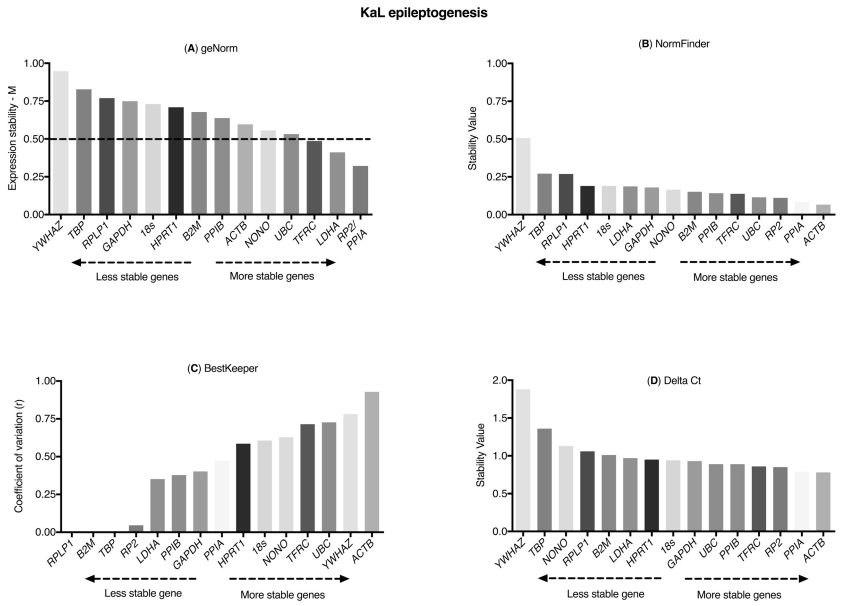

Supplementary Figure 6: Ranking of candidate reference genes for the KaL epileptogenesis group according to (A) geNorm, (B) NormFinder, (C) BestKeeper, and (D) Delta Ct. Panel A shows ranking based on geNorm, where the y-axis represents the average expression stability (M) value and the x-axis shows the candidate reference genes ranked from the least to the most stable. The dashed line represents the cut-off value of 0.5, below which genes are considered sufficiently stable. Panel B represents ranking based on NormFinder, where the y-axis shows the stability value and the x-axis represents the ranking of reference genes. Panel C represents BestKeeper, where the y-axis shows the co-efficient of variation (r) values and the x-axis has the ranking of the least to the most stable reference genes. RPLP1, B2M, and TBP do not have bars since the values were negative. Panel D shows the ranking based on Delta Ct method, where y-axis represents the stability value and the x-axis presents the ranking of candidate reference genes. All colors are consistent in all panels in all figures, e.g. HPRT1 is always dark blue.

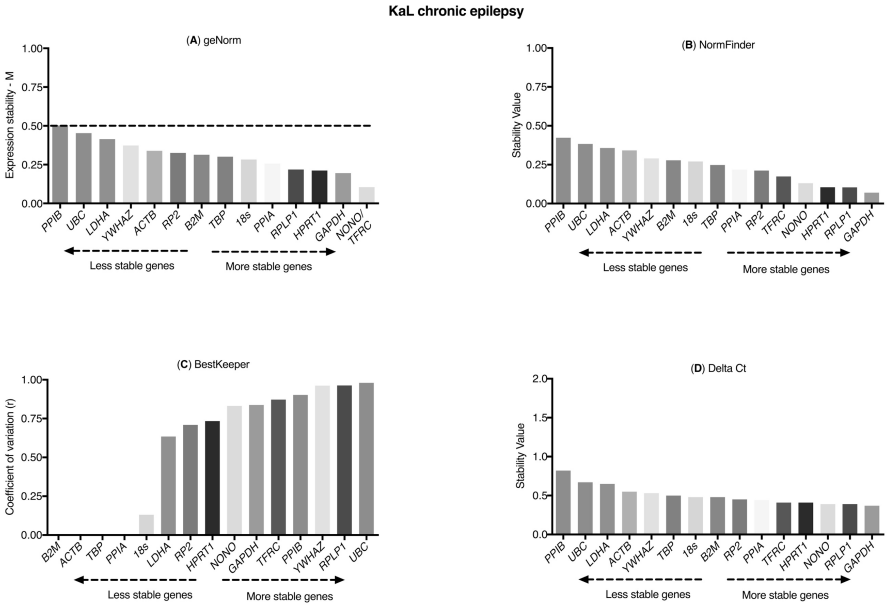

Supplementary Figure 7: Ranking of candidate reference genes for the KaL chronic epilepsy group according to (A) geNorm, (B) NormFinder, (C) BestKeeper, and (D) Delta Ct. Panel A shows ranking based on geNorm, where y-axis represents the average expression stability (M) value and x-axis shows the candidate reference genes ranked from the least to the most stable. The dashed line represents the cut-off value of 0.5, below which genes are considered sufficiently stable. Panel B represents ranking based on NormFinder, where the y-axis represents the stability value and the x-axis represents the ranking of reference genes. Panel C represents BestKeeper, where the y-axis represents the coefficient of variation (r) values and the x-axis shows the ranking of reference genes from least to most stable. B2M, ACTB, TBP, and PPIA do not have bars since the values were negative. Panel D represents the ranking based on the Delta Ct method, where y-axis represents stability values, the ranking of candidate reference genes is shown on the x-axis. All colors are consistent in all panels in all figures, e.g. HPRT1 is always dark blue.

Gene name	Abbreviation	Forward Primer	Reverse Primer	Length (bp)	r^2 value	Efficiency
Actin β	*ACTB*	TGACAGGATGCAGAAGGAGA	GGACAGTGAGGCCAGGATAG	121	0.96	97.533
Beta 2 Microglobulin	*B2M*	GCAGCCTAGCAGTTCAATCC	CACACAGGCTTGCAGACATT	166	0.98	98.067
Glyceraldehyde-3-phosphate dehydrogenase	*GAPDH*	CAAGTTCAACGGCACAGTCA	TACTCAGCACCAGCATCACC	128	1	100.08
Hypoxanthine Phosphoribosyl-transferase 1	*HPRT1*	CAGTCAACGGGGGACATAAA	GGTCCTTTTCACCAGCAAG	180	1	101.86
Lactate Dehydrogenase	*LDHA*	CCGTTACCTGATGGGAGAAA	ACGTTCACACCACTCCACAC	108	1	100.034
Non-POU domain containing Octamer binding	*NONO*	GGTCCACTTGATCCTGCTGT	GCCTGGGTCCTTTGAGTATG	83	0.99	100.3
Peptidylprolyl Isomerase A	*PPIA*	AGGCATGAGCATTGTGGAAG	GCCGCAAGTCAAAGAAA	193	0.99	100.84
Peptidylprolyl Isomerase B	*PPIB*	GGCTCCGTTGTCTTCCTTTT	CGTCCTACAGGTTCGTCTCC	119	0.99	100.19
Ribosomal Protein Large P1	*RPLP1*	GACGGTCACGGAGGATAAGA	AACAAGCCAGGCCAGAAAG	78	0.99	102.18
Retinitis Pigmentosa 2	*RP2*	TGGAAAATGCTGAGGAGGAG	TGGTGATACGCTTCTGGTTG	87	0.99	100.09
TATA box binding protein	*TBP*	TTACGGCACAGGGCTTACTC	TGCTGCTGTCTTTGTTGCTC	81	1	100.11
Toll-like receptor 4	*TLR4*	CACCAACGGCTCTGGATAAA	GAGGACTGGGTGAGAAACGA	188	0.96	98.968
Transferin receptor	*TFRC*	GGCTGCAGATGAGGAAGAAA	CCCAGGTAGCCGATCATAAA	141	0.98	99.786
Ubiquitin C	*UBC*	ACTCGTACCTTTCTCACCACAG	AGACACCTCCCCATCAAACC	76	1	100
Tyrosine 3-	*YWHAZ*	AGACGGAAGGTGCTGAGAAA	CCTCAGCCAAGTAGCGGTAG	192	1	101.09

monooxygenase						
18s ribosomal RNA	*18s*	ATACCGCAGCTAGGAATAATGG	CCTCTTAATCATGGCCTCAGTT	78	1	99.523

Supplementary Table 1: Primer sequences and efficiencies for the reference genes and genes of interest.

Supplementary Table 1: Primer sequences and efficiencies for the reference genes and genes of interest.

Appendix

List of academic teachers

The following list represents my academic teachers in India (IN), Sweden (SE), Germany (DE), Austria (OE) and United States of America (USA).

Beyeler (USA)
Dechant (OE)
Deisseroth (USA)
Jazin (SE)
Kore (IN)
Kullander (SE)
Monory (DE)
Nawani (IN)
Norwood (DE)
Rawas (OE)
Rosenow (DE)
Saria (OE)
Schmidt (SE)
Schratt (DE)
Thornqvist (SE)
Vida (DE)
Wani (IN)
Winberg (SE)

Acknowledgements

I would like to express my deepest gratitude to my supervisors, **Prof. Gerhard Schratt and Prof. Felix Rosenow,** for giving me an opportunity to conduct my PhD research as a member of their group. You have been excellent supervisors and motivators.

Thank you, **Dr. Braxton Norwood**, for always encouraging and supporting me, taking out time for endless discussions, and always answering my queries.

I would like to thank **Dr. Sebastian Bauer** for our discussions and suggestions during my lab presentations and meetings. Thanks to **Silke Caspari** for providing excellent technical support.

I would like to thank my lab colleagues, **Lara Costard** and **Valentin Neubert,** for all the fun times we had. It would have been impossible to be in the office without you guys. I also thank both of you for helping me with surgeries and all the German-English translations.

I would like to thank the entire **AG Schratt** team for helping me setup Western Blot and troubleshoot the technique. I have learnt about Western Blot from each one of you. Thank you, **Martin Lackinger** and **Helena Martins**, I will miss our dark room times. I would also like to thank **Shadan Zulfiqar**, for all the motivation, talks and discussions, and for showing me how to knock out genes using CRISPR.

I would also like to thank my friends. **Dr. Kanishk Abhinav** for troubleshooting molecular biology problems, especially Western Blots. Thank you for visiting us and I wish you good luck with your future goals. **Dr. Deepak Modi** for our discussions on real-time PCR experiments. **Dr. Stephen Marino** for providing me with the motivation and helping me decide my next steps as a scientist. Stephen, you have been a guiding angel since my time in Berlin. Thank you for being so supportive. **Jubin Thomas**, for listening to all my blabbering about neuroscience. Being a mechanical engineer, you had all the patience to listen to me. We have to celebrate and visit our hidden den soon, in Delhi. **Dr. Anuradha Kaistha** and **Dr. Brajesh Kaistha**, thank you for your encouraging and motivating words, and for helping me understand the German PhD system better.

Lastly, I would like to thank my family. **Mom** and **Dad,** this is for you. Thank you for being there with me and supporting all my decisions to pursue my career in science. Thank you for giving me complete freedom, without your support I could not have achieved so much. My wife, **Pratichi Dixit**, thank you for providing me with

unlimited cups of coffee and making delicious food. Thank you for helping me proofread my manuscripts and thesis, and for coloring the graphs. It made my thesis and publications better. I wish you good luck with your endeavors. You have been a patient listener and I am sure you have learnt many things about neuroscience by now. You still have a lot to listen about neuroscience, perhaps forever. I would also like to thank your parents **Nandita** and **Dillip Dixit**, for being kind, patient, and supportive of all our decisions. Last, but not the least, I owe my deepest gratitude to **Sai Baba**, who has always been there with me during my difficult and happy times. I would like to thank you for your blessings.